

https://dspace.org/

# Nutrient and Salinity Loading Based On The Temporal And Spatial Water Quality Data In The Upper Crocodile River Basin

**Mistry, Nikhil Jayant**

**2024-03**

University of the Witwatersrand, Johannesburg

https://hdl.handle.net/10539/45308

Mistry, Nikhil Jayant. (2024). Nutrient and Salinity Loading Based On The Temporal And Spatial Water Quality Data In The Upper Crocodile River Basin. [Master's dissertation, University of the Witwatersrand, Johannesburg]. WIReDSpace. https://hdl.handle.net/10539/45308

Downloaded from a DSpace repository. https://dspace.org/

# NUTRIENT AND SALINITY LOADING BASED ON THE TEMPORAL AND SPATIAL WATER QUALITY DATA IN THE UPPER CROCODILE RIVER BASIN, JOHANNESBURG

A research report by

NIKHIL MISTRY

1864537

Submitted to the Faculty of Science, the University of the Witwatersrand, Johannesburg in partial fulfilment of the requirements for the degree of

Master of Science in Hydrogeology

**Supervisor**: Professor Tamiru Abiye

School of Geosciences, University of the Witwatersrand, Johannesburg

**Co-supervisor**: Professor K Adam Ali

University of Charleston, South Carolina, the USA

MARCH 2024

## PLAGIARISM DECLARATION

I, Nikhil Jayant Mistry, hereby declare that this research report titled Nutrient and Salinity Loading Based on the Temporal and Spatial Water Quality Data in the Upper Crocodile River Basin, Johannesburg' is my own, unaided work. This research is to be submitted to the Degree of Master of Science in Hydrogeology at the University of the Witwatersrand, Johannesburg and has not been submitted previously for any degree or examination to any other university. Information which has been obtained from sources has been indicated and acknowledged by detailed and complete referencing.



_____

Nikhil Mistry

11 August 2024

## ABSTRACT

The Upper Crocodile River Basin has undergone a drastic change through anthropogenic factors such as rapid urban growth, industrial activities, agriculture and mining in the past thirty-eight years. This has led to an increase in nutrient and salinity loads with decreasing water quality. The Upper Crocodile River Basin wastewater treatment works struggle to maintain loading rates, causing partially treated wastewater to enter the river systems that increased the salinity loads. Water chemistry and discharge data from the DWS were collected, cleaned and processed; data were summated across the necessary river channels in which they are located to determine the nutrient and salinity loads in all rivers in the Upper Crocodile River Basin. The results indicated that the Hennops, Jukskei and Crocodile Rivers are responsible for the largest nutrient and salinity loading rates. Changes in land use activities and climate over the past thirty-eight years, since 1980, have drastically impacted the rate at which nutrient and salinity loads enter into the UCRB. During the early 1980s to 1990s a significant drop was observed in nutrient and salinity loading rates, spiking in the late 1990s and early 2000s, influenced by changes in water management and climatic events like the La Niña and the El Niño phenomena. The inter-basin transfer in the early 2000s and subsequent two decades have led to an overall rise in nutrient and salinity loading rates, posing serious water quality and health risks to people in the UCRB area. Mining activities, poor landfill management and leaking tailing storage facilities have resulted in increased sulphate loading rates into the UCRB. Nitrogen loading has risen due to uncontrolled waste disposal from informal settlements, industrial activities and sewage spills in the Johannesburg region. Phosphorus loading rates have risen due to agricultural fertiliser runoff, with the Jukskei River being the largest contributor to these loads in the Upper Crocodile River Basin. The loads entering the Hartbeespoort dam during summer and winter seasons in the 2016-2018 period for sulphate is 6819.24 kg/hr, 4873.62kg/hr; for nitrogen 4179.24 kg/hr, 4021.55 kg/hr and for phosphorus 40.08 kg/hr, 34.724 kg/hr, respectively. Salinity loads entering the Hartbeespoort dam during summer and winter are 42952.87 kg/hr and 27548.39 kg/hr,

respectively. According to the findings, water resource management must act quickly to improve the overall quality of the water; in the upcoming ten years, as loading rates are expected to rise exponentially as a result of increased demand and stressed water use, which will lead to poor water quality.

This will pose serious health and economic risks to the people of the Upper Crocodile River Basin and the populace of South Africa.

## ACKNOWLEDGEMENTS

Thank you to my supervisor, Professor Tamiru Abiye for your patience and understanding during my research, as it took longer than expected. Thank you too, for your guidance and for allowing me the opportunity to participate in the Hydrogeology Programme, which has given me invaluable knowledge and which has allowed me to prosper as a hydrogeologist.

Thank you to the Department of Water and Sanitation for giving me the opportunity to use their large data reserves, enabling me to complete this project.

To my sister, mother and father, thank you for the financial opportunity, love and motivation through some stressful and dire situations. Without you, this research would not have been possible.

To my cousins, Ishani, Seemeen and Ranaa, and to my friends, Reece, Nishen, Liam, Reece, Akshay, Vimal, Prabir, Trisha, Zakhna and Aliyah: thank you for the support and for offering me your homes to work in and load shedding immunity to get this project done; and when it was tough, for getting me to campus for my lectures.

I'd like to dedicate this research project to my late friend and brother, Nishen Pather 07/09/1999 – 24/03/2024

WITS UNIVERSITY

## TABLE OF CONTENTS

PLAGIARISM DECLARATION ..... ii

ABSTRACT ..... iii

ACKNOWLEDGEMENTS ..... v

TABLE OF CONTENTS ..... vi

LIST OF FIGURES ..... viii

LIST OF TABLES ..... x

LIST OF ACRONYMS ..... xi

1. INTRODUCTION ..... 1

1.1. Background ..... 1

1.2. Study Area ..... 1

2. AIM AND OBJECTIVES ..... 5

2.1. Aim ..... 5

2.2. Objectives ..... 5

3. LITERATURE REVIEW ..... 6

3.1. Assessing the Influence of Nutrient and Salinity Loading ..... 6

3.2. Effects of Eutrophication ..... 9

3.3. Case Study ..... 10

3.4. Description of the Study Area ..... 12

3.5. Geological Setting ..... 13

3.5.1. Karoo Supergroup ..... 14

3.5.2. Transvaal Supergroup ..... 14

3.5.3. Ventersdorp Supergroup ..... 15

3.5.4. Witwatersrand Supergroup ..... 15

3.5.5. Crystalline Basement ..... 15

3.6. Hydrogeological Setting ..... 16
3.7. Topography and Drainage in UCRB ..... 17
3.8. Climate Setting ..... 18
3.9. Land Use and Land Cover ..... 20
4. METHODOLOGY ..... 22
4.1. Desktop Work ..... 23
4.2. Data Collection ..... 23
4.3. Excel Work ..... 23
4.3.1. Discharge Data Processing and Validation ..... 23
4.3.2. Water Chemistry Data Processing and Validation ..... 26
4.3.3. Total Dissolved Solids Calculation ..... 26
4.3.4. Nutrient and Salinity Loading Determination ..... 27
4.3.5. Nutrient and Salinity Loading Basin Calculation ..... 29
5. RESULTS ..... 32
5.1. Hennops River Nutrient and Salinity Loading ..... 32
5.2. Jukskei River Nutrient and Salinity Loading ..... 38
5.3. The Crocodile River Nutrient and Salinity Loading ..... 45
5.4. Skeerpoort River Nutrient and Salinity Loading ..... 51
5.5. Swartspruit River Nutrient and Salinity Loading ..... 56
5.6. Brandvlei River Nutrient and Salinity Loading ..... 61
5.7. Gauging station A2H012Q01 ..... 65
6. DISCUSSION ..... 72
7. CONCLUSION ..... 81
8. RECOMMENDATIONS AND LIMITATIONS ..... 82
9. REFERENCES ..... 83

## LIST OF FIGURES

Figure 1: Locality of the UCRB, river network and sites ..... 2

Figure 2: Quaternary catchments, stream networks and dams in the UCRB ..... 12

Figure 3: Geological map with stratigraphic legend of the UCRB ..... 13

Figure 4: UCRB mean changes above sea level (digital elevation)(USGS) ..... 17

Figure 5: CHIRPS, annual precipitation across four decades in the UCRB (CHIRPS) ..... 19

Figure 6: Mean temperature from 1981–2018 in the UCRB(NASA/POWER CERES/MERRA2)19

Figure 7: Multivariate ENSO Index Version 2 indicating El Nino and La Nina events from 1980-2020 (https://climatedataguide.ucar.edu/climate-data/southern-oscillation-indices-signal-noise-and-tahitidarwin-slp-soi) ..... 20

Figure 8: Land use and land change of the UCRB ..... 21

Figure 9: Nutrient and salinity loading result methodology for each UCRB site ..... 22

Figure 10: UCRB nutrient and salinity summation order ..... 29

Figure 11: The stream network and stream order of the UCRB ..... 30

Figure 12: Hennops River gauging station summation ..... 32

Figure 13: Hennops River temporal sulphate load spanning 38 years ..... 33

Figure 14: Hennops River temporal nitrogen load spanning 38 years ..... 34

Figure 15: Hennops River temporal phosphorus load spanning 38 years ..... 35

Figure 16: Hennops River temporal salinity load spanning 38 years ..... 36

Figure 17: Jukskei River gauging station summation ..... 39

Figure 18: Jukskei River temporal sulphate load spanning 38 years ..... 39

Figure 19: Jukskei River temporal nitrogen load spanning 38 years ..... 41

Figure 20: Jukskei River temporal phosphorus load spanning 38 years ..... 43

Figure 21: Jukskei River temporal salinity load spanning 38 years ..... 44

Figure 22: Crocodile River gauging station summation ..... 46

Figure 23: Crocodile River temporal sulphate load spanning 38 years ..... 47

Figure 24: Crocodile River temporal nitrogen load spanning 38 years ..... 48

Figure 25: Crocodile River temporal phosphorus load spanning 38 years ..... 49
Figure 26: Crocodile River temporal salinity load spanning 38 years ..... 50
Figure 27: Skeerpoort River gauging station summation ..... 51
Figure 28: Skeerpoort River sulphate load spanning 38 years ..... 52
Figure 29: Skeerpoort River nitrogen load spanning 38 years ..... 53
Figure 30: Skeerpoort River temporal phosphorus load spanning 38 years ..... 54
Figure 31: Skeerpoort River temporal salinity load spanning 38 years ..... 55
Figure 32: Swartspruit River gauging station summation ..... 56
Figure 33: Swartspruit River temporal sulphate load spanning 38 years ..... 57
Figure 34: Swartspruit River temporal nitrogen load spanning 38 years ..... 58
Figure 35: Swartspruit River temporal phosphorus load over 38 years. ..... 59
Figure 36: Swartspruit River temporal salinity load spanning 38 years ..... 60
Figure 37: Brandvlei River gauging station summation ..... 61
Figure 38: Brandvlei River temporal sulphate load spanning 38 years ..... 62
Figure 39: Brandvlei River temporal nitrogen load spanning 38 years ..... 62
Figure 40: Brandvlei River temporal phosphorus load spanning 38 years ..... 63
Figure 41: Brandvlei River temporal salinity load spanning 38 years ..... 64
Figure 42: A2H012Q01 Main Crocodile River gauging station summation ..... 65
Figure 43: A2H012Q01 temporal sulphate load spanning 38 years ..... 66
Figure 44: A2H012Q01 temporal nitrogen load spanning 38 years ..... 68
Figure 45: A2H012Q01 temporal phosphorus load spanning 38 years ..... 69
Figure 46: A2H012Q01 temporal salinity load spanning 38 years ..... 70

## LIST OF TABLES

Table 1 :Discharge data obtained from the DWS for 18 sites..... 24

## LIST OF ACRONYMS

| | | |
|---|---|---|
| AMD | – | Acid Mine Drainage |
| BIF | – | Banded Iron Formation |
| DO | – | Dissolved Oxygen |
| DWA | – | Department of Water Affairs |
| DWAF | – | Department of Water Affairs and Forestry |
| DWS | – | Department of Water and Sanitation |
| HAB | – | Harmful Algal Bloom |
| kg/hr | – | Kilograms per hour |
| ITCZ | – | Intertropical Convergence Zone |
| LULC | – | Land Use and Land Change |
| MASL | – | Metres Above Sea Level |
| TDS | – | Total Dissolved Solids |
| TN | – | Total Nitrogen |
| TP | – | Total Phosphorus |
| UCRB | – | Upper Crocodile River Basin |
| CWMWMA | – | Crocodile West & Marico Water Management Area |

# 1. INTRODUCTION

## 1.1. Background

Water, one of the most valuable resources in the world is coming under significant stress as a result of rapid urbanisation and population growth (Naidoo et al., 2014). The stresses on the resource have led to reduced water quality and availability. Owing to the peculiar characteristics of water, it can retain matters with which it comes intCo contact, making a key transport mechanism for harmful microbes, nutrients and chemicals. Contaminants persisting in this water could result in serious health implications when consumed by humans and surrounding ecosystems (Ritter et al., 2002). Contamination developments are a consequence of general land use activity and uncontrolled waste disposal. The degradation in water quality is attributed mainly to contact with mineralised rocks, pathogens, nutrients (nitrate, phosphate, sulphate), hydrocarbons, inorganic chemicals, radioactive substances, emerging medical pollutants and e-waste. The latter has become a new contaminant, increasing heavy metal concentration in water. As electronic devices reach their end-of-use, they are disposed of, and remain in landfills; on contact with water, these devices tend to leach mercury, lead and cadmium into the water, which is then passed through the soil before ending up in streams or groundwater (Michael et al., 2013).

## 1.2. Study Area

This study was conducted in the Upper Crocodile River Basin (UCRB), which is located within the geographical limits of 25.678˚S, 27.341˚E and -25.678˚S, 28.472˚E. The UCRB is situated in the northern regions of the city of Johannesburg with the southern water divide being located along the city centre. The overall slope decreases northwards, leading to the Hartbeespoort Dam (Figure 1), and thus the surface water direction flow is towards the North. The basin, which encompasses a total surface area of 4107 $km^2$, includes the city of Johannesburg, the Hartbeespoort Dam, the town of Brits and southern Tshwane (Department of Water Affairs and Forestry, 2008b). The catchment area is

managed by the Crocodile West and Marico Water Management Area (CWMWMA), and the study area is hydrologically classified within the A21 catchment – including the A21A to A21H quaternary catchments. The majority of the study area falls within the highly urbanised, populated and industrialised city of Johannesburg.

The Upper Crocodile River Basin is characterised by a subtropical highland climate which receives a mean annual precipitation of 700 mm (Abiye, 2011). The UCRB experiences cold, dry winters between May and July, and summer between October and March, which is when most of the precipitation occurs.

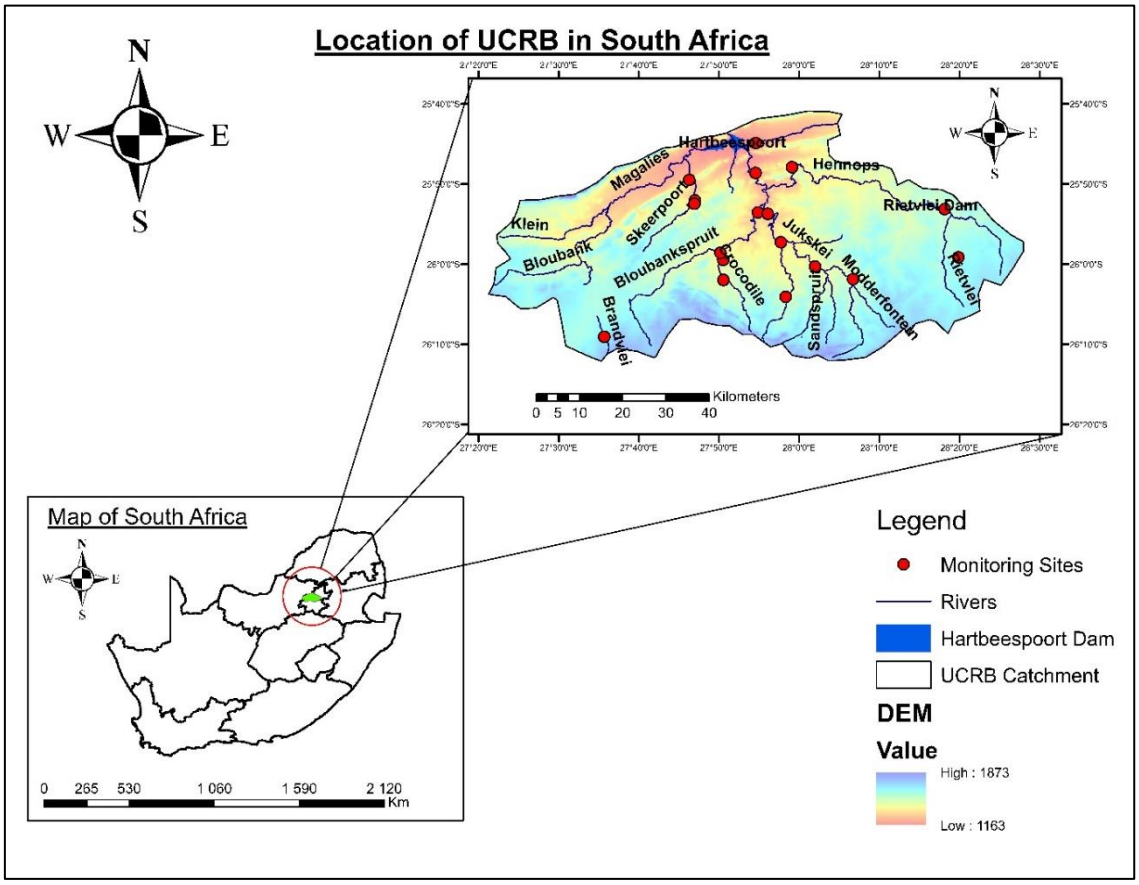



*Figure 1: Locality of the UCRB, river network and sites*

The area has dynamic and variable land and water use patterns extending across the basin. Johannesburg's dense population and well-developed formal sector consume an extremely high volume of water (500 million $m^3$ per year), subsequently placing severe stress on the city's water supply (Department of

Water Affairs and Forestry, 2008a). The water demand is assisted through the water transfer supply from the Vaal catchment (Department of Water Affairs and Forestry, 2008a). The current supply of water is focused primarily on the use of surface water reserves with minor groundwater abstractions concentrated in the southern end of the catchment where industries and minor settlements are dominant. Groundwater is used extensively in the northern and central regions of the UCRB. The surface water in these regions of the basin relies heavily on the main reservoirs, which are located along the edges of valleys through which the Crocodile River flows. Land is predominantly used for agricultural activities (Leketa, 2019). It has been noted by Leketa (2019), that poor surface water quality has been a major issue for several decades, particularly in the Hartbeespoort Dam, which receives wastewater from the city of Johannesburg (Department of Water Affairs and Forestry, 2008a).

The UCRB is negatively impacted by climatic and anthropogenic factors that are influential and threaten the overall future of South Africa's water resources (Leketa, 2019). According to the Department of Water Affairs of South Africa (DWAF) (DWAF, 2008), the UCRB is characterised as having the greatest human impact in South Africa due to its large urban settlements in Johannesburg, Midrand and southern Pretoria (Tshwane). The urban centres from various economic sectors (including mining, industrial and agricultural), have furthered considerable water demand (Abiye et al., 2015). The overall water demand was calculated to be around 556 million $m^3$ per year (DWAF, 2008). However, it is noted that water resources within the UCRB could not meet the demands, and water supply through the neighbouring Vaal Basin has mitigated the increased water demands (Leketa and Abiye, 2019); this necessitated enhancement from the Vaal Basin of 556 million $m^3$ per year which increased wastewater disposal from the water treatment plants draining into the UCRB (Leketa and Abiye, 2019). This discharge exacerbates the decrease in overall surface water quality in the UCRB (DWAF, 2008). According to the DWAF (2008), the overall demand for water in urban settlements will have increased from 292 million $m^3$ to 409 million $m^3$ by 2025, which will place pressure on wastewater treatment plants and subsequently compromise the water quality in the UCRB. It is postulated that the

Hartbeespoort Dam could be impacted the most by increased urban wastewater disposal as it is the first downstream restrictive water body to receive water from Johannesburg and Pretoria. The known pollution crisis faced by the Hartbeespoort Dam is due to the high influx of nutrient loads from wastewater treatment plants, poor maintenance of leaking sewers and urban and agricultural runoffs (Dudula, 2007). It has therefore been labelled as one of the water bodies in South Africa most severely affected by eutrophication (Cukic and Venter, 2012).

Consequently, it has been projected that the UCRB will adversely be affected by changes from anthropogenic and climatic activities. Rapid climatic shifts, reduced rainfall and temperature increases, combined with effluent discharge and exponential population growth, pose drastic threats to surface and groundwater reserves in the UCRB (Kusangaya et al., 2014). In addition, the rising discharge of effluent attributable to the exponential urbanisation and industrialisation in the UCRB is anticipated to further aggravate the overall pollution in the area. The increased natural flow of water which would dilute the overall effluent is envisaged to dilute and lower the pollution of wastewater (Leketa and Abiye, 2019). The Hartbeespoort Dam has been associated with the use of water for agricultural activity (Harding, 2004; Venter, 2004). The radically expanding mining industry upstream of the dam has drawn foreign and local interest and has aided the growth of Johannesburg and Pretoria. Decades of development, rapid urbanisation and population growth have increased the quantity of sewage entering the dam, increasing the overall influx of contaminants in the area (Ashton et al., 1985; DH Environmental, 2004; Harding, 2004; Venter, 2004). In recent times, not only has the dam been an agricultural water source for the local community, but it has also become a tourist attraction for recreational purposes (Harding, 2004; Venter, 2004). In the last two decades, earlier evaluations revealed that residents and surrounding communities had noticed a bad odour and masses of algae in the water source, while the surrounding flora and fauna experienced increased health issues and land desertification (Thornton et al., 1989). Additionally, residents around the Hartbeespoort Dam experienced increased incidences of gastroenteritis and rashes (Thornton et al., 1989). This

drew in attention of scientists and the Department of Water Affairs (DWA), which led to the implementation of a remediation plan.

A rise in nutrient influx from rivers in the UCRB was observed to accelerate the eutrophication rates, resulting in algal blooms (Toerien and Walmsley, 1978; Harding, 2004; Venter, 2004). The upstream industrial and mining activities in Johannesburg and Pretoria injected heavy metal pollutants such as Acid Mine Drainage (AMD), into the dam, which exacerbated health issues experienced by humans, animals and plants (Wittmann and Forstner, 1975; Abiye et al., 2015).

Nutrient influx is an issue in the UCRB; the volume and water chemistry need temporal and spatial evaluation, and the rate at which nutrient influx enters the UCRB needs to be determined to mitigate the effects on flora and fauna.

## 2. AIM AND OBJECTIVES

### 2.1. Aim

The main aim of this research was to understand the temporal and spatial change in nutrient and salinity loading in the streams that make up the UCRB by using water chemistry data collected at designated gauging stations across the UCRB.

### 2.2. Objectives

1. Determine the spatial and temporal variation in nutrient and salinity loading coupled with variation in the hydrochemistry of streams at different gauging stations in the basin.
2. Quantify volumes of nutrient and salinity loading at different discharge gauging stations.
3. Identify the source of nutrients entering surface water by evaluating past and present land use activities.
4. Evaluate the changes in land use activity across four decades in coherence with hydrochemical data.

# 3. LITERATURE REVIEW

## 3.1. Assessing the Influence of Nutrient and Salinity Loading

Loading is described broadly as the rate of supply of a particular entity to receiving water and is commonly expressed as a rate of supply (kg(mg)/S). Eutrophication in most surface water is directly linked to the rate at which nutrients and organic matter are added to a system. Physical and chemical characteristics and processes like surface area, volume, vertical mixing, stratification, residence time, depth and flushing rate are common factors that affect the export, transport, retention and transformation of nutrients in a basin. The are many methods and procedures for calculating nutrient loading, although the most common calculation is to multiply the nutrient concentration (mg/L) by the river discharge rate ($m^3/s$), (Pinckney et al., 2001).

$$Nutrient\ Loading = Concentration\left(\frac{mg}{L}\right) \times Discharge(Q)\left(\frac{m^3}{s}\right)$$

$$\therefore Nutrient\ Loading = \left(\frac{mg}{L}\right) \times \left(\frac{1000L}{s}\right)$$

$$\therefore Nutrient\ Loading = \frac{mg}{s} or \frac{kg}{s}$$

The accuracy of the calculation is determined primarily by the accuracy of measurement of the two variables, discharge and concentration. The frequency at which measurements are taken is critical when the basin is affected by episodic events where there is an injection of large volumes of water. During such an event, the injection of nutrients can exceed the total loading for an entire year in only a few days. Given that discharge is directly proportional to loading, the dilution caused by the high volumes of water means that overall loading rates will be high (Pinckney et al., 2001). Nutrients in the form of nitrogen and phosphorus can be derived from point and nonpoint sources (Pinckney et al., 2001). Point sources of nutrients are derived from wastewater treatment plants, stormwater drains, sewage outfalls and industrial wastewater, whilst nonpoint sources of

nutrients are atmospheric depositions including rainfall and groundwater in the form of baseflow and runoff. Nonpoint sources are subjected to increased nutrient loads when dominated by agricultural activities and are difficult to control when compared to point sources, which are a dominant source of nitrogen (Pinckney et al., 2001).

The impact of a given nutrient load is primarily dependent on how fast the inputs are transferred through the system. Nutrients are exported through tidal flushing or microbial processes and so converted into an elemental form. The $N_2$ nitrification and denitrification are common microbial processes where forms of N conversion are determined by the dissolved oxygen values and the presence of microbes (Pinckney et al., 2001). In oxic conditions, ammonium transforms to $NO_2^-$ and then $NO_3^-$ and this is commonly referred to as nitrification. In anoxic conditions, $NO_2^-$ and $NO_3^-$ are converted to $N_2$ gas by microbes, referred to as denitrification. During winter months, phosphate ($PO_4^{-3}$), can be limiting or colimiting when concentrations N increase (Pinckney et al., 2001).

Studies conducted in parts of North America and Europe have quantified the overall nutrient contributions to watersheds. The results of nutrient loading (N and P) in the Mississippi River have shown that an estimated ten  % (Howarth et al., 1996), to twenty  % (Goolsby et al., 2000), of the total N flux and twenty  % of the total P flux is directly related to point sources including sewage and industries. Basins that are heavily populated with relatively small surface areas are subjected to N pollution through wastewater, with sixty per cent of nitrogen inputs (organic and inorganic); as an example, Long Island Sound, New York City due to sewage (Pinckney et al., 2001).

Regeneration within a known basin compounded by recycling processes is deterministic in the overall water systems response and recovery from increased nutrient loading.

Total Dissolved Solids (TDS), are a common indicator of water salinity, measured as mg/l. Salinity loading is the rate at which TDS is transported in a given  as (Venkatesan et al., 2011):

$$Salinity\ Loading = TDS\left(\frac{mg}{L}\right) \times Discharge(Q)\ \left(\frac{m^3}{s}\right)$$

$$\therefore Salinity\ Loading = \left(\frac{mg}{L}\right) \times \left(\frac{m^3}{s}\right)$$

$$\therefore Salintiy\ Loading = \left(\frac{mg}{L}\right) \times \left(1000\frac{L}{s}\right)$$

$$\therefore Salinity\ Loading = \left(\frac{mg}{s}\right) or\ \left(\frac{kg}{s}\right)$$

The impact of salinity on surface water and groundwater systems is a global concern. TDS is altered through primary and secondary sources. The primary sources affecting rivers and groundwater resources are both natural and anthropogenic. Agricultural runoff, soil leaching, and high wastewater treatment plant discharges directly increase the overall TDS concentration, as the ionic composition of water is altered. TDS is strongly related to the ionic composition of water (Chapman et al., 2000), and high TDS values are a threat to the economy as they compromise infrastructure due to their ability to corrode. These also affect crop yield directly as the water contains toxic ions that affect biotic communities (Chapman et al., 2000); this is a threat to the overall health and biodiversity of the region. Salinity problems are prevalent in semi-arid to arid countries, as evaporation enriches the overall ionic concentration (Williams, 1987).

Studies conducted by the United States Bureau of Reclamation on the Colorado River strongly propose that stream flow, natural runoff, climatic conditions, reservoir storage and water resource development are major factors that control the impact of salinity concentrations (United States Bureau of Reclamation: USBR, 2005). Natural sources that increase the overall ionic concentration and salt composition are evaporation, groundwater discharge, saline springs and sediment erosion, with agricultural practices being the second largest driver of increased salinity (Venkatesan et al., 2011).

It has been found that the use of water softeners and dishwashers in residential and commercial locations is a major contributor to TDS in wastewater effluents.

Increased water consumption driven by a growing population in arid and semi-arid countries has increased the overall wastewater generation. For example, in the Colorado Basin, this increased water use increases the wastewater generation resulting in greater TDS discharges. The increase in commercial, residential and industrial water use has exponentially increased wastewater discharges (USBR, 2005).

### 3.2. Effects of Eutrophication

Eutrophication refers to algal infestation of water bodies due to high nutrient content, or it refers to the rate of supply of organic matter into a given habitat rather than the overall trophic state (Paul, 2013). Eutrophication is frequently quantified using organic matter. Different forms of organic matter occur in diverse ecosystems and are strongly influenced by land use characteristics of the overall watershed or catchment (Guo et al., 1990; Farrington, 1992; Paerl et al., 1997). Allochthonous organic matter is a primary source of organic matter that occurs in an estuary, transported through runoff (Pinckney et al., 2001). This organic matter is generated internally within the system through photosynthesis; within estuarine environments, phytoplankton, benthic microalgae and other aquatic vegetation are responsible producers of organic matter (Pinckney et al., 2001).

Eutrophication is caused by an overall increase in organic matter loading. This happens naturally by increased allochthonous organic matter when the overall estuarine vegetation increases. Eutrophication occurs within chronic and episodic changes that occur in watershed hydrodynamics, geomorphology and climate, and then is rapidly altered during catastrophic events; these events affect the overall organic matter input rate in the basin (Odum et al., 1995). According to Pinckney et al. (2000), the ecological context of eutrophication involves time and space scales that transcend into ephemeral and seasonal events; this changes the overall input rates of organic matter and needs to be assessed on annual or decadal scales to evaluate changes in the organic matter by ecosystem responses to increased loading rates.

The rate of supply of nutrients is a driving factor in regulating eutrophic events that take place within a watershed. In estuarine ecosystems, nitrogen is a limiting nutrient for phytoplankton buildup. In contrast, allochthonous nitrogen can be used for phytoplankton growth and production, and it is captured and returned to the estuary (Pinckney et al., 2001).

Phosphate ($PO_4^{-3}$), is a colimit during winter months or when nitrogen concentrations are elevated (Fisher et al.,1992; Conley, 2000). Rapid regeneration of nutrients and short turnover can mask true nutrient limitation and availability. Hence, the rate of nutrients entering a given estuarine needs to be quantified to understand the overall controls of eutrophication.

The increased nutrient and salinity loading are pertinent in the Hartbeespoort Dam – as a central convergence dam, into which all large rivers in the upper Crocodile River feed. Anthropogenic nitrogen has caused a growth in estuarine vegetation leading to a strong stimulation of algal blooms. Further coupled with water anoxia, with water animal and ecosystem life declining due to the reduction of overall oxygen levels, this is inherently detrimental and can exacerbate the overall eutrophication issue. During the summer and spring seasons, there is optimal growth for phytoplankton (cyanobacteria). It is important to understand the overall temporal variability based on the seasons in the UCRB, to manage the future of the basin more effectively.

### 3.3. Case Study

A recent study monitored the temporal and spatial changes across the UCRB through the utilisation of remote sensing. The use of Landsat 5/7 was obtained to extract data over the period of 1995–2010. Landsat 8 and Sentinel 2 images were used across the UCRB from 2013. Data gathered from remote sensing has been thoroughly evaluated with water quality data obtained from the Department of Water and Sanitation (DWS), and in turn, carefully checked for Total Phosphorus (TP) concentrations. TP is known to be the limiting nutrient in ecosystems controlling many biological processes, especially the rates of photosynthesis (Ali et al., 2022). Furthermore, data has been gathered on physiochemical processes

including Dissolved Oxygen (DO) and temperature at various depths to understand the stronghold of the Harmful Algal Blooms (HAB), experienced at the Hartbeespoort Dam (Ali et al., 2022).

As an index for HAB quantification chlorophyll-a was used, which is known to be a universal pigment indicator for HABs and phytoplankton. Through the evaluation of the study, strong relationships between TP, DO and chlorophyll-a were noted. Furthermore, the evaluation of various time series plots over five-year and decadal intervals verified oscillatory fluctuations in the limiting nutrient phosphorus, which is due to climatic and anthropogenic controls. Climatic controls involved the El Niño and La Niña effects which induced periods of flooding and drought, with anthropogenic controls being mining, industrial and agriculture (Ali et al., 2022).

The research conducted by Ali et al. (2022) prompted this study to investigate and attempt to quantify the nutrient and salinity loads that are contributing to the degradation of water quality in the UCRB. This raised the question of how much nutrient is moving in the basin, and what the spatial controls on surface water in the basin are, and if the surface water quality in the UCRB declined because of anthropogenic activities including industrial, agriculture and mining activities. By closely evaluating the time series plots and remote sensing data across the period of four decades, one would be able to understand the nutrient and salinity load moving through the basin, leading to the degradation of water quality. Furthermore, through the evaluation of TDS as a salinity indicator, an understanding of surface water quality would be in perspective.

As highlighted, the TP total nitrogen and sulphate loads were temporally evaluated across four decades to provide greater insight into the reasons for water quality degradation in the UCRB, compounded with the spatial evaluation. The spatial evaluation provided by Ali et al. (2022), illustrates the need for further research to evaluate the major anthropogenic controls on the UCRB. The need to understand the temporal and spatial relationships in the UCRB across thirty-eight years will be of importance to control and attenuation in basins across the world, as water demand increases and water quality plummets.

## 3.4. Description of the Study Area

The Upper Crocodile River Basin is located in parts of the Gauteng and North-West Provinces of South Africa. The catchment area extends from the water divide in the South to the Hartbeespoort Dam in the North (Figure 2). The basin has an aerial extent of 4107 km$^2$ and is located within the geographical coordinates of 25.678˚S, 27.341˚E and -25.678˚S, 28.472˚E. The catchment is managed by the Crocodile West and Marico Water Management Area (WMA), and the study area of focus is hydrologically classified within the A21 catchment, including the A21A to A21H quaternary catchments. The majority of the study area falls within the highly urbanised, populated and industrialised city of Johannesburg.

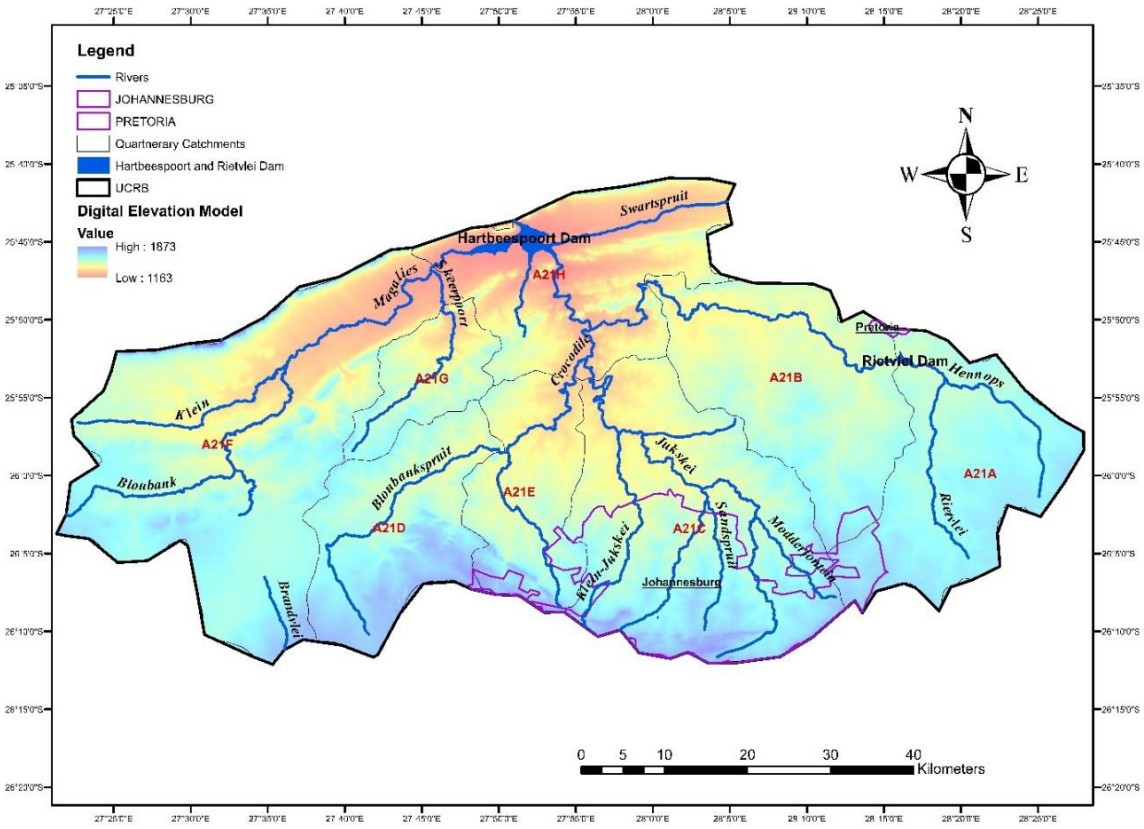



*Figure 2: Quaternary catchments, stream networks and dams in the UCRB*

## 3.5. Geological Setting

The UCRB is underlain by rocks from the Archean to the Paleoproterozoic era. The eroded, weathered and tectonically-altered granitic, gneissic and granodioritic rocks make up the crystalline Archean basement (McCarthy and Rubdige, 2005; Abiye, 2011). The crystalline Archean basement is overlain by the Witwatersrand Supergroup, comprising a succession of argillaceous and arenaceous sedimentary rocks, which make up the West Rand and Central Rand Groups of the Witwatersrand Supergroup (McCarthy and Rubidge, 2005).

The conformable Witwatersrand Basin unconformably overlies the Archean basement rocks (McCarthy and Rubidge, 2005). The Transvaal Supergroup is made up of various volcanic, sedimentary, carbonate (dolomite), and chemical Banded Iron Formation (BIF) rocks (McCarthy and Rubidge, 2005). The succession of the various supergroups forms a dome shape that extends across the UCRB catchment. Across the range of the UCRB catchment, notable structural deformation features were noted, including shear zones and lateral

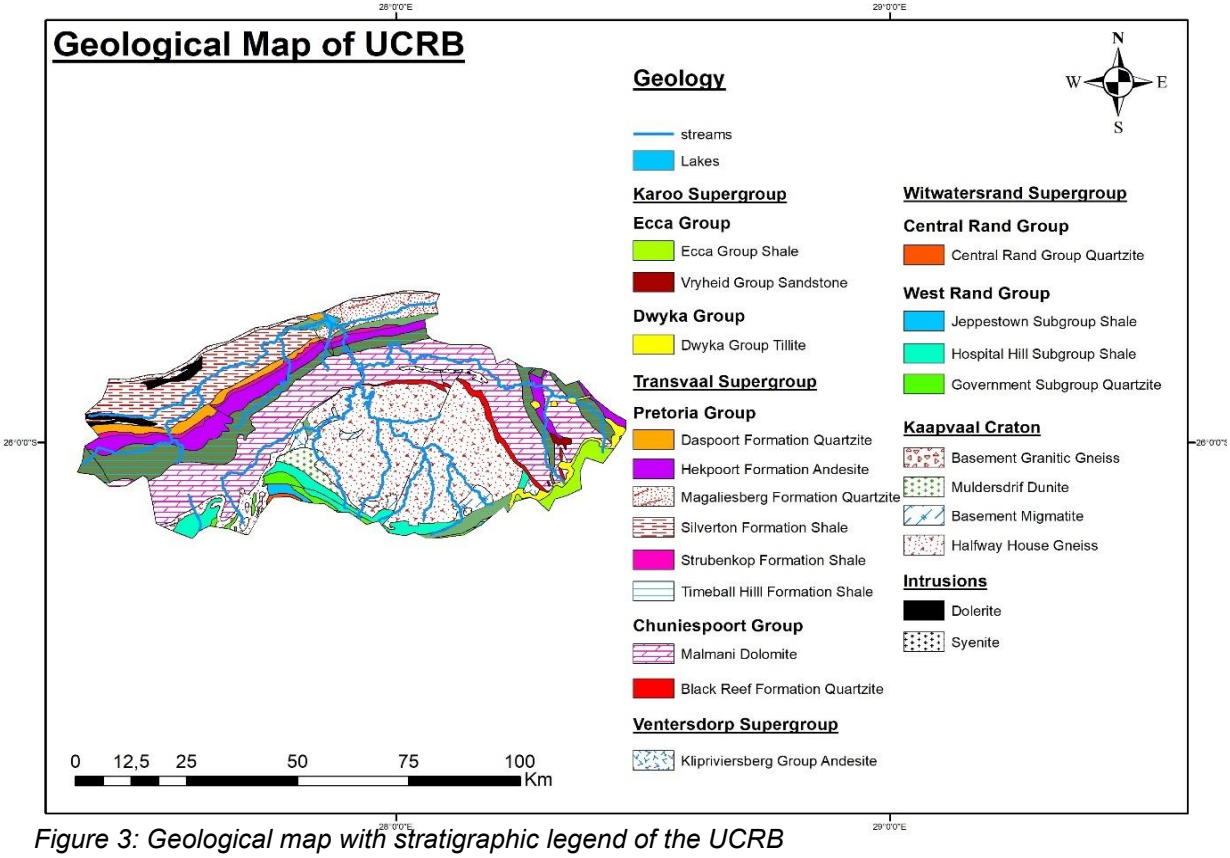



*Figure 3: Geological map with stratigraphic legend of the UCRB*

strike-slip faults which are seen to intersect various lithological units in the catchment (Abiye, 2011; Abiye et al., 2011).

### 3.5.1. Karoo Supergroup

The Karoo Supergroup is a sedimentary basin comprising the youngest lithological sequence in the UCRB; it is classed into two Groups– the Dwyka Group made up of mudstone, sandstone and tillite, and the Ecca Group made up of sandstone, shale and coal (Leketa, 2019).

### 3.5.2. Transvaal Supergroup

The Transvaal Supergroup was approximated to have been deposited 2650 Ma. ago. As a result of thermal subsidence due to the rifting of the shallow continental shelf, a basin formed where the Transvaal Supergroup was deposited (McCarthy and Rubidge, 2005). This supergroup is further divided into three groups: Pretoria, Chuniespoort and the Black Reef Formation (McCarthy and Rubidge, 2005).

The Black Reef Formation, which conformably overlies the Ventersdorp Supergroup, was the first of the three groups to be deposited and is made up of quartzites and conglomerates. The Chuniespoort Group is further classed into the Malmani Subgroup where there are chert-rich and chert-poor dolomitic formations, the Penge Formation (containing metamorphosed sedimentary rocks and BIFs), and the unconformable Duitschland Formation, which overlies the Penge Formation comprising mainly diamictite, lava and various carbonaceous rocks (McCarty and Rubidge, 2005). Shale and quartzite can be seen along the extension northeast to southwest across the catchment of the Malmani Dolomites and Pretoria Group. The topography of the area where dolomite is present has a characteristic undulating topography (Abiye, 2011), while the more resistant quartzite of the Pretoria Group forms ridges and the less resistant shale forms valleys in response to mechanical and chemical erosion.

### 3.5.3. Ventersdorp Supergroup

The Ventersdorp Supergroup is characterised by sedimentary, volcano-sedimentary and intermediate to mafic volcanic rock units, which were emplaced after 2714 Ma (Van der Westhuizen et al., 1991; Robb and Meyer, 1995). Within the UCRB, outcrops of the Ventersdorp Supergroup are predominantly tuffs and andesites of the Klipriviersberg Group (Barnard, 2000).

### 3.5.4. Witwatersrand Supergroup

During the Precambrian era in an extensional geological setting, the rocks of the Witwatersrand Supergroup were deposited, and this supergroup comprises two groups. The younger Central Rand Group is made up of two subgroups: the Johannesburg Subgroup and the Turffontein Subgroup; the subgroups consist primarily of shale and quartzite. The older West Rand Group consists of three subgroups, Jeppestown, Government and Hospital Hill, characterised by conglomerates, shale and quartzite. The subgroups are further typified by fluvial conglomerates, shale, interbedded shale and quartzite units, andesitic lava, diamictite and quartzite (McCarthy and Rubidge, 2005). An outcrop of the West and Central Rand Groups can be seen in the South of the study area (Figure 3).

### 3.5.5. Crystalline Basement

The crystalline Archean basement is formed from the oldest dated rock types in the catchment and contains greenstone remnants. The gneissic, granitic and granodioritic rocks are the oldest in the UCRB catchment, which are unconformably overlain by the Witwatersrand Supergroup (McCarthy and Rubidge, 2005; Abiye, 2011). In the geological map (Figure 3), a very noticeable circular feature can be seen – this is known as the Johannesburg Dome. As perceived, the dome is surrounded by the Witwatersrand, Ventersdorp and Transvaal Supergroups.

## 3.6. Hydrogeological Setting

The UCRB has undergone a series of deformational events resulting in different geological structures. The structures present include shear zones and strike-slip faults which cross-cut different lithologies (Abiye, 2011). Due to the penetration of the diverse rock units by shear zones and strike-slip faults, this resulted in aquifers with varied hydraulic properties where their yields are dependent on secondary structures and weathering (Abiye et al., 2015). According to multiple resources, there are four types of aquifers: fractured, karstic, intergranular and fractured and intergranular aquifers (Barnard, 2000; Abiye, 2011; Abiye et al., 2011; Abiye et al., 2015).

Fractures, joints and fissures make up the transmitting structures characteristic of fractured aquifers and these structures carry large quantities of water. The fractured aquifers are commonly found in the Archean Basement and in the Witwatersrand Supergroup quartzite of the UCRB (Leketa, 2019).

The dolomitic aquifers too, have undergone karstification which has resulted in large transmission and storage cavities for water to move through. There are large conduits present within the karstic aquifers which transmit and retard groundwater flow. According to Abiye (2011), karstic aquifers are found in the Malmani Subgroup (Figure 3), which have been noted to have greater productivity and transmissivity compared to fractured aquifers in the UCRB.

Intergranular aquifers are primarily made up of gravel, sand and unconsolidated porous materials which have undergone strong deformation, resulting in the porous state. These aquifers are found along the peripheries of riverbanks and within the weathered regions of granite complexes across the UCRB (Leketa, 2019).

Intergranular and fractured aquifers comprise rocks containing both unconsolidated material and fractures (Barnard, 2000). The fractures also, comprise a sequential system of high-permeability regolith, overlaying a highly fractured rock aquifer. The aquifer systems can be seen in the basement granites (Barnard, 2000).

### 3.7. Topography and Drainage in UCRB

The digital elevation map (Figure 4), suggests that the catchment has a decreasing elevation from South to North, with the upstream areas having an elevation of 1626–1660 metres above sea level, and downstream regions with an approximate elevation of 1163–1199 metres above sea level. The catchment area is drained by the Crocodile River with an overall flow direction from southwest to the North, draining into the Hartbeespoort Dam impoundment.

The catchment area is fed by the Crocodile River, which is supplied by subsidiary tributaries including the Hennops River in the Eastern part of the catchment area. On the West of the catchment, the Jukskei River, the Rietspruit River and Magaliesburg River feed into the Crocodile River. The rivers are perennial, with their recharge sustained by a combination of runoff, baseflow and wastewater discharge.

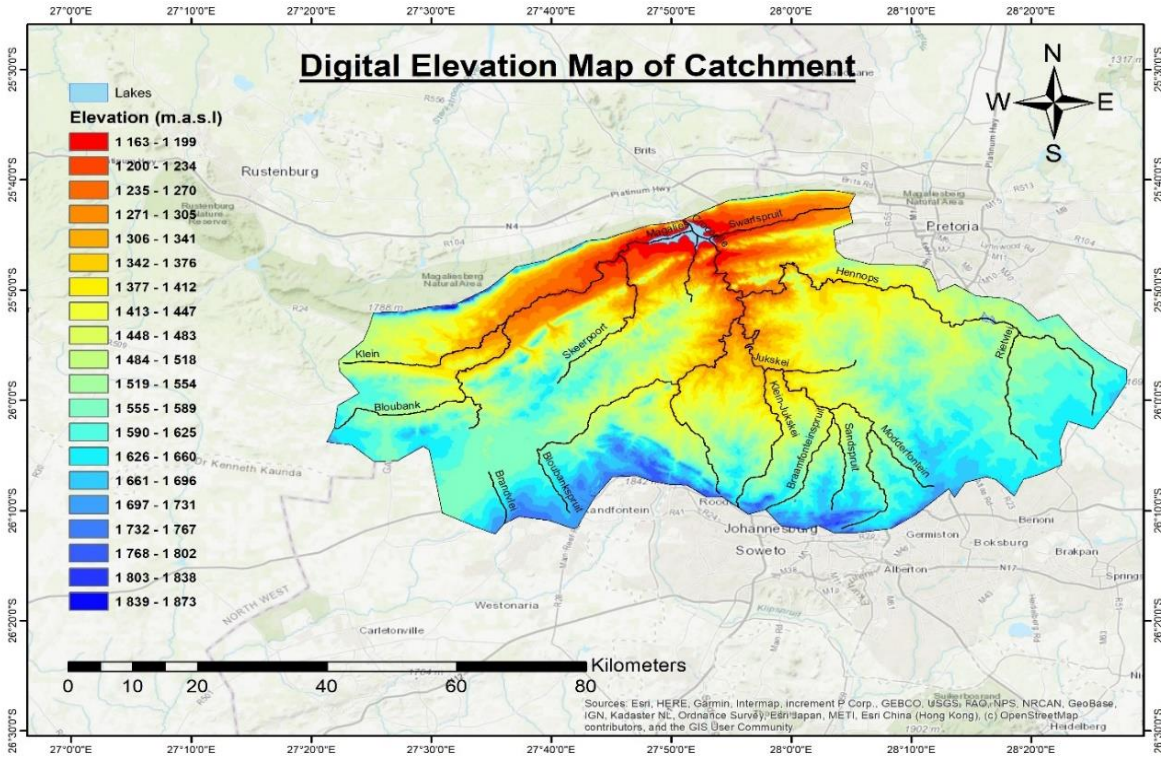



*Figure 4: UCRB mean changes above sea level (digital elevation)(USGS)*

The catchment is topographically characterised by large quartzite ridges in the Northern and Southern parts, while the low-lying areas are made up of dolomite and shale. The overall surface water drainage is South to North due to the general dip of the lithologies towards the North.

The water bodies of importance in the study include the Rietvlei Dam within the A21A quaternary catchment and the Hartbeespoort Dam in the A21H quaternary catchment. The Hartbeespoort Dam is the focus of the study as it is strongly affected by the recharge originating from industrial, mining and agricultural activities.

### 3.8. Climate Setting

The UCRB has been classified as a semi-arid environment. The contributing seasons of influence are the wet summer season (October and March) and the dry winter season (April and September), where limited rainfall occurs (DWAF 2004; DACE, 2004). The wet and dry seasons experienced across the Upper Crocodile River Basin are due to the Southern Hemisphere climate systems and the position of the Intertropical Convergence Zone (ITCZ). During summer, the ITCZ migrates southward which results in the generation of low-pressure cells that are commonly associated with localised thunderstorms and frontal rainfall over the interior (DWAF, 2004; DARD, 2011). During the winter months, air circulation is dominated by the Kalahari high-pressure cells. The subtropical high-pressure system is driven by the shift in the ITCZ position resulting in the movement of cold dry air across the interior from polar regions (DACE, 2004; Abiye, 2016). Figure 5 shows the mean annual monthly distribution of rainfall. Data has been extracted from CHIRPS, through interpolating the catchment boundary into the Google Earth Engine and then integrated into the climate engine and to the Google Earth Engine. The rainfall data were sourced from 1981 to 2020 by running the code. In Figure 5 we see the mean annual precipitation across the UCRB with a mean annual rainfall of 698.22mm.

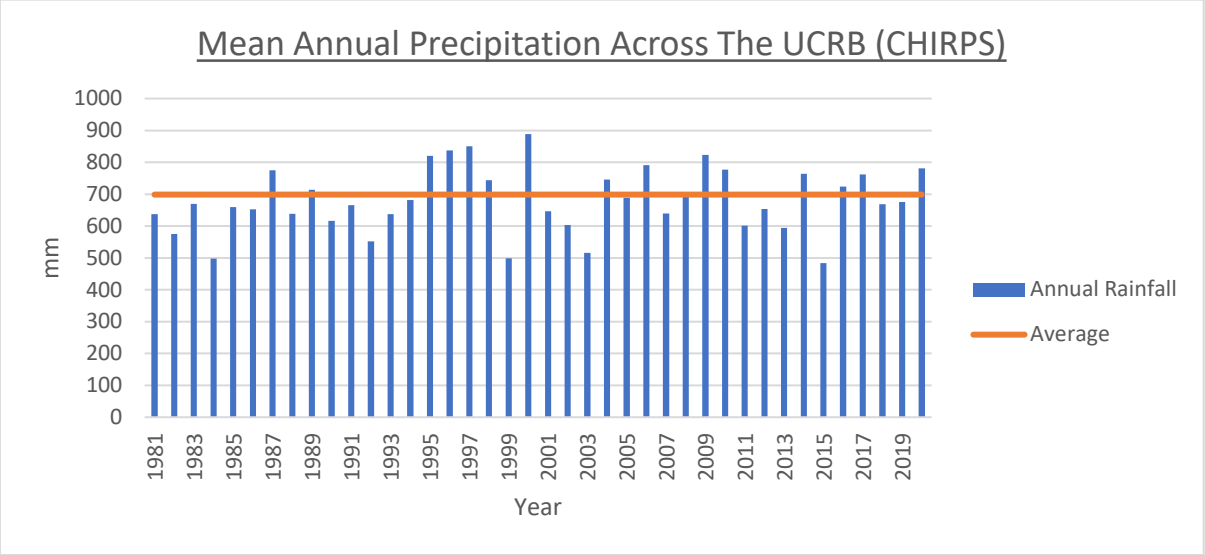



*Figure 5: CHIRPS, annual precipitation across four decades in the UCRB (CHIRPS)*

As per the Koppen Classification, the UCRB climate is characterised by hot summer and dry winter temperatures. In December and January, the UCRB experiences its highest temperatures, while the coldest temperatures are observed during July (Figure 6). The mean annual temperature is calculated to be around 19.2˚C.

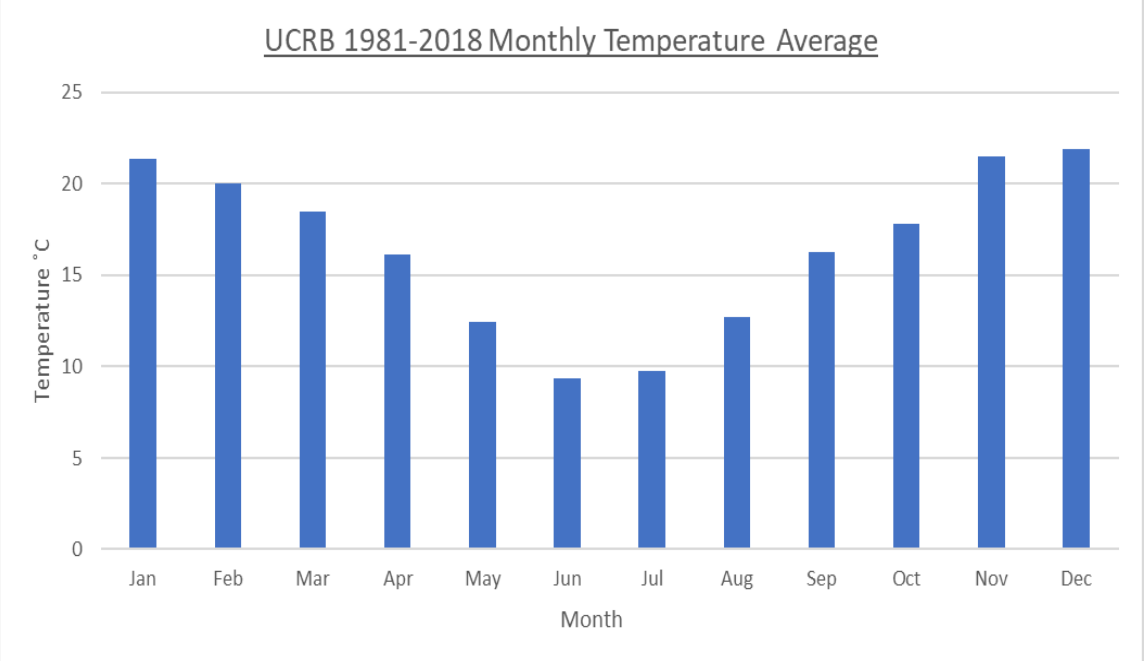



*Figure 6: Mean temperature from 1981–2018 in the UCRB(NASA/POWER CERES/MERRA2)*

The Oceanic “Temperature” Index is an indicator for monitoring the El Nino and La Nina phenomena This illustrates the periods of extensive precipitation (La Nina) and periods of drought (El Nino) represented in Figure 7.

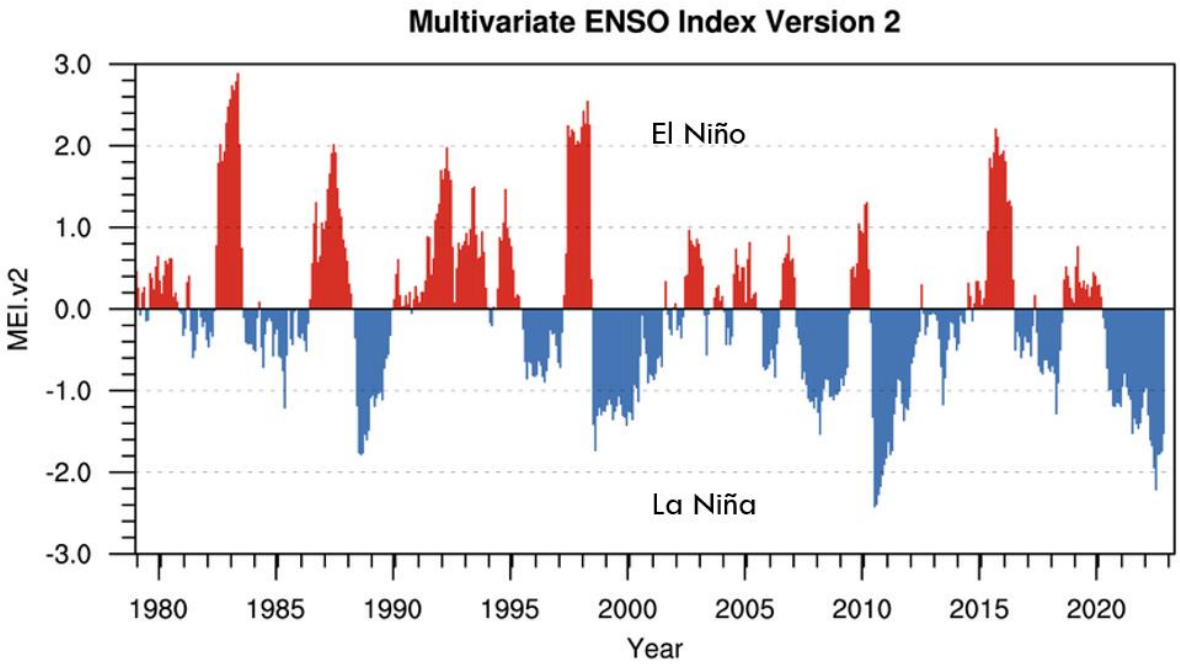



*Figure 7: Multivariate ENSO Index Version 2 indicating El Nino and La Nina events from 1980-2020 (https://climatedataguide.ucar.edu/climate-data/southern-oscillation-indices-signal-noise-and-tahitidarwin-slp-soi)*

### 3.9. Land Use and Land Cover

Land use and land cover are important in understanding the surface biophysical environmental controls on the surface water resources in the UCRB (Figure 8). Vegetation primarily controls the hydrology, ecosystems and physical environment. The southern area of the catchment’s dominant land use controls includes urbanisation, agriculture, industrial and mining activities. The agricultural practices in the UCRB are primarily mixed, and irrigation farming (largely dependent on groundwater), further cash crops, formal irrigation, game farming and livestock farming are common in the area. Within the southeast end of the Magaliesburg catchment is bushveld vegetation typical of a semi-arid environment. The UCRB is inherent to grassland (veld), proteas, and acacias.

Mining activities include small open-cast stone mining, platinum and chrome, with sand quarries located along river valleys.

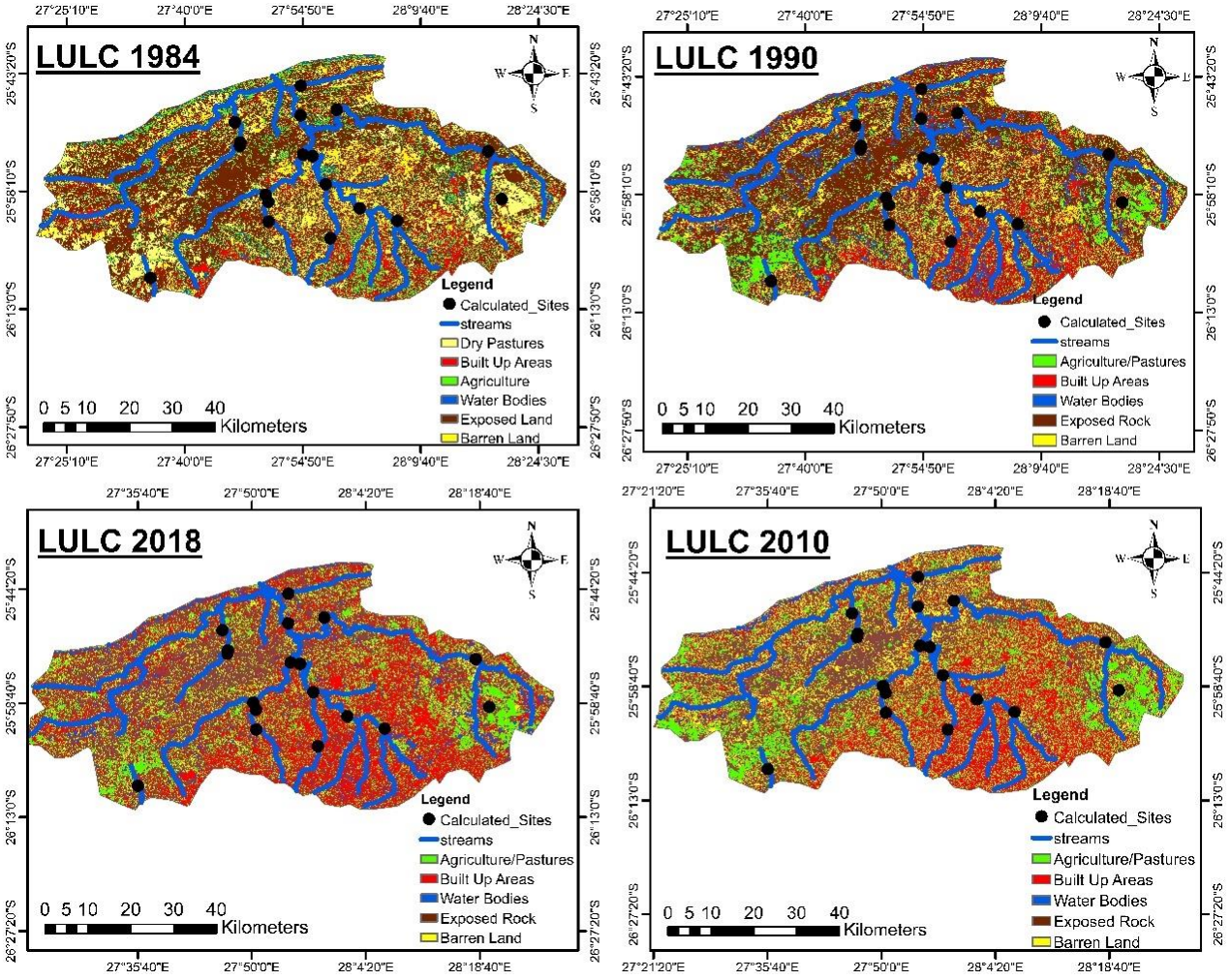



*Figure 8: Land use and land change of the UCRB*

## 4. METHODOLOGY

The estimation of nutrient and salinity loading which describes the complex and large UCRB catchment, required the collection and refinement of water chemistry and discharge data, which defines the physical characteristics of the basin. Water chemistry data and discharge data were gathered from the DWS; the data gathered was to be assessed for validity and errors, and subject to scrutiny to determine its suitability for nutrient and salinity loading description in the UCRB.

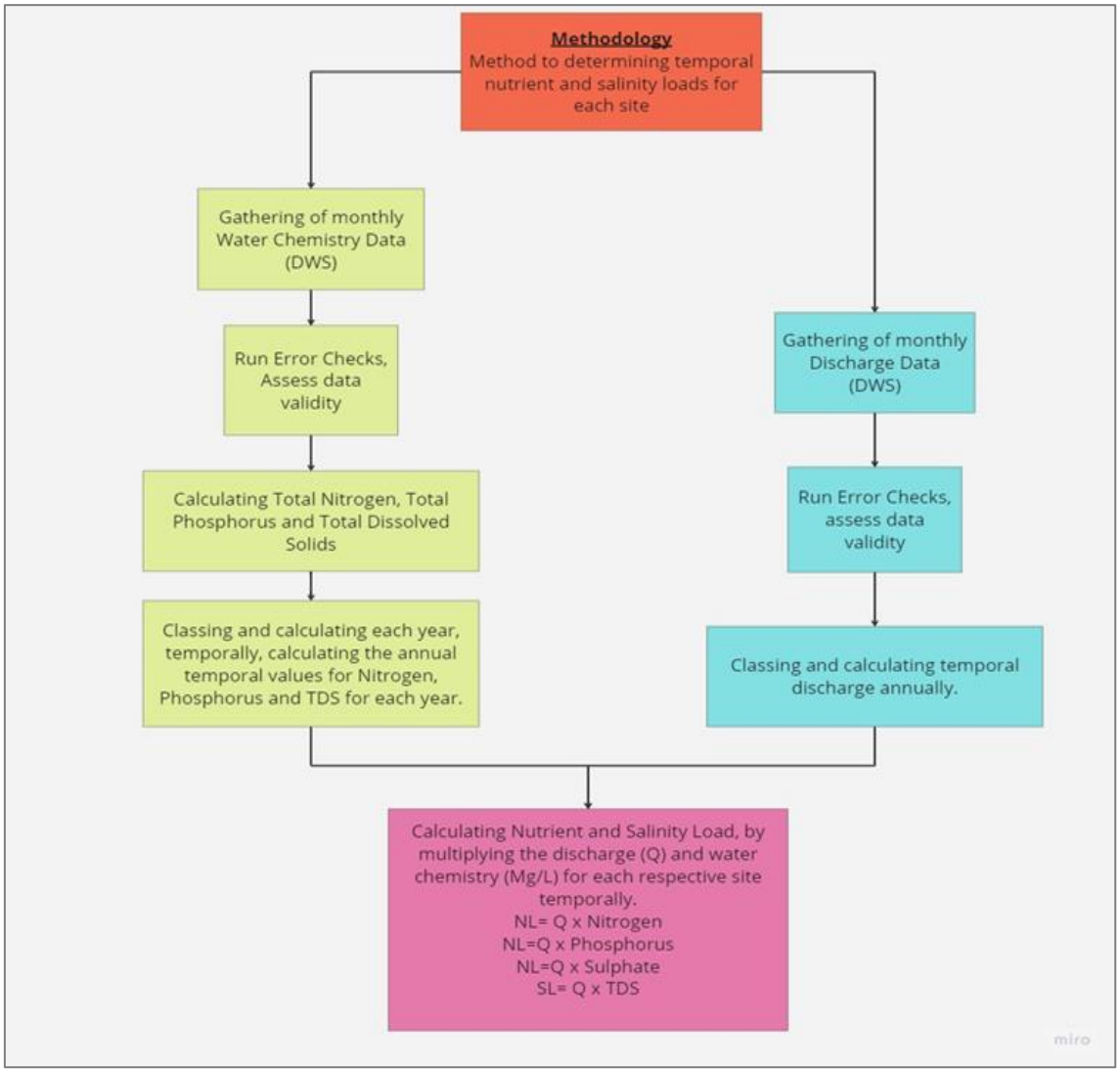



*Figure 9: Nutrient and salinity loading result methodology for each UCRB site*

For the temporal and spatial evaluation of the UCRB's nutrient and salinity loading changes, discharge and water chemistry data spanning Thirty-eight years

from 1980 were required. According to Pinckney et al. (2001), the discharge (Q), $m^3/s$ must be multiplied by its respective concentration (C), mg/L to obtain the nutrient load. To determine the spatial changes, Google Earth images, coupled with ArcGIS processing tools, were used to create land use change maps. The temporal/seasonal variations were calculated through Microsoft Excel and the use of data analytical tools. The sequence of data validation, processing, calculation and interpretation is represented in a flow chart (Figure 9).

## 4.1. Desktop Work

The desktop work involved a review of necessary research material applicable to the study, including the literature review on understanding nutrient and salinity loading, environmental impact and the influence of human activities and the driving factors controlling loading rates and processes, which could affect the rate of loading. This was done by evaluating other studies across the world.

## 4.2. Data Collection

Long-term discharge and water chemistry data (time-series data), were obtained from the DWS. Hydrometeorological data (CHIRPS), were obtained through the climate engine, using Google Earth. Geographical Information System (GIS), software included gathering shapefiles from the RQIS database of the Department of Water and Sanitation. Digital Elevation Maps (DEM.tif), were obtained from the USGS National Elevation Dataset and spatial data were obtained from Google Earth and then further processed.

## 4.3. Excel Work

### 4.3.1. Discharge Data Processing and Validation

Discharge data were obtained from the DWS for a list of sites in the catchment area. The collected data had eighteen sites with data spanning different monitoring periods as seen in Table 1.

*Table 1: Discharge data obtained from the DWS for 18 sites (each first and last data set measured)*

| ID | MONITORING POINT NAME | LATI TUDE | LONGITUDE | LOCATED ON TYPE | DRAINAGE REGION | FIRST DATE | LAST DATE |
|---|---|---|---|---|---|---|---|
| 90218 | A2H090Q01 HENNOPS RIVER AT V RIEBEECK NAT RES UP/S RIETVLEI | -25.88556 | 28.30278 | Rivers | A21A | 25 04 1986 | 20 08 2018 |
| 90161 | A2H008 ELANDSFONTEIN 412 JR ON ELANDSFONTEIN EYE | -25.98583 | 28.33111 | Spring/Eye | A21A | 29 01 1980 | 17 10 1998 |
| 90191 | A2H047 KLIPFONTEIN/RANDBURG ON KLEIN-JUKSKEIRIVIER | -26.06818 | 27.97203 | Rivers | A21C | 06 12 1971 | 05 06 2018 |
| 90187 | A2H042Q01 JUKSKEI RIVER AT LONE HILL | -26.00528 | 28.03333 | Rivers | A21C | 06 12 1971 | 13 10 1997 |
| 90186 | A2H040Q01 DWJ37 AT WATERVAL D/S R101 ON JUKSKEI | -26.03139 | 28.11222 | Rivers | A21C | 06 12 1971 | 21 08 2018 |
| 90169 | A2H023 NIETGEDACHT 535 JQ DWJ26 ON JUKSKEIRIVIER | -25.95466 | 27.96217 | Rivers | A21C | 02 05 1979 | 21 05 2018 |
| 90195 | A2H051 VAN WYKS RESTANT 182 IQ AT MULDERSDRIFT ON KROKODILRIVIER | -26.03311 | 27.84269 | Rivers | A21E | 02 05 1979 | 19 12 2016 |
| 90194 | A2H050Q01 ZWARTKOP 250 JQ HOI-HOI AT HOI-HOI ON CROCODILE RIVER | -25.99136 | 27.84208 | Rivers | A21E | 02 05 1979 | 21 05 2018 |

| ID | MONITORING POINT NAME | LATI TUDE | LONGI-TUDE | LOCATED ON TYPE | DRAINAGE REGION | FIRST DATE | LAST DATE |
|---|---|---|---|---|---|---|---|
| 90193 | A2H049 ZWARTKOP 525 JQ ON BLOUBANKSPRUIT / RIETSPRUIT | -25.97681 | 27.83644 | Rivers | A21E | 23 05 1979 | 21 05 2018 |
| 90171 | A2H024 BRANDVLEI 261 IQ ON BRANDVLEIRIVIER | -26.15119 | 27.59486 | Rivers | A21F | 09 02 1978 | 30 04 2018 |
| 90181 | A2H035Q01 SKEERPOORT RIVER AT HARTBEESHOEK | -25.8675 | 27.78333 | Rivers | A21G | 03 02 1980 | 29 01 1999 |
| 90180 | A2H034 SCHEERPOORT 477 JO ON SKEERPOORTRIVIER | -25.82483 | 27.77175 | Rivers | A21G | 21 01 1976 | 23 05 2018 |
| 90179 | A2H033Q01 NOUKLIP EYE AT HARTBEESHOEK | -25.87444 | 27.78222 | Spring/Eye | A21G | 03 03 1980 | 29 05 2018 |
| 90202 | A2H058 IFAFA 457 JQ AT RIETFONTEIN / SYFERFONTEIN ON SWARTSPRUIT | -25.74819 | 27.90986 | Rivers | A21H | 08 09 1982 | 29 05 2018 |
| 90190 | A2H045 VLAKFONTEIN 494 JQ DWJ31 ON CROCODILE RIVER | -25.89264 | 27.91437 | Rivers | A21H | 02 05 1979 | 23 05 2018 |
| 90189 | A2H044 VLAKFONTEIN 494 JQ ON JUKSKEIRIVIER | -25.8955 | 27.93481 | Rivers | A21H | 06 12 1971 | 21 05 2018 |
| 90164 | A2H012Q01 KALKHEUWEL 493 JQ ON CROCODILE RIVER | -25.81048 | 27.90955 | Rivers | A21H | 04 07 1971 | 12 07 2018 |
| 90166 | A2H014 SCHURVEBERG 488 JQ AT SKURWEBERG ON HENNOPSRIVIER | -25.79842 | 27.98533 | Rivers | A21H | 27 01 1976 | 08 05 2018 |

Discharge data were gathered and first evaluated for any errors and subject to scrutiny for use, and then considered for the study. The data were recorded in $m^3/s$ for every month, and these monthly data were then paired with the corresponding season of winter, months from April to September and summer, months from October to March. This was done for each month for every year for the period of the annual measurement. The discharge data were then averaged using a pivot table for every season for each year across its monitoring period.

### 4.3.2. Water Chemistry Data Processing and Validation

Water chemistry data were obtained for eighteen sites across the UCRB through the Department of Water and Sanitation (Figure 9). Like the discharge data, the data were error-checked and scrutinised before processing. The data gathered for processing were reported daily for major ions, *calcium, chloride, fluoride, potassium, magnesium, ammonium* as N, *nitrate and nitrite, sodium, phosphate as* P, *sulphate and silicon*. The major cations and anions were labelled as dissolved concentrations measured in mg/l. Physicochemical parameters such as pH, electrical conductivity, total hardness and total alkalinity are included in the reported water chemistry data for each site. Total nitrogen was calculated from $NO_3$-N for each site using a conversion factor of mg/l x 4.4268. Total phosphorus was calculated from $PO_4$-P using a quotient factor of 1/3.07 against phosphate to represent total phosphorus. Each daily data measurement was changed to a monthly conversion and paired with its corresponding season. Using a pivot table, data were averaged for each season (summer and winter), for the respective measuring period; the wet summer season (October–March), and the dry winter months (April–September). This resulted in an annual seasonal average.

### 4.3.3. Total Dissolved Solids Calculation

The TDS was calculated by summing all the major cations and anions in the water chemistry data; this was done using the following formula as per (McCleskey et al., 2023):

$$TDS = \sum Cations + \sum Anions + \sum Non\ charged$$

(McCleskey et al., 2023)

TDS is used as a salinity indicator for studies in surface water by summing all speciated ion concentrations (McCleskey et al., 2023). The calculation was completed using Excel *=SUM(Mg+Na+Ca+$NH_4$+K+Cl+F+N+P+$SO_4$+$CaCO_3$)*, and was completed for every daily measurement and for every site in the basin. The daily data were converted to monthly data, which were coupled with the respective seasons for each measurement. At that point, the TDS data were averaged using a pivot table to determine the annual seasonal average for the period of measurement (Table 1).

### 4.3.4. Nutrient and Salinity Loading Determination

To calculate the nutrient and salinity load, the discharge data were grouped according to the season for every year (as previously explained) and then matched with their respective processed annual seasonal average water chemistry data. The discharge (Q), data were multiplied with the water chemistry (Mg/L), data to calculate the overall load. The nutrient load was calculated for sulphate, nitrogen and phosphorus. This was done using the equation:

$$Nutrient\ Loading = Concentration\left(\frac{mg}{L}\right) \times Discharge(Q)\left(\frac{m^3}{s}\right)$$

$$\therefore Nutrient\ Loading = \left(\frac{mg}{L}\right) \times \left(\frac{1000L}{s}\right)$$

$$\therefore Nutrient\ Loading = \frac{g}{s}$$

$$Nutrient\ Loading = \frac{g}{s} \times \frac{3600s}{1hr}$$

$$\therefore Nutrient\ Loading = g/hr$$

$$Nutrient\ Loading = (g/hr)/1000$$

$$\therefore Nutrient\ Loading = kg/hr$$

(Pinckney et al., 2001)

The salinity load was calculated from TDS using the equation:

$$Salinity\ Loading = TDS\left(\frac{mg}{L}\right) \times Discharge(Q)\ (\frac{m^3}{s})$$

$$\therefore Salinity\ Loading = \left(\frac{mg}{L}\right) \times \left(\frac{m^3}{s}\right)$$

$$\therefore Salintiy\ Loading = \left(\frac{mg}{L}\right) \times \left(1000\frac{L}{s}\right)$$

(Venkatesan et al., 2011)

$$\therefore Salinity\ Loading = \left(\frac{g}{s}\right)$$

$$Salinity\ Loading = \frac{g}{s} \times \frac{3600s}{1hr}$$

$$\therefore Salinity\ Loading = g/hr$$

$$Salinity\ Loading = \frac{\frac{g}{hr}}{1000}$$

$$\therefore Salintiy\ Loading = kg/hr$$

The calculation was used for each of the eighteen sites in the basin. The discharge was multiplied by the concentration of total nitrogen, phosphorus and sulphate in the basin and the TDS. The resulting nutrient and salinity load data were then added to the pivot table, and a range criterion was set out to analyse the data on a five-year interval period i.e., 1980–1985, 1986–1990, 1991–1995, 1996–2000, 2001–2005, 2006–2010, 2011–2015, 2016–2018 (three years); due to the COVID-19 pandemic, there were no available data for 2019 and 2020. This range would allow for more accurate interpretation, smoothing episodic and cyclic climatic variations that could otherwise skew the interpretations (Pinckney et al., 2001).

### 4.3.5. Nutrient and Salinity Loading Basin Calculation

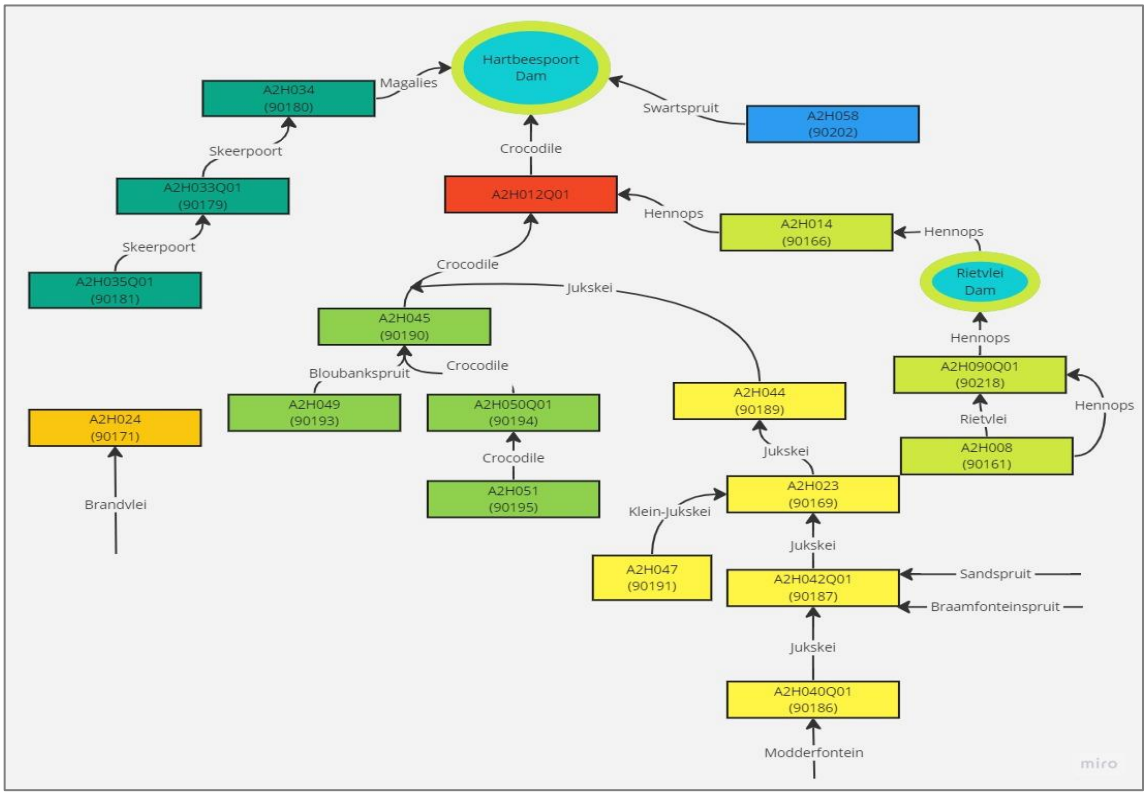



*Figure 10: UCRB nutrient and salinity summation order*

The net nutrient and salinity loading was determined using the results of the nutrient and salinity load calculated for each site, compiled in order, from upstream to downstream (Figure 9). Data were then summated based on the streams that flow into one another as determined using a stream order map, derived using GIS processing tools (Figure 10).

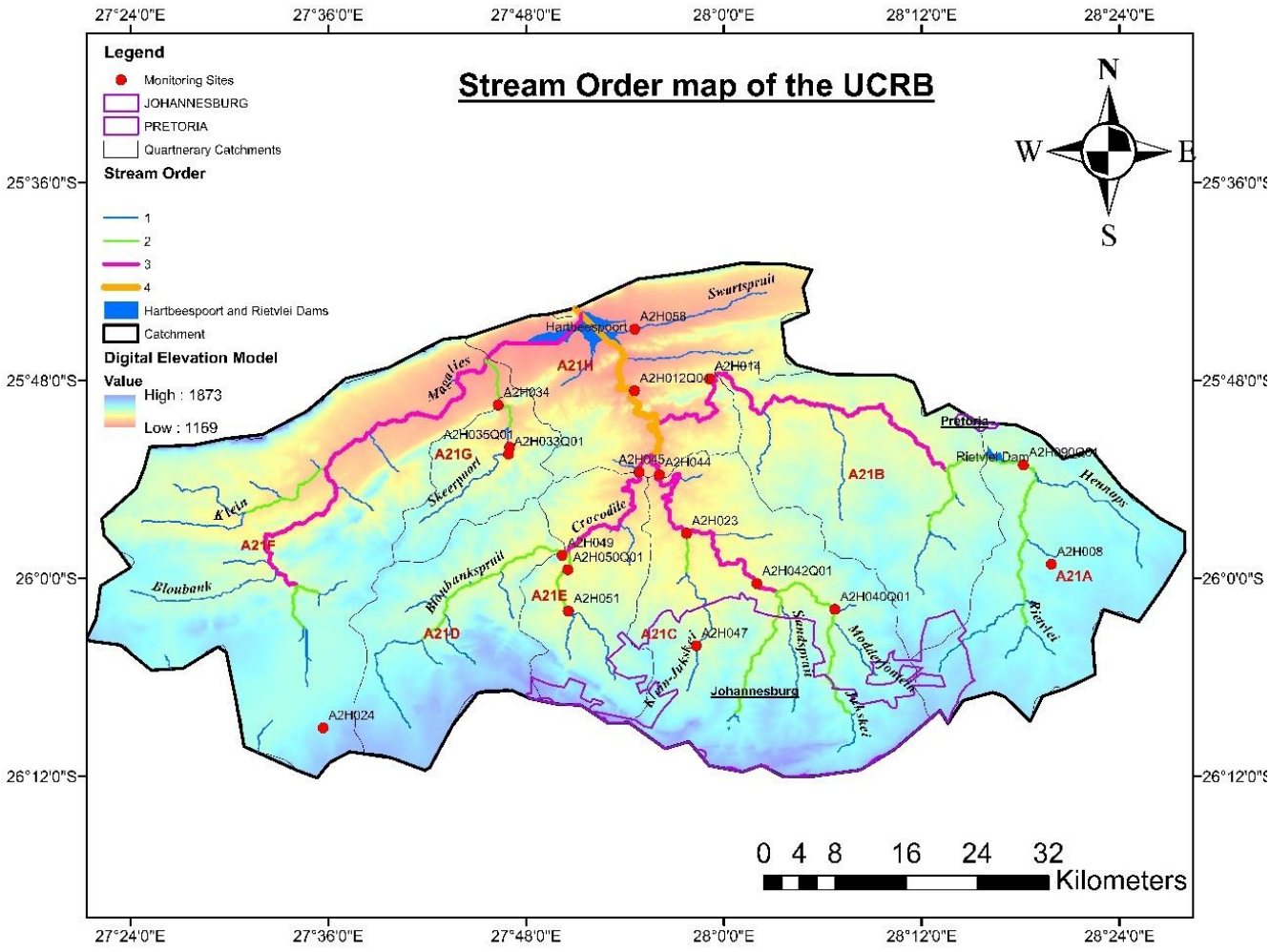



*Figure 11: The stream network and stream order of the UCRB*

The nutrient and salinity load for sulphate, nitrogen, phosphorus and TDS for each site along each stream were summed up from upstream to downstream direction (Figure 11). The data for the Hennops River, the Skeerpoort River, the Jukskei River and the Crocodile River were added to get net nutrient and salinity loading results, prior to their entry into the Hartbeespoort Dam. This was temporally evaluated for the years 1980–2020, and the nutrient and salinity loading evaluated summation plan was determined using a stream order map (Figure 11). The nutrient and salinity load improved with increasing stream orders. This required a dilution factor to be calculated as concentration decreased downstream while volume increased downstream towards the Hartbeespoort Dam; the dilution factor was determined by dividing the final volume by the initial

volume for each site. The initial volume was taken as 1980 and the final volume as 2018, and a dilution factor was determined for all rivers as DF= $C_f/C_i = V_f/V_i$ where C is concentration and V is a volume (Colman et al., 2016). The rivers' dilution factors were determined to be 1:2.56 for the Hennops River, 1:2.22 for the Jukskei River, 1:4.38 for the Crocodile River and 1:0.785 for the Skeerpoort River. For site A2H012Q01, an average was taken of all the major rivers feeding into the Hartbeespoort Dam from the South, which came to 1:3.05. The ratios were then used by dividing the nutrient and salinity loading results by the ratio to account for dilution.

As seen by the colour schemes in Figure 10, light green represents the Hennops River, with three sites, which were added in the following order: A2H008→A2H090Q01→A2H014. The river network consists of the Rietvlei River and the Hennops River that feed into A2H090Q01. The yellow scheme denotes the Jukskei River network which comprises the Modderfontein River which feeds into monitoring point A2H040Q01 into the Jukskei River. The Braamfonteinspruit, the Sandspruit and the Jukskei River join at site A2H042Q01. A net nutrient load was calculated at A2H023, which is where all the river networks merge into the Jukskei River – with a stream order of three (Figure 11). A2H047 is a monitoring point along the Klein Jukskei River which feeds into A2H023. The Jukskei River network is further evaluated at A2H044, the last monitoring point before it merges with the Crocodile River, depicted in dark green. To determine the Crocodile River nutrient and salinity loads (represented in dark green) sites which were calculated using summation as follows: A2H051→A2H050Q01→A2H045. A2H045 is a monitoring point where two river networks intersect, the Bloubankspruit and the Crocodile River seen with a stream order three. The Jukskei River (shown in yellow), the Hennops River (shown in light green) and the Crocodile River (shown in dark green), all meet at A2H012Q01, which then forms part of the greater Crocodile River which enters the Hartbeespoort Dam; this monitoring represents the highest stream order of four. The Skeerpoort River (turquoise), is monitored and added in the following order A2H035Q01-A2H033Q01-A2H034, feeds into the Magalies River and the Hartbeespoort Dam. A2H058 (blue scheme), is the only monitoring site along the Swartspruit River which enters the Hartbeespoort

Dam. A2H024 as seen in Figure 10, forms part of the Brandvlei River network but does not form part of a larger river network, and therefore the nutrient and salinity load is calculated as an individual monitoring point.

## 5. RESULTS

### 5.1. Hennops River Nutrient and Salinity Loading

The Hennops River nutrient and salinity load was determined using three gauging stations, A2H008; A2H090Q01 located before the Rietvlei Dam and A2H014, which is the northernmost gauging station along the Hennops River. The river falls in the A21A and A21B quaternary catchments as seen in Figure 12.

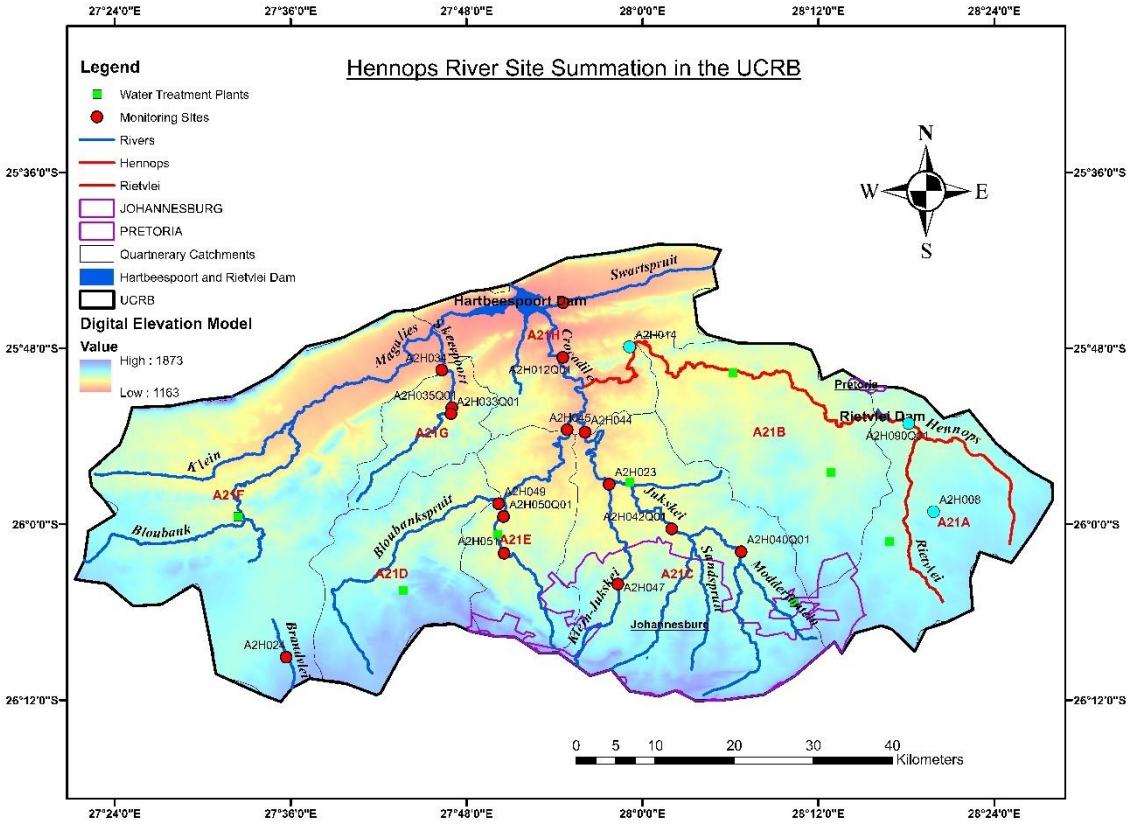



*Figure 12: Hennops River gauging station summation*
*(including quaternary catchments, sites and water treatment plants)*

The results represented show the Rietvlei and Hennops River networks. The spatial controls around the gauging stations are predominantly agricultural, urban and industrial activities. These result in strong leaching and seepage of N- and

S-rich effluent discharge entering from the southeast of the study area. Abandoned mines and landfill sites located southeast of the study area contribute significantly to high sulphate loads entering the Hennops River and Rietvlei River system (Figure 13).

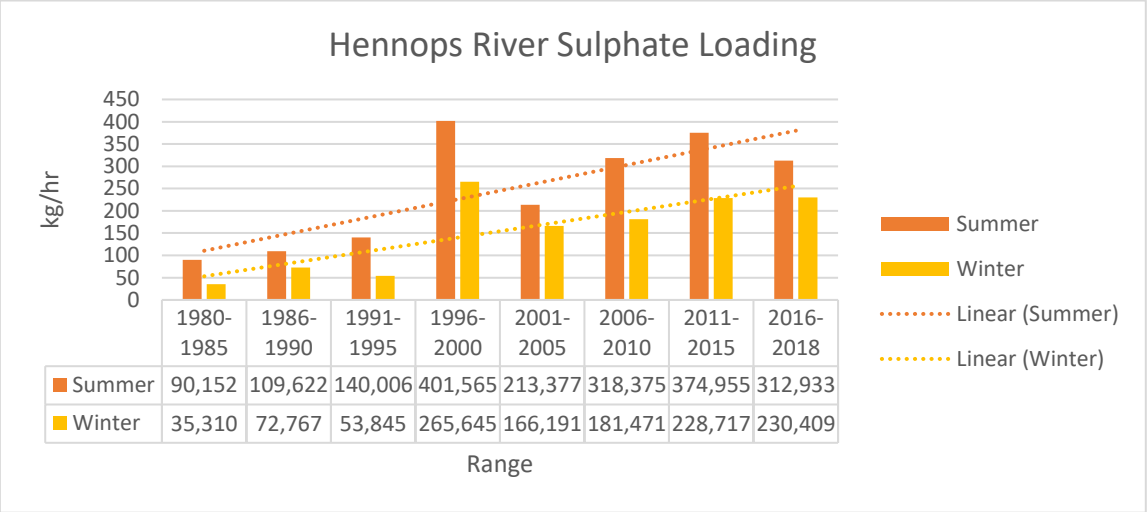
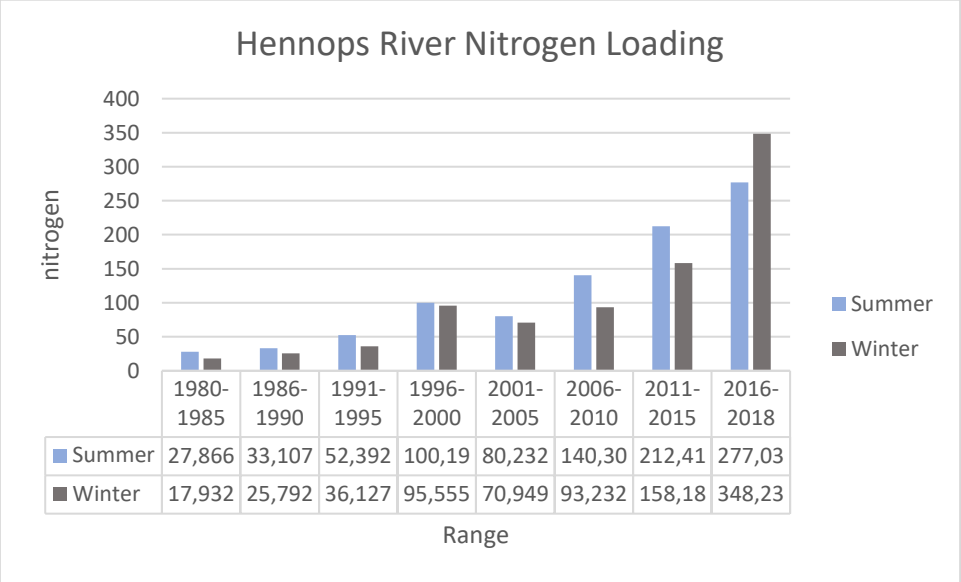



*Figure 13: Hennops River temporal sulphate load spanning 38 years*

In Figure 13, the seasonal and temporal sulphate load of the Hennops River was determined. The results show an increasing trend towards the latter years, for the summer and winter months. During the 1980–1985 period, the sulphate load in summer was higher than the winter sulphate load at 90.152 kg/hr and winter 35.310 kg/hr respectively. The sulphate load increased in winter and summer months for the period 1986–1990 with results of 109.622 kg/hr and 72.767 kg/hr. From 1991 to 1995, the summer sulphate load increased further to 140.006 kg/hr and the winter load dropped to 53.845 kg/hr. From 1996 to 2000, the overall sulphate load peaked at 401.565 kg/hr and the winter load of 265.645 kg/hr was the highest in the basin across the thirty-eight years of the evaluation. A steady decline followed into the 2001–2005 period, with almost half of the sulphate loading rate in summer at 213.377 kg/hr and the winter rate at 166.191 kg/hr. An increase was seen in the 2006–2010 period with rates of 318.375 kg/hr for summer and 181.471 kg/hr for winter. A further increase occurs through the 2011–2015 period in summer and winter loading rates at 374.955 kg/hr and 228.717 kg/hr respectively. A gentle decrease in sulphate load is seen during the

2016–2018 period with summer loading rates of 312.933 kg/hr and winter rates of 230.409 kg/hr. This is a result of leakage, seepage and runoff from mining activities, tailings storage facilities and landfill sites into the Hennops River.

Nitrogen loading rates in the Hennops River (Figure 14), showed an increase in winter and summer loadings from 1980 to 2018.



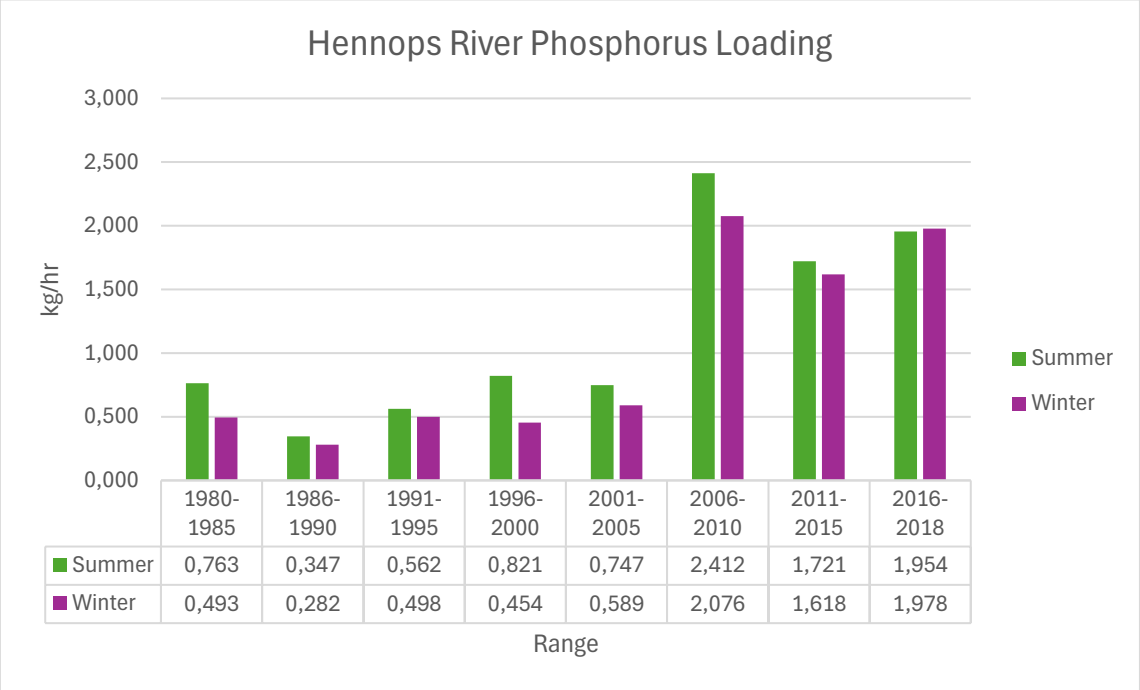

| | 1980-1985 | 1986-1990 | 1991-1995 | 1996-2000 | 2001-2005 | 2006-2010 | 2011-2015 | 2016-2018 |
|---|---|---|---|---|---|---|---|---|
| Summer | 27,866 | 33,107 | 52,392 | 100,19 | 80,232 | 140,30 | 212,41 | 277,03 |
| Winter | 17,932 | 25,792 | 36,127 | 95,555 | 70,949 | 93,232 | 158,18 | 348,23 |

*Figure 14: Hennops River temporal nitrogen load spanning 38 years*

During the 1980–1985 period, nitrogen loading rates of 27.866 kg/hr in summer and 17.932 kg/ hr in winter were determined. The overall summer and winter loading rates increased during the 1986–1990 period with a summer nitrogen loading rate of 33.107 kg/hr and a winter loading rate of 25.792 kg/hr. The nitrogen loading rate followed a gradual increase into the 1991–1995 period, with calculated values of 52.392 kg/hr for summer and 36.127 kg/hr for winter. Across the two decades, high loading was observed during 1996–2000 period with summer rates of 100.19 kg/hr and winter rates of 95.555 kg/hr, which could be attributed to the La Niña event, which occurred during 1999. Following El Niño in 2002, the loading rate lowered to 80.232 kg/hr in summer and winter to 70.949 kg/hr due to drought experienced across the area. The nitrogen loading rate thereafter increased successively throughout 2006–2018, reaching a high throughout 2016–2018 period at 277.03 kg/hr in summer and winter at 348.23

kg/hr. With time, the increase in nitrogen loading rates is a result of greater discharge due to water demand increases and supply by the WMA (Department of Water Affairs and Forestry 2008a). Nitrogen levels are consistently increasing as human activities increase, and the overall discharge has driven up the volume as seen through the *Land Use-Land Cover* maps from 1990 to 018. Agricultural runoff from manure and fertiliser is directly attributed to increased summer and overall nitrogen loading rates due to land use changes. Unaccounted sewage spills in and around the Johannesburg region have been observed, contributing to an increase in the nitrogen content in the Hennops River and inducing large degradation in water quality.

Phosphorus loading was determined and is represented in Figure 15 for summer and winter. Both of the seasons' loading rates increased over the thirty-eight years.



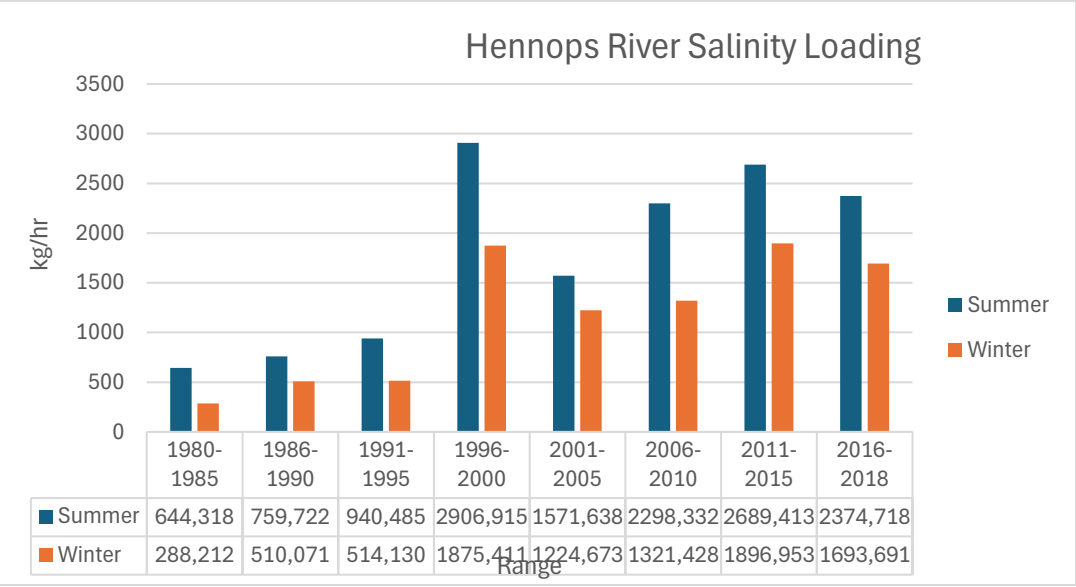

| | 1980-1985 | 1986-1990 | 1991-1995 | 1996-2000 | 2001-2005 | 2006-2010 | 2011-2015 | 2016-2018 |
|---|---|---|---|---|---|---|---|---|
| Summer | 0,763 | 0,347 | 0,562 | 0,821 | 0,747 | 2,412 | 1,721 | 1,954 |
| Winter | 0,493 | 0,282 | 0,498 | 0,454 | 0,589 | 2,076 | 1,618 | 1,978 |

*Figure 15: Hennops River temporal phosphorus load spanning 38 years*

Phosphorus loading rates were drastically lower than nitrogen and sulphate loading rates for both seasons. The reduced loading rate indicated a lower discharge of phosphorus entering from the river network in the UCRB (even

though phosphorus-containing fertilisers are often used in the agricultural sector). The summer phosphorus loading rates were consistently higher than those of winter loading rates due to the runoff into the river network when summer rainfall occurs. The phosphorus load during the summer of 1980–1985 was the highest rate until 1995 at a rate of 0.763 kg/hr. In the 1991–1995 period, the loading of total phosphorus was reduced as a result of El Niño in 1992, bringing dry conditions across the interior and reducing precipitation, which is the primary discharge mechanism (Ali et al., 2022). During the 1996–2000 period, the overall summer loading rate increased to 0.821 kg/hr due to the La Niña, which had occurred over 1998–1999 period. After the period from 2001 to 2005 phosphorus loading rates increased exponentially, reaching their peak in the 2006–2010 period at 2.412 kg/hr, because of the La Niña phenomenon driving up precipitation rates during 2008. Phosphorus loading rates consistently stayed high thereafter due to an increased discharge rate and effluent discharge attributed to the increased anthropogenic influence in the UCRB with amplified urbanisation and fertiliser from agricultural runoff (Huizenga and Harmse, 2005).

In Figure 16 the Hennops River salinity loading rate was determined, and the results are representative of a gradual increase in overall salinity in the winter and summer months through the thirty-eight years.




| | 1980-1985 | 1986-1990 | 1991-1995 | 1996-2000 | 2001-2005 | 2006-2010 | 2011-2015 | 2016-2018 |
|---|---|---|---|---|---|---|---|---|
| Summer | 644,318 | 759,722 | 940,485 | 2906,915 | 1571,638 | 2298,332 | 2689,413 | 2374,718 |
| Winter | 288,212 | 510,071 | 514,130 | 1875,411 | 1224,673 | 1321,428 | 1896,953 | 1693,691 |

*Figure 16: Hennops River temporal salinity load spanning 38 years*

During the 1980–1985 period, the salinity load in summer was high at a rate of 644.318 kg/hr compared to 288.212 kg/hr in winter. A gradual increase in the overall rate followed through 1986–1990 period with a loading rate of 759.722 kg/hr in summer and 510.071 kg/hr in winter. The salinity rate further increased through 1991–1995 period with salinity loading rates of 940.485 kg/hr in summer and 514.130 kg/hr in winter. The salinity loading rate peaked during the 1996–2000 period at 2906.915 kg/hr in summer and 1875.411 kg/hr in winter. During the 2001–2005 period, a steady decline in summer (1571.638 kg/hr) and winter salinity rates (1224.673 kg/hr) were determined with the winter rate set at the lowest through the second decade. The 2006–2010 period was met with an overall increase in summer and winter salinity rates, determined at 2298.332 kg/hr and 1321.428 kg/hr respectively. A gentle increase in rate was seen through the 2011–2015 period, with a summer value of 2689.413 kg/hr and 1896.953 kg/hr in winter. A moderate decrease was followed through 2016–2018 period at 2374.718 kg/hr in summer and a winter rate of 1693.691 kg/hr.

The salinity load along the Hennops River during the summer season was consistently higher than in the winter season. The peak salinity load was observed in the 1996–2000 period with a summer and winter loading rate of 2906.915 kg/hr and 1875.411 kg/hr, respectively. Throughout 1980–1995 salinity loading rates remained relatively low. During the 1996–2000 period, salinity loading levels peaked, this is strongly attributed to a rise in overall chloride levels as observed in the water chemistry data. The chloride levels rose rapidly which could be attributed to wastewater from backwash of water softeners and swimming pools, discharge from dishwashers and disposal of untreated or partially-treated municipal wastewater, causing an increase in overall TDS values. Salinity loading rates consistently increased throughout the 2006–2018 period with a rise in winter and summer loading rates. The salinity loading rate could be exacerbated by increased evaporation due to temperature increases with time (Venkatesan et al., 2011).

The rapid rise in overall salinity loading rates was attributed to the overall urban expansion throughout the UCRB, compounded by agricultural runoff, partially

untreated wastewater and higher wastewater discharges. This caused an increase in the overall TDS values in the UCRB, supplemented with increased discharge causing an increase in overall salinity loading with time.

### 5.2. Jukskei River Nutrient and Salinity Loading

The Jukskei River has the largest river network in the basin, made up of the Klein-Jukskei River, the Modderfontein River, the Sandspruit River and the Braamfontein Spruit which flow from South to North. The subsidiary rivers that feed into the Jukskei River carry a large nutrient load (primarily from urban discharge from the city of Johannesburg). Urban expansion has been on the rise, resulting in increased nonpoint sources and then in boosted nutrients, and an amplified effluent discharge. The Jukskei River's nutrient and salinity loading rates were estimated using five gauging stations along the river, A2H047, A2H040Q01 A2H042Q01 A2H023 and A2H044, seen in Figure 17. The Jukskei River, as previously indicated in Figure 11, falls under stream order three and this postulates a high overall nutrient and salinity loading rate due to the discharge, and the drainage network feeding into the Jukskei River.

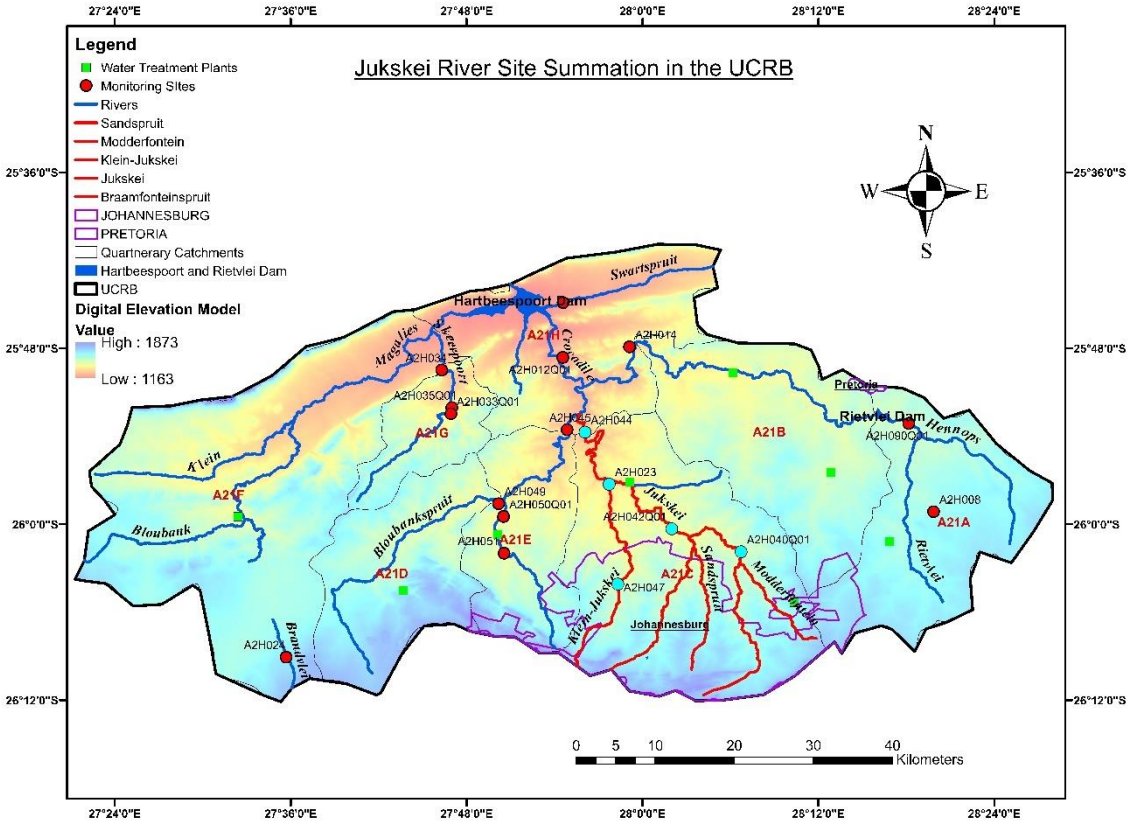
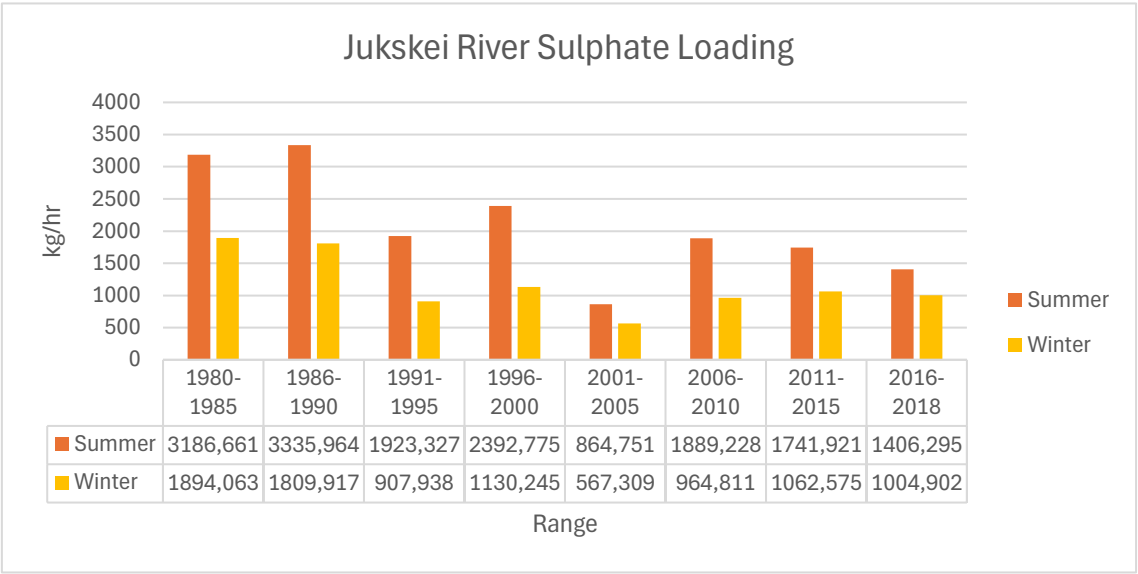



*Figure 17: Jukskei River gauging station summation*
*(including quaternary catchments, sites and water treatment plants)*




| | 1980-1985 | 1986-1990 | 1991-1995 | 1996-2000 | 2001-2005 | 2006-2010 | 2011-2015 | 2016-2018 |
|---|---|---|---|---|---|---|---|---|
| Summer | 3186,661 | 3335,964 | 1923,327 | 2392,775 | 864,751 | 1889,228 | 1741,921 | 1406,295 |
| Winter | 1894,063 | 1809,917 | 907,938 | 1130,245 | 567,309 | 964,811 | 1062,575 | 1004,902 |

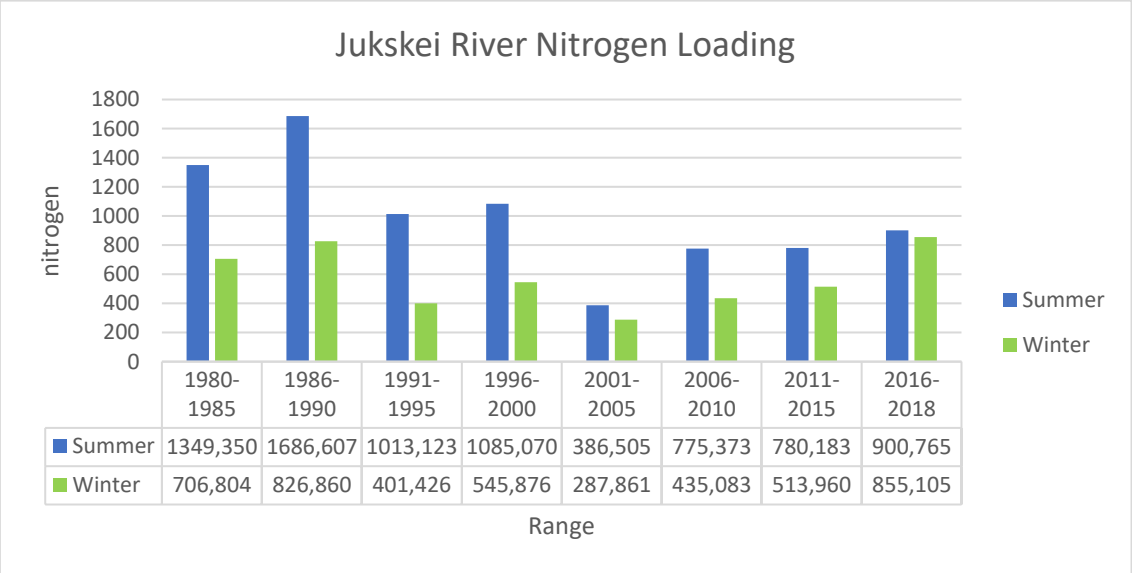
*Figure 18: Jukskei River temporal sulphate load spanning 38 years*

Sulphate loading determined for the Jukskei River is represented in Figure 18, the summer and winter loading rates along the Jukskei River showed a general decline in overall sulphate loading rate with time.

From 1980 to 1985, the sulphate seasonal loading rates were estimated at 3186.661 kg/hr in summer and peak winter sulphate loads for the period of evaluation at 1894.063 kg/hr. The loading rate was considerably higher than that of the Hennops River which was attributed to the discharge volume feeding into the river network from the city of Johannesburg. Sulphate loads were considerably high due to the abandonment of old mines, continued mining and landfill site leaching; they are located South of the study area contributing to the overall high sulphate loads seen in the Jukskei River (Huizenga and Harmse, 2005). Converse to the rising rates of sulphate throughout time in the Hennops River, a declining trend in terms of winter and summer loads was observed, although the loading rates were much higher, posing a threat to overall water quality in the area. The decline in general sulphate loading could be due to the presence of two wastewater treatment works along the Jukskei River, resulting in an overall decrease in loading rates with time (Figure 17). During the 1986–1990 period, a peak summer sulphate loading rate was observed at 3335.964 kg/hr with a peak winter loading rate during the 1980–1985 period at 1894.063 kg/hr. The overall high loading rate was attributed to the average rainfall amount of 698 mm which occurred during 1984–1985, which spiked discharge levels and prompted loading rates to be high. An overall increase in sulphate loading was observed in the 1996–2000 period, which was directly attributed to the 1999–2000 La Niña occurrence (as previously noted in the Hennops River), and this resulted in a high summer sulphate loading rate of 2392.775 kg/hr moving to the North. A decline was observed in the 2001–2005 period due to heavy droughts experienced during 2002 due to El Niño, reducing the primary driver of increased discharge rates and precipitation (Ali et al., 2022). Following the lower rates in the 2001–2005 period, sulphate loading rates increased in the 2006–2010 period to 1889.228 kg/hr in summer and 964.811 kg/hr in winter respectively. During the years 2011–2015, the summer sulphate loading rate dropped to 1741.921 kg/hr and the winter rate rose to 1062.575 kg/hr. A decrease in summer and winter

loading rates was seen in the 2016–2018 period to 1406.295 kg/hr and 1004.902 kg/hr respectively. From 2011 to 2018, a decline in summer and winter sulphate loading rates was observed, attributed to improved management of the wastewater treatment works (Huizenga and Harmse, 2005). Summer sulphate loading rates were normally far higher than winter sulphate loading rates, directly attributed to summer precipitation and dry winters that follow; across the interior of South Africa in response to the shifting of the ITCZ (Abiye and Leketa, 2021).

Over time, nitrogen loading in the Jukskei River showed a general declining trend in seasonal nutrient loading rates (Figure 19).




| | 1980-1985 | 1986-1990 | 1991-1995 | 1996-2000 | 2001-2005 | 2006-2010 | 2011-2015 | 2016-2018 |
|---|---|---|---|---|---|---|---|---|
| Summer | 1349,350 | 1686,607 | 1013,123 | 1085,070 | 386,505 | 775,373 | 780,183 | 900,765 |
| Winter | 706,804 | 826,860 | 401,426 | 545,876 | 287,861 | 435,083 | 513,960 | 855,105 |

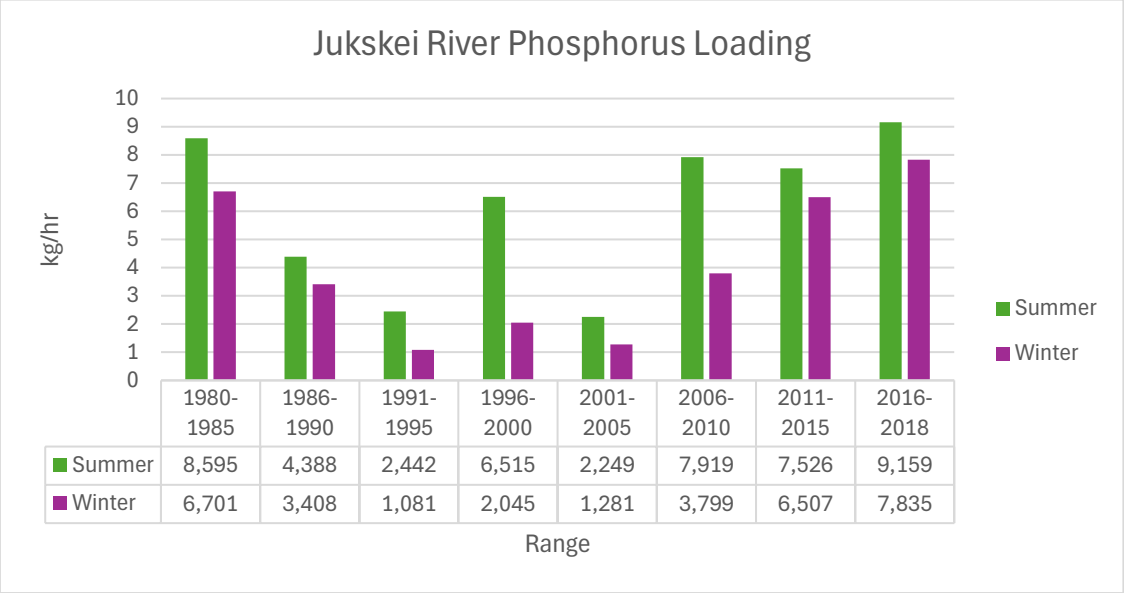
*Figure 19: Jukskei River temporal nitrogen load spanning 38 years*

From 1980 to 1985, the summer nitrogen loading rate was reported at 1349.350 kg/hr and the winter rate at 706.804 kg/hr. From 1986 to 1990, the peak nitrogen loading in the Jukskei River was noted at an overall rate of 1686.607 kg/hr in summer and 826.860 kg/hr in winter. From 1991 to1995, a general decline in both seasons' nutrient loading rates was reported at 1013.123 kg/hr in summer and 401.426 kg/hr in winter; this was due to El Niño which occurred during 1992, inducing drought and reducing overall discharge rates. An increase in 1996–2000 in the summer nitrogen loading rate was determined at 1085.070 kg/hr and in winter at 545.876 kg/hr. A drastic decrease was noted during the years from 2001 to 2005 in both seasons' nitrogen loading rates by more than half of the summer

and winter loading rates of 1996–2000 to 386.505 kg/hr and 287.861 kg/hr. A steady increase in summer and winter loading rates occurred during 2006–2010 to 775.373 kg/hr and 435.083 kg/hr respectively. Over the 2011–2015 period, the summer loading rate increased to 780.183 kg/hr and 513.960 kg/hr, followed by a substantial increase in the 2016–2018 period. During this period, the overall nitrogen load across summer and winter increased to 900.765 kg/hr and 865.105 kg/hr, respectively. It is to be noted that the overall nitrogen summer loading rates were higher than winter loading rates. The increase in overall nitrogen loading rates recorded during the thirteen years (2005–2018), was the result of additions of fertiliser, due to agricultural practices occurring along A2H023 and A2H042Q01. After the 2001–2005 period, the overall winter nitrogen loading rates increased from 287.861 kg/hr to 855.105 kg/hr in the 2016–2018 period. This is strongly attributed to increased sewage spills, industrial effluent discharge and dishwasher use. The augmented WMA supply to meet urban demands from Johannesburg (Department of Water Affairs, 2008a), indicates that effluent discharge rates are certain to increase over time, driving up overall nitrogen loading along the Jukskei River in the UCRB.

Agricultural practices are known to occur downstream from the Jukskei River and have increased as a result of raised levels of TP. TP is known to be the limiting reactant in all algal blooms and eutrophic matters. The increase in phosphorus loading (directly attributed to increased phosphorus loading rates over time from the Jukskei River), poses a threat to the water quality in the Hartbeespoort Dam. Along the Jukskei River around gauging stations A2H023 and A2H042Q01, agricultural practices have been observed leaching into the river; downstream movement with reduced dilution will lessen overall water quality with elevated temperature with time, as noted by (Huizenga and Harmse, 2001).

In Figure 20, the total phosphorus loading rates illustrate an overall increase in summer and winter phosphorus loading rates over time.



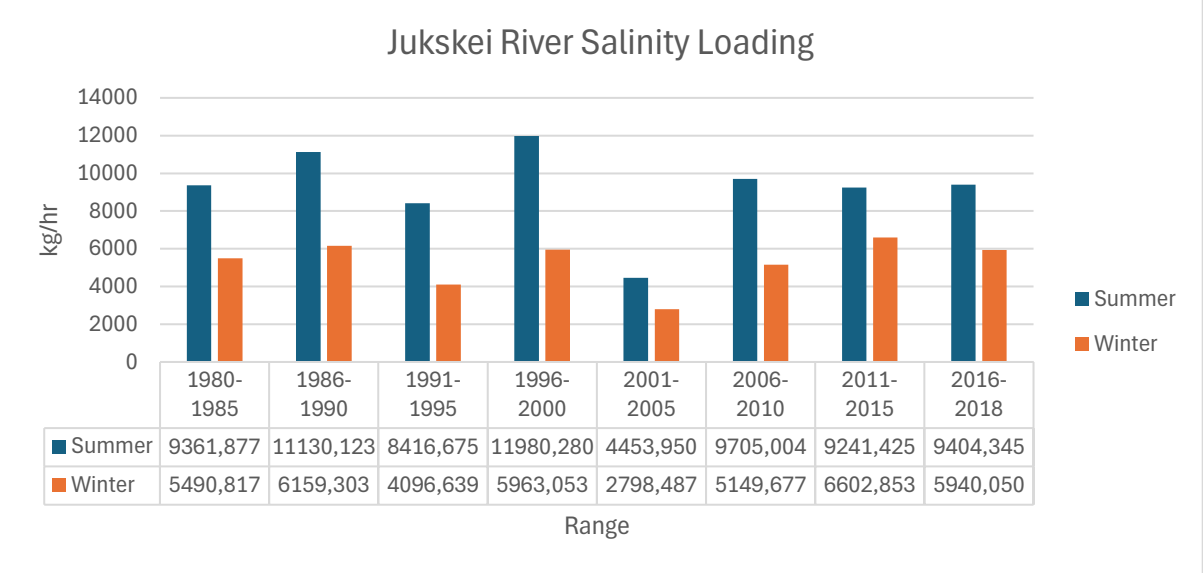

| | 1980-1985 | 1986-1990 | 1991-1995 | 1996-2000 | 2001-2005 | 2006-2010 | 2011-2015 | 2016-2018 |
|---|---|---|---|---|---|---|---|---|
| Summer | 8,595 | 4,388 | 2,442 | 6,515 | 2,249 | 7,919 | 7,526 | 9,159 |
| Winter | 6,701 | 3,408 | 1,081 | 2,045 | 1,281 | 3,799 | 6,507 | 7,835 |

*Figure 20: Jukskei River temporal phosphorus load spanning 38 years*

The Jukskei River poses the largest threat to contamination of the Crocodile River further downstream (which feeds the Hartbeespoort Dam), as it has the highest phosphorus loading rate before joining the Crocodile River. As observed in Figure 20, in the 1980–1985 period, a summer loading rate of 8.595 kg/hr and a winter loading rate of 6.701 kg/hr were evident. The phosphorus loading rate, however, decreased in the summer and winter of 1986–1990 to 4.388 kg/hr and 3.408 kg/hr, respectively, followed by a further decline during the summer and winter of 1991–1995 to 2.442 kg/hr and 1.081 kg/hr, respectively. In 1996–2000, the summer phosphorus rate increased by more than double to 6.515 kg/hr and 2.045 kg/hr, followed by a decrease in the 2001–2005 period to 2.249 kg/hr and 1.281 kg/hr for summer and winter. This was due to El Niño during 2002 (with drought across the interior), causing a decrease in the loading rate, which reduced discharge and further loading. Thereafter, a rapid increase, by more than double the summer and winter phosphorus loading rate was observed in the 2006–2018 period. Phosphorus loading rates reached an all-time high during the 2016–2018 period at 9.159 kg/hr in summer and 7.835 kg/hr in winter. This is strongly attributed to the increased ingress discharge into the basin from the WMA supply and an urban expansion which simultaneously increased the demand for crop

yields and subsequently fertiliser, which induced an overall increase in the Jukskei River's phosphorus loading rates.

The summer and winter salinity loading rates which are converse to phosphorus, sulphate and nitrogen, indicated consistent summer salinity loads that are higher than those in winter. Winter loading rates are seen to gradually increase with time relative to summer salinity loading rates (Figure 21).




| | 1980-1985 | 1986-1990 | 1991-1995 | 1996-2000 | 2001-2005 | 2006-2010 | 2011-2015 | 2016-2018 |
|---|---|---|---|---|---|---|---|---|
| Summer | 9361,877 | 11130,123 | 8416,675 | 11980,280 | 4453,950 | 9705,004 | 9241,425 | 9404,345 |
| Winter | 5490,817 | 6159,303 | 4096,639 | 5963,053 | 2798,487 | 5149,677 | 6602,853 | 5940,050 |

*Figure 21: Jukskei River temporal salinity load spanning 38 years*

From 1980 to 1985, salinity loading was determined to be 9361.877 kg/hr in summer and 5490.817 kg/hr in winter. During 1986–1990, the summer and winter loading rates increased to 11130.123 kg/hr and 6159.303 kg/hr respectively. In 1991–1995 a decrease in the salinity load for both summer and winter to 8416.675 kg/hr and 4096.639 kg/hr was evident. In the 1996–2000 period, the summer loading rate peaked at 11980.280 kg/hr and the winter loading rate increased to 5963.053 kg/hr. A sharp decrease was seen in the 2001–2005 period to more than half the rate of 1996–2000 to 4453.950 kg/hr in summer and 2798.487 kg/hr in winter. During the 2006–2010 period, the loading rate increased to double that of the 2001–2005 period to 9705.004 kg/hr in summer and 5149.677 kg/hr in winter. In the 2011–2015 period, the summer salinity loading rate decreased to 9241.425 kg/hr and peaked in winter to 6602.853 kg/hr.

A small increase in summer salinity load is seen to occur in the 2016-2018 period, to 9404.345 kg/hr and decrease in winter to 5940.050 kg/hr.

The summer salinity load consists of greater than 9000 kg/hr with the exception of the 2001–2005 and the 1991–1995 periods, which were low compared to the nutrient loading graphs of the Jukskei River; this was due to El Niño in 2002 and 1992 that adversely affected parts of South Africa, bringing drought in the rainy summer season. Summer loading rates were considerably higher than those in winter due to the UCRB being dominated by the most precipitation in the rainy summers – which increased the discharge rates by increasing runoff and drainage into river systems. Summer salinity loads were mainly driven by an increase in overall chloride (mainly backwashing water from a large number of swimming pools in Johannesburg), which ended up in the major rivers and increased salinity (Ali et al., 2022). During the 1996–2000 period, peak summer salinity loading rates were seen to be at 11980.280 kg/hr and winter peak during the 2011–2015 period, at 6602.853 kg/hr. The strong control of salinity is TDS which increased immensely due to sodium and chloride in the water during summer months. The increase in salinity loading rates can be attributed to the use of water softeners by water treatment plants and the disposal of untreated wastewater into the Jukskei River (Venkatesan et al., 2011).

### 5.3. The Crocodile River Nutrient and Salinity Loading

The Crocodile River flows from South to North which enters the Hartbeespoort Dam. The river network within the study area is made up of the Bloubankspruit and Crocodile Rivers. The loading rates along the river network were determined until directly before A2H012Q01. The results are representative of the summation of gauging stations A2H051, A2H050Q01, A2H049 and A2H045 (Figure 22), and are an indication of the southwest river network directly before A2H012Q01. The river network flows through the A21E and A21D quaternary catchments.

South of the main Crocodile River, the city of Johannesburg has varied land use activities like mining and landfill sites. The level of activity of the mines lasted for

more than a century, and it is known that they adversely affect the water quality. Figure 23 represents the temporal sulphate loading rate.

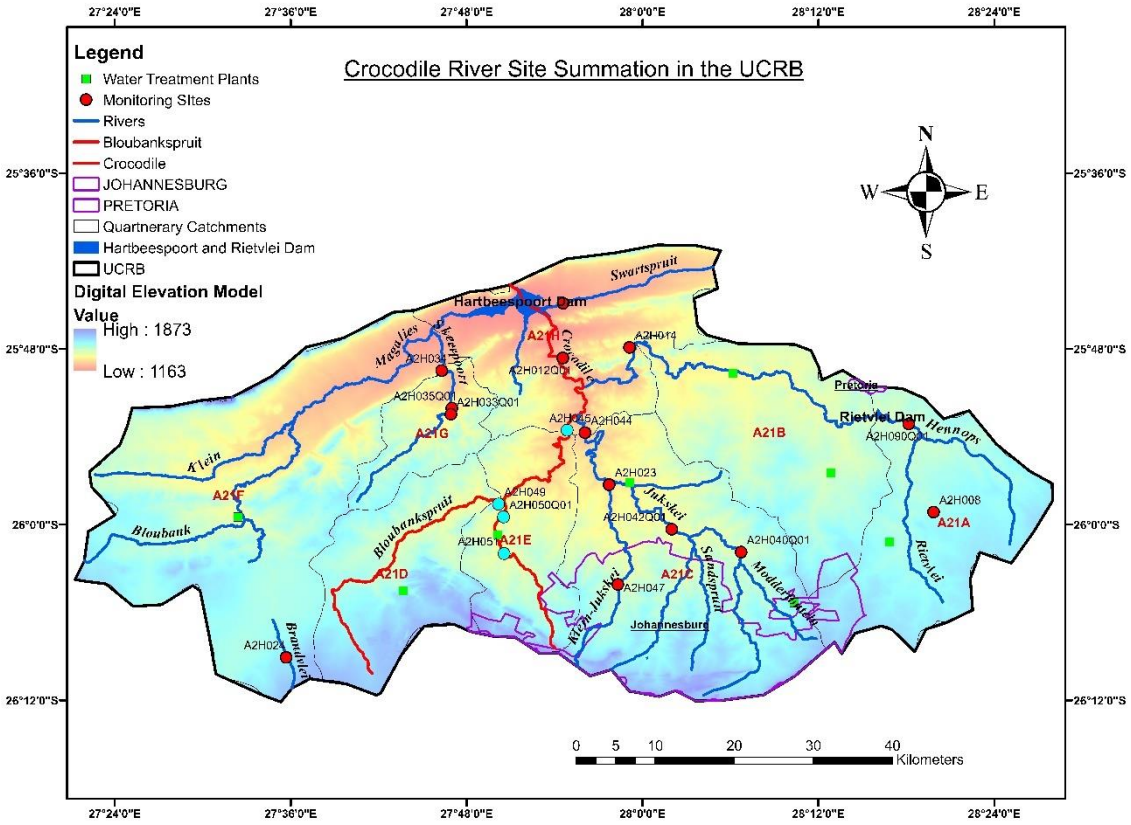



*Figure 22: Crocodile River gauging station summation*
*(including quaternary catchments, sites and water treatment plants)*

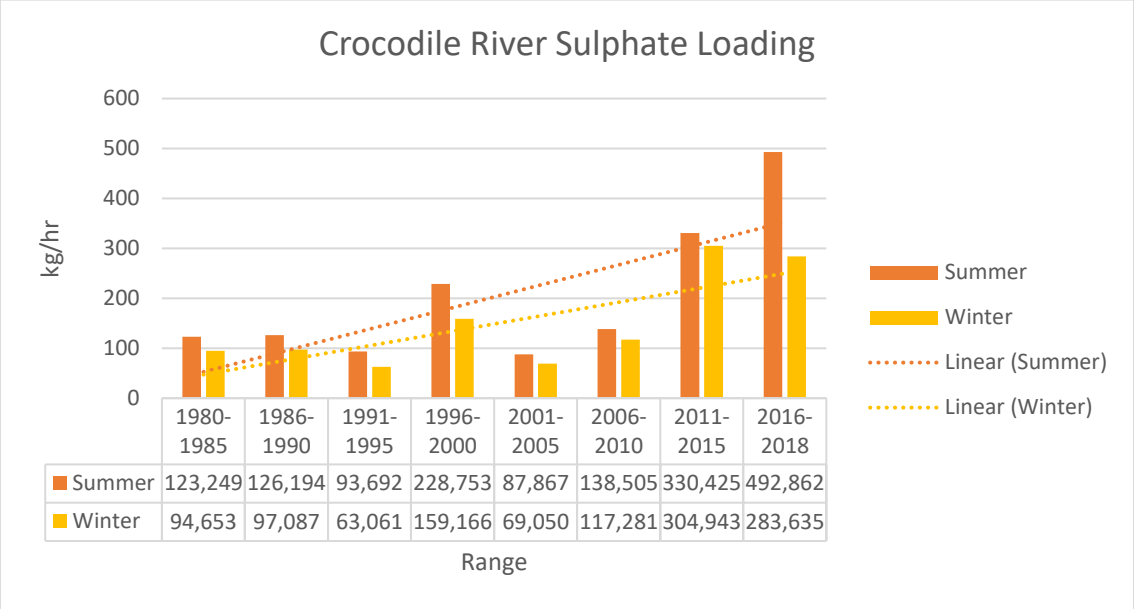
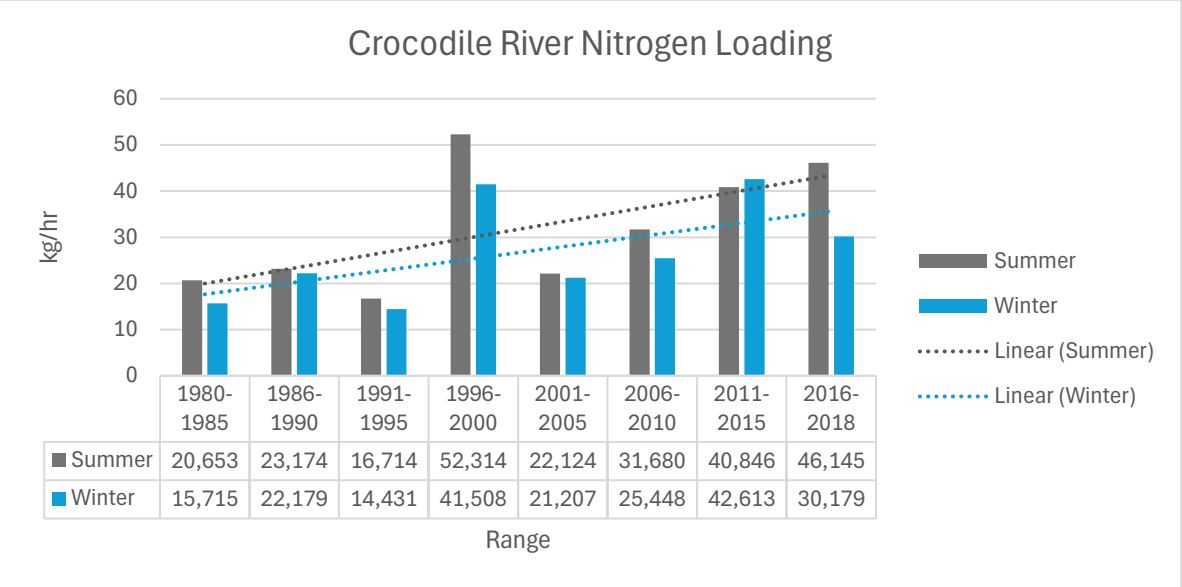



*Figure 23: Crocodile River temporal sulphate load spanning 38 years*

Sulphate loading rates have shown a general trend of increasing over time during both summer and winter. The origin of sulphate within the Crocodile River was due to mining activities occurring to the South of the study area. The sulphate loading rates were considerably lower than that of the Jukskei River and illustrate a trend similar to the Hennops River sulphate loading rate. As hypothesised, summer sulphate loading rates were higher than that of winter loading rates due to the direct relationship between precipitation and discharge. The time series illustrates a pattern that has been observed in the Hennops River. During the period 1980–1985, the summer sulphate load was 123.249 kg/hr and the winter load was at 94.653 kg/hr. The sulphate load increased through 1986–1990 during summer and winter, to 126.194 kg/hr and 97.087 kg/hr respectively. The rate of sulphate loading decreased in 1991–1995 in summer and winter to 93.692 kg/hr and 63.061 kg/hr due to El Niño in 1992 and then to La Niña in the 1999–2000 period, caused a spike in loading rates in the 1996–2000 period. The sulphate loading rate peaked in summer and winter during the first two decades in 1996–2000 to 228.753 kg/hr in summer and 159.166 kg/hr in winter. This followed a drastic decrease in 2001–2005 to more than half the previous five-year interval due the El Niño in 2002 (Ali et al., 2022). An increase followed from 2006 to 2018

for summer and winter sulphate loading rates which peaked during the 2016–2018 period at 492.862 kg/hr and 283.635 kg/hr respectively. This has been concluded due to the increased discharge of additional water from the Vaal management area into the UCRB, exacerbated by La Niña in 2016 and abandoned landfills driving sulphate into the UCRB.

Nitrogen loading showed an increasing trend over time in summer and winter loading rates (Figure 24). Nitrogen loading rates within the Crocodile River (Figure 24) were seen to gradually increase although they were not as high as in the Jukskei River (Figure 19), but had similar nitrogen loading rates to the Hennops River system (Figure 14).



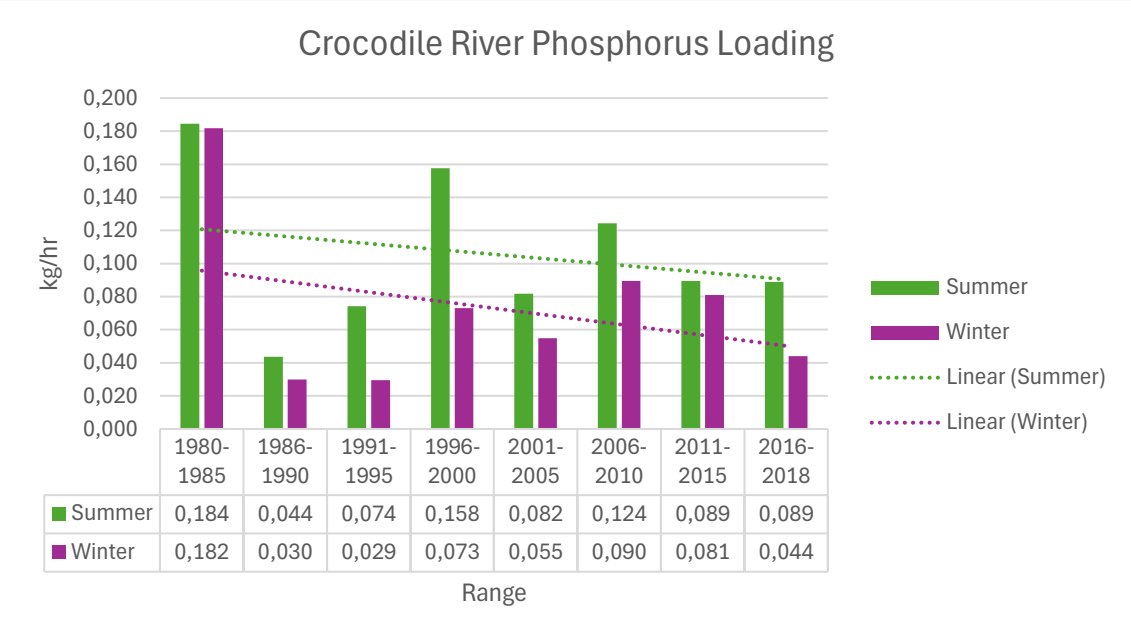

| | 1980-1985 | 1986-1990 | 1991-1995 | 1996-2000 | 2001-2005 | 2006-2010 | 2011-2015 | 2016-2018 |
|---|---|---|---|---|---|---|---|---|
| Summer | 20,653 | 23,174 | 16,714 | 52,314 | 22,124 | 31,680 | 40,846 | 46,145 |
| Winter | 15,715 | 22,179 | 14,431 | 41,508 | 21,207 | 25,448 | 42,613 | 30,179 |

*Figure 24: Crocodile River temporal nitrogen load spanning 38 years*

A trend was noted of low nitrogen loading rates before the Hennops River flows into the Crocodile River during the decade 1980–1990, with a peak summer and winter nitrogen loading rate of 23.174 kg/hr and 22.179kg/hr during 1986–1990. This was followed by a decrease during 1991–1995 due to El Niño in 1992, which induced drought. The all-time nitrogen loading rate high of 52.314 kg/hr during the four decades was seen in the summer of 1996–2000, primarily due to the increase in the discharge rates, resulting in more nitrogen entering the river with the occurrence of La Niña in 1999 and ultimately increasing nitrogen loading. A decrease in the 2001–2005 period was followed by an increase through 2006–

2018 period in summer and winter loading rates. The 2001–2005 drop in loading rates has been attributed to reduced discharge values reducing the overall nitrogen loading rates. The increase which followed thereafter has been attributed to the nonpoint sources and point sources like urban development, as roads and secondary infrastructure development have driven up surface runoff and increased discharge and hence loading. The use of dishwashers and industries found in the southwest of the study area have contributed to increasing nitrogen loads. Unaccounted-for loss in discharge due to burst sewage pipes in the Johannesburg region discharged large amounts of nitrogen that adversely affected the water quality and subsequently spiked nitrogen loads (Ali et al., 2022). This resulted in the increase observed from 2016 to 2018 with values of 46.145 kg/hr during summer and 30.179 kg/hr during winter.

Phosphorus loading rates within the Crocodile River showed very low loading rates with a steady decline in these overall loading rates from 1980 to 2018 (Figure 24). The phosphorus loading rate peaks during the summer and winter of 1980–1985 period at 0.184 kg/hr and 0.182 kg/hr, respectively (Figure 25).




| | 1980-1985 | 1986-1990 | 1991-1995 | 1996-2000 | 2001-2005 | 2006-2010 | 2011-2015 | 2016-2018 |
|---|---|---|---|---|---|---|---|---|
| Summer | 0,184 | 0,044 | 0,074 | 0,158 | 0,082 | 0,124 | 0,089 | 0,089 |
| Winter | 0,182 | 0,030 | 0,029 | 0,073 | 0,055 | 0,090 | 0,081 | 0,044 |

*Figure 25: Crocodile River temporal phosphorus load spanning 38 years*

A drastic decline was observed from 1986 to 1995, where the summer and winter loading phosphorus loading rose rapidly during the 1996–2000 period to 0.158 kg/hr and 0.073 kg/hr in summer and winter, respectively; this was attributed to the La Niña occurrence. A decrease followed in 2001–2005 period due to El Niño in 2002. An increase followed from 2006 to 2018 was attributed to fertiliser runoff. Summer rates were higher throughout the years considered in the study as hypothesised due to summer rainfall.

Salinity loading throughout the section of the Crocodile River shows an expected trend, with summer peaking during 1996–2000 and 2016–2018, and with winter peaking during the 1996–2000 and 2011–2015 periods (Figure 26).

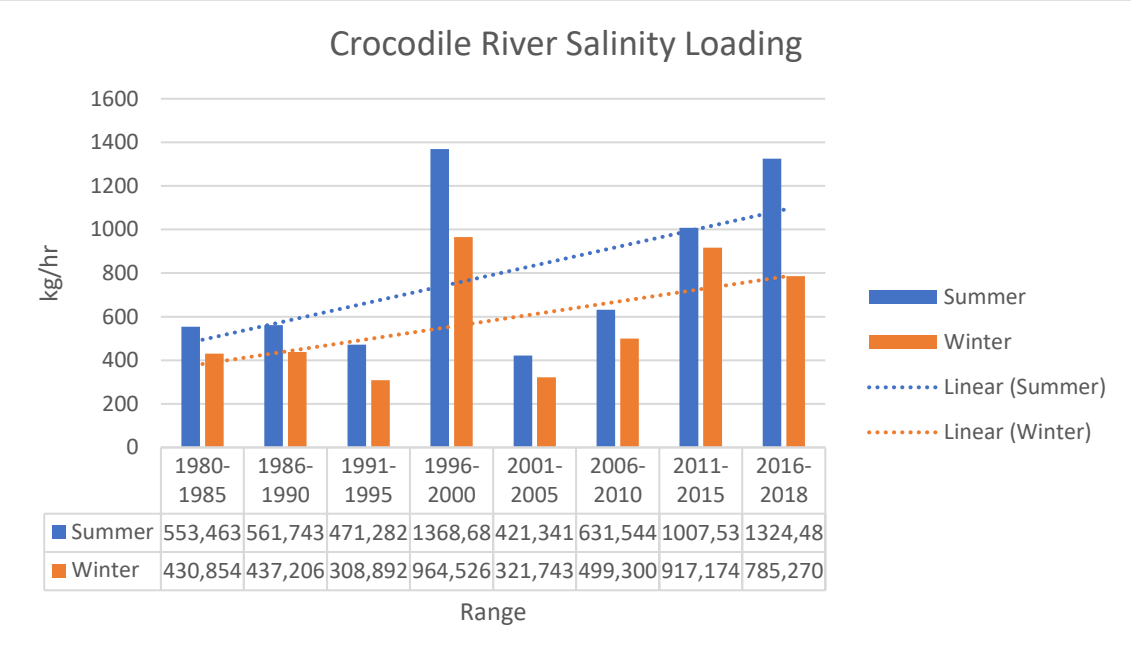



*Figure 26: Crocodile River temporal salinity load spanning 38 years*

Expected lows due to El Niño during 2002, were noted in the 1991–1995 and 2001–2005 periods, and the highs were due to La Niña in 1999. During summer, temperatures were higher which resulted in increased evaporation that increased TDS values and drove up the overall salinity loading rates (Ali et al., 2022). Chloride and sodium levels increased with time due to the use of water softeners and swimming pool backwashes resulting in higher TDS values throughout the summer seasons from 1980 to 2018. Discharge rates drove up the overall salinity

loads as with previously mentioned nutrients, which occurred in summer seasons, resulting in higher summer salinity loads relative to those in winter. As a result of consistent urban expansion and agricultural runoff along the Bloubankspruit feeding into the Crocodile River, TDS values were expected to rise.

## 5.4. Skeerpoort River Nutrient and Salinity Loading

The Skeerpoort River results were derived using three gauging stations (A2H033Q01, A2H035Q01, and A2H034), which are found within the A21G and A21H quaternary catchments. The Skeerpoort River intercepts with the Magalies River that feeds into the Hartbeespoort River (Figure 27). Data gathered from the DWA had few Skeerpoort River measurements from 1990, as lower sample measurement conclusions were made and these had a high level of uncertainty.

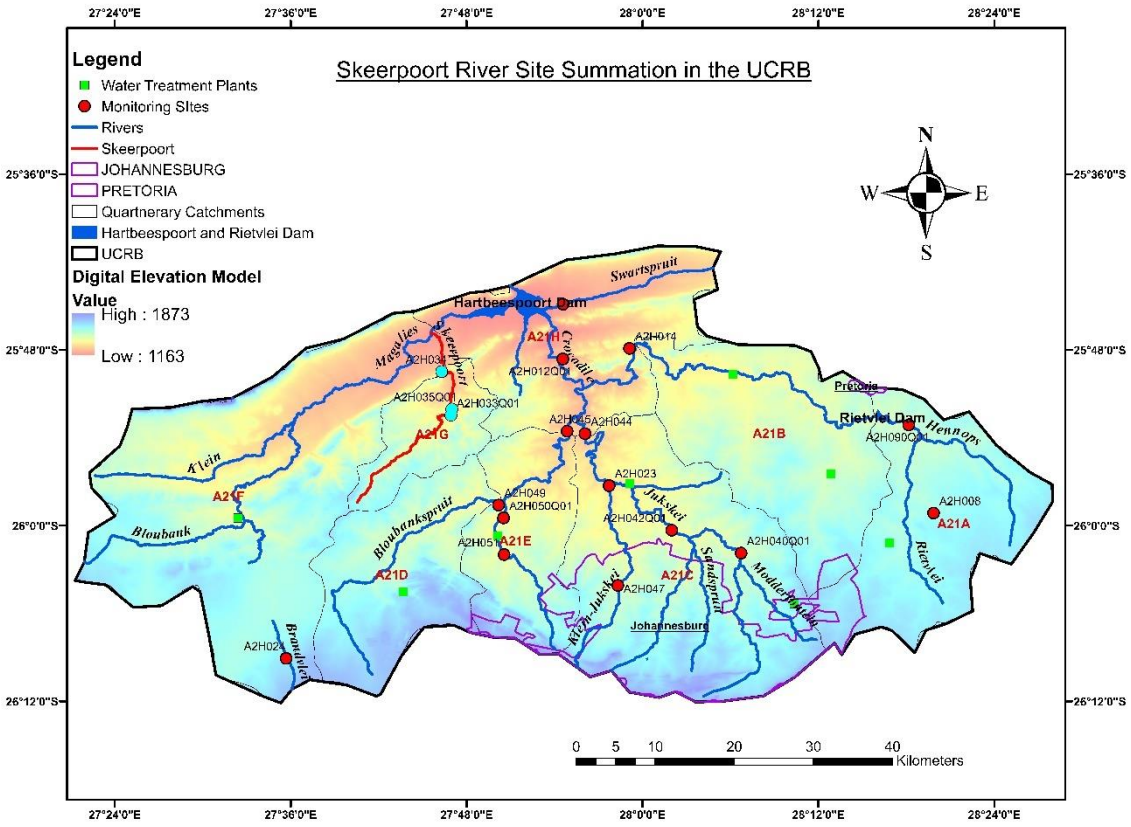



*Figure 27: Skeerpoort River gauging station summation*
*(including quaternary catchments, sites and water treatment plants)*

In Figure 28, the minimum sulphate load is higher in summer than in winter and is calculated using the period 1980–1995.

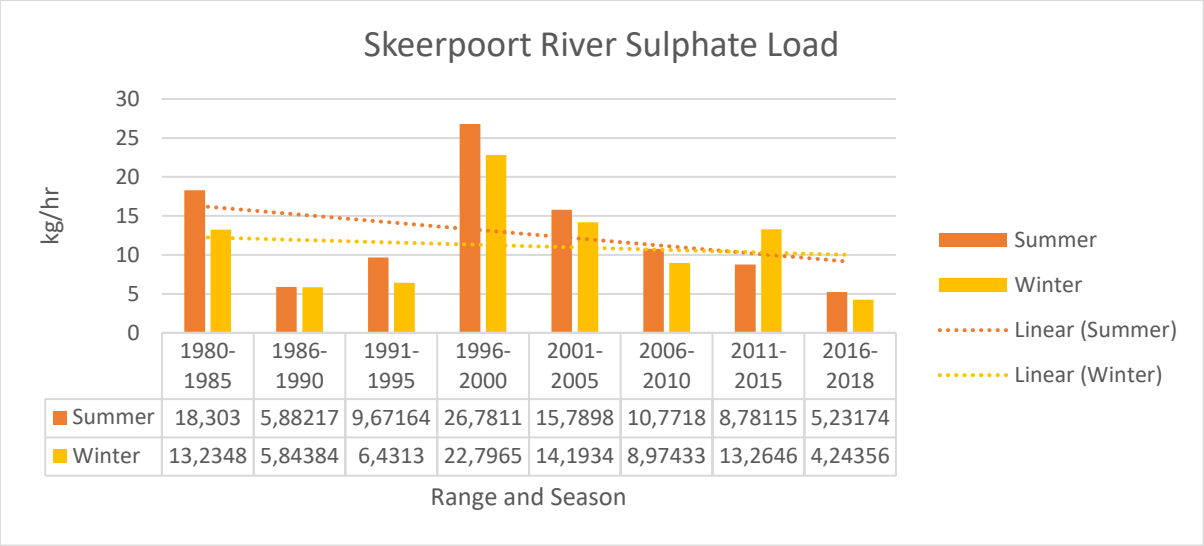
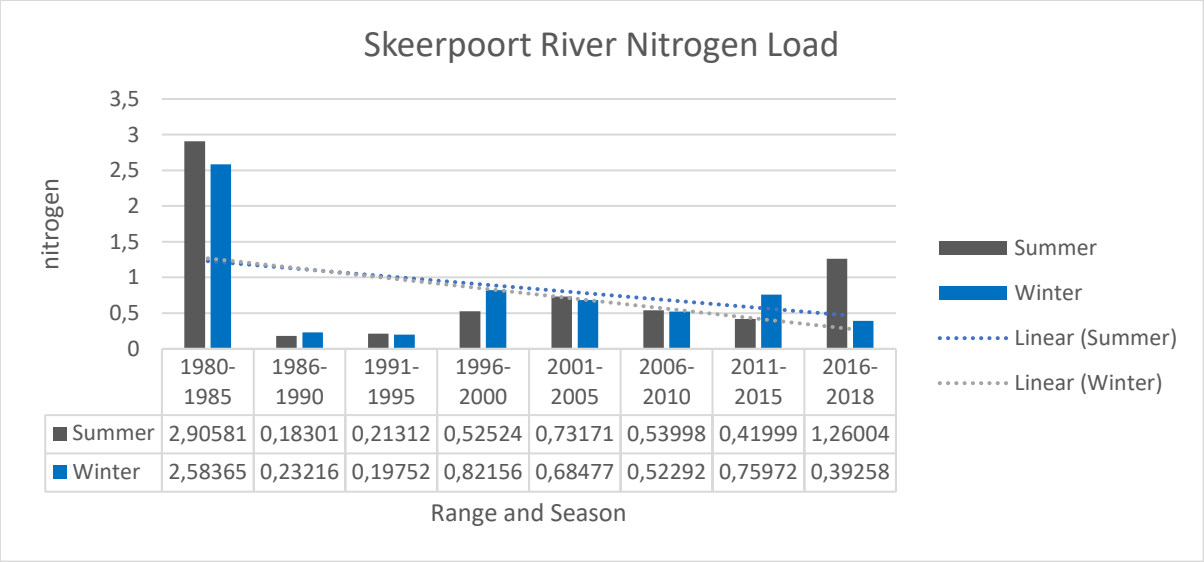



*Figure 28: Skeerpoort River sulphate load spanning 38 years*

The sulphate loading rate within the Skeerpoort River was low relative to the Hennops River, the Jukskei River and the Crocodile River, due to the very low influence of mining in the region. The presence of sulphate in the water was directly attributed to groundwater interaction with surface water from the Malmani Dolomites which have proven to affect surface water and sulphate content in the river adversely. The overall sulphate loading rates were high during the 1980–1985 and 1996–2000 periods due to La Niña, with summer loading rates calculated to be at a minimum of 18.303 kg/hr and 26.7811 kg/hr for summer and winter respectively. A noteworthy finding shows that summer and winter loading rates were higher during the 2001–2005 period than the 2006–2018 period; this trend was not seen in prior river loading rates. Sulphate loading rates decreased from 2006 to 2018 with results showing 5.23174 kg/hr in summer and 4.24356 kg/hr in winter. The anomaly within the results was due to insufficient water

chemistry and discharge data from 2006 to 2018, which were retrieved from the Department of Water Affairs.




| | 1980-1985 | 1986-1990 | 1991-1995 | 1996-2000 | 2001-2005 | 2006-2010 | 2011-2015 | 2016-2018 |
|---|---|---|---|---|---|---|---|---|
| Summer | 2,90581 | 0,18301 | 0,21312 | 0,52524 | 0,73171 | 0,53998 | 0,41999 | 1,26004 |
| Winter | 2,58365 | 0,23216 | 0,19752 | 0,82156 | 0,68477 | 0,52292 | 0,75972 | 0,39258 |

*Figure 29: Skeerpoort River nitrogen load spanning 38 years*

From the data retrieved, a decline in nitrogen loading is observed with a peak nitrogen loading rate in the 1980–1985 period at 2.90581 kg/hr during summer and 2.58365 kg/hr during winter (Figure 29). A steady decline was noted during the 1986–1995 period with an increase in summer and winter loading rates between 1996 and 2000, although the overall nitrogen levels were very low relative to other rivers. An increase in the 2016–2018 period is seen in Figure 28, calculated as a minimum of 1.26 kg/hr.

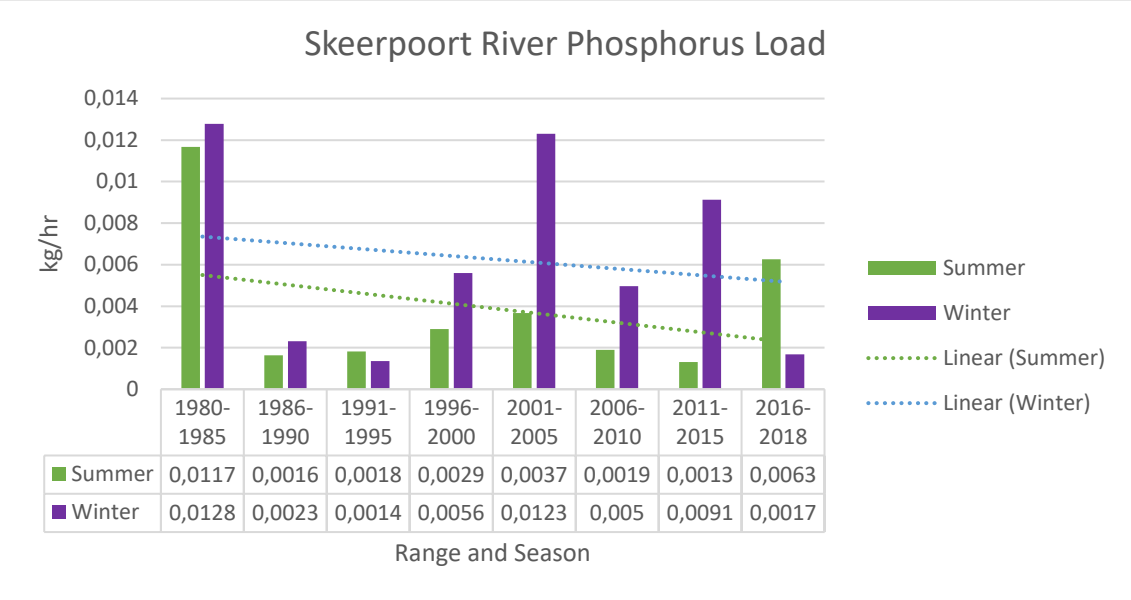



*Figure 30: Skeerpoort River temporal phosphorus load spanning 38 years*

During the 1980–1985 period, the Skeerpoort River rate of phosphorus loading is the highest within the four decades of evaluation (Figure 30). With the overall winter load at 0.01278 kg/hr and the rate at 0.01168 kg/hr, the winter rate was higher than that of summer. There was a drastic decrease in the phosphorus load in the period 1986–1995. The phosphorus load increased in the 1996–2000 period with the winter load calculated at 0.0056 kg/hr and the summer load at 0.0029 kg/hr. During the 2001–2005 period, the overall summer and winter load increased to 0.00367 kg /hr and 0.0123 kg/hr in winter. In the 2006–2010 period, the phosphorus load decreased during both seasons, summer to 0.0019 kg/hr, and winter to 0.00497 kg/hr. From 2011 to 2015, a gradual spike in winter loads was seen with a reported value of 0.00913 kg/hr and 0.00132 kg/hr in summer. Lastly, a strong summer loading event was noted during the 2016–2018 period, with an increase of 0.00626 kg/hr, and a serious decrease in winter to 0.00168 kg/hr.

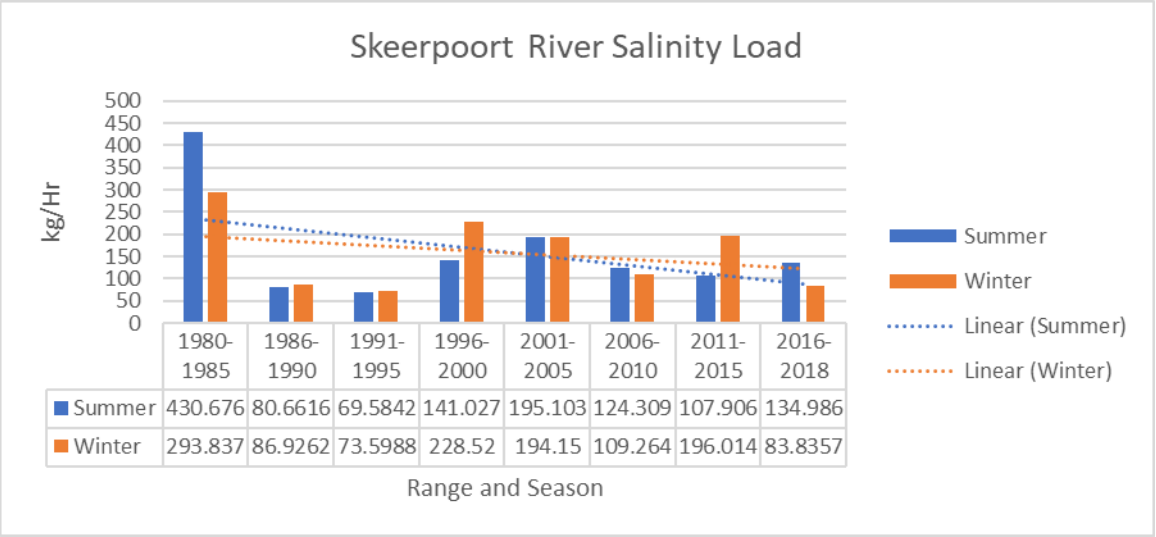



*Figure 31: Skeerpoort River temporal salinity load spanning 38 years*

Salinity loading rates throughout their respective seasons showed relatively low TDS values (Figure 31). The years 1980–1985 showed the highest summer and winter loading rates due to the completeness of data, with a steady decline observed from 1986 to 1995 (Figure 31). A steep increase during the 1996–2000 period was seen in summer and winter loading rates at 141.0266 kg/hr and 228.51954 kg/hr, respectively. This was followed by a steady decline over the subsequent two decades. The summer salinity loading rates were higher than those in winter during the 1980–1985, 2001–2005 and 2016–2018 periods. Winter loading rates stayed higher than summer loading in the remainder of the periods, including 1986–1990, 1991–1995, 1996–2000, 2006–2010 and 2011–2015 periods.

The lower nutrient salinity levels seen in the Skeerpoort River indicate that urbanisation harms water quality. The Skeerpoort region is a sparsely populated region with reduced land use activities. It is mainly dominated by barren land and exposed rock; thus, lower loading rates were observed throughout the river system.

## 5.5. Swartspruit River Nutrient and Salinity Loading

The Swartspruit River nutrient and salinity load was calculated using one gauging station A2H058, located along the eastern side of the Hartbeespoort Dam. The site falls within the A21H quaternary catchment area (Figure 32). The site provided valuable information concerning minimum loading rates entering the Hartbeespoort Dam. Data measurements, particularly discharge data, were limited and consequently increased the uncertainty of results obtained when using these data sets. No winter discharge measurements were taken between 1980 and 1985.

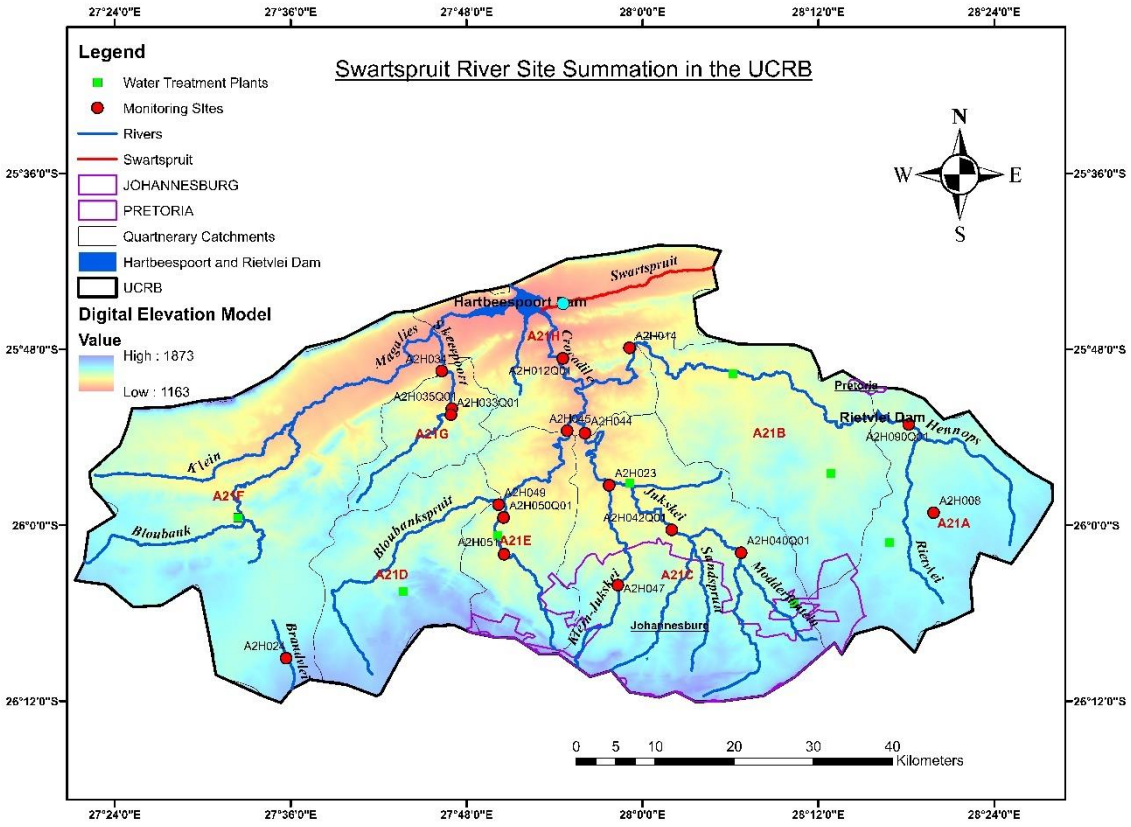



*Figure 32: Swartspruit River gauging station summation*
*(including quaternary catchments, gauges and water treatment works)*

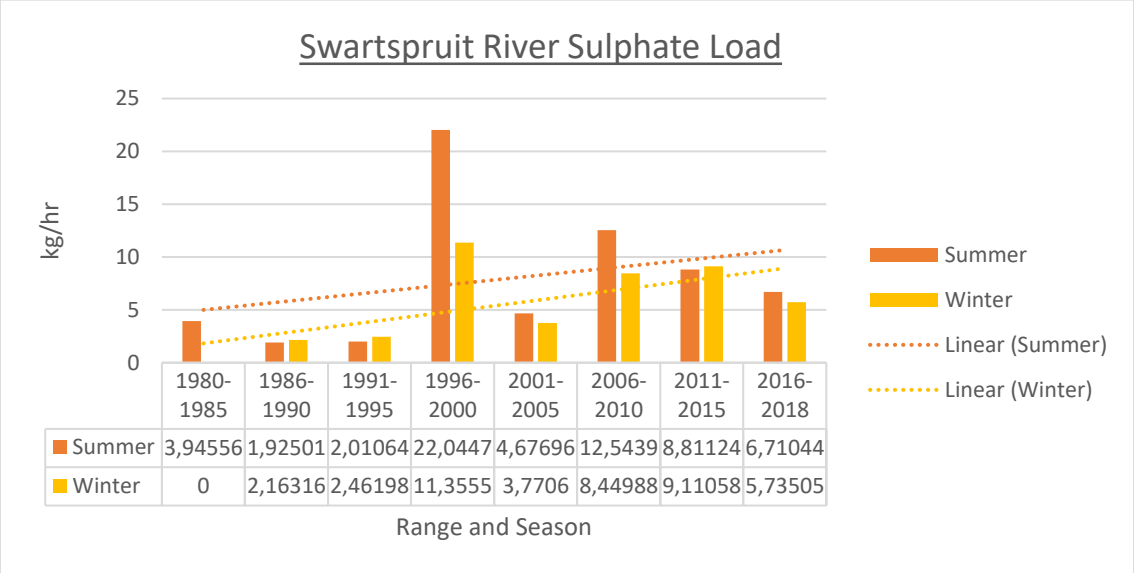



*Figure 33: Swartspruit River temporal sulphate load spanning 38 years*

The sulphate load is presented in Figure 33; no records for the winter season were noted during the 1980–1985 period as no discharge data were available. Figure 33 shows that sulphate loads were fairly low throughout the period of study relative to other rivers like the Hennops River, the Jukskei River and the Crocodile River. Summer sulphate loading rates were considerably higher than winter loading rates. An overall spike was observed, as previously seen during 1996–2000 with summer loading rates reaching a high of 22.0447 kg/hr and winter loading rates of 11.355 kg/hr, due to the La Niña effect. This was followed by a drop in 2001–2005 due to the El Nino-inducing drought. A rise in overall sulphate load increased in the 2006–2010 period to 12.5439 kg/hr and winter of 8.44 kg/hr respectively, which was followed by a drop thereafter into the 2016–2018 period. The overall loading rates were relatively low compared to the Crocodile River, the Jukskei River and the Hennops River, partly due to the relatively low numbers of industries occupying the area and in addition to limited urbanisation in the river's vicinity.

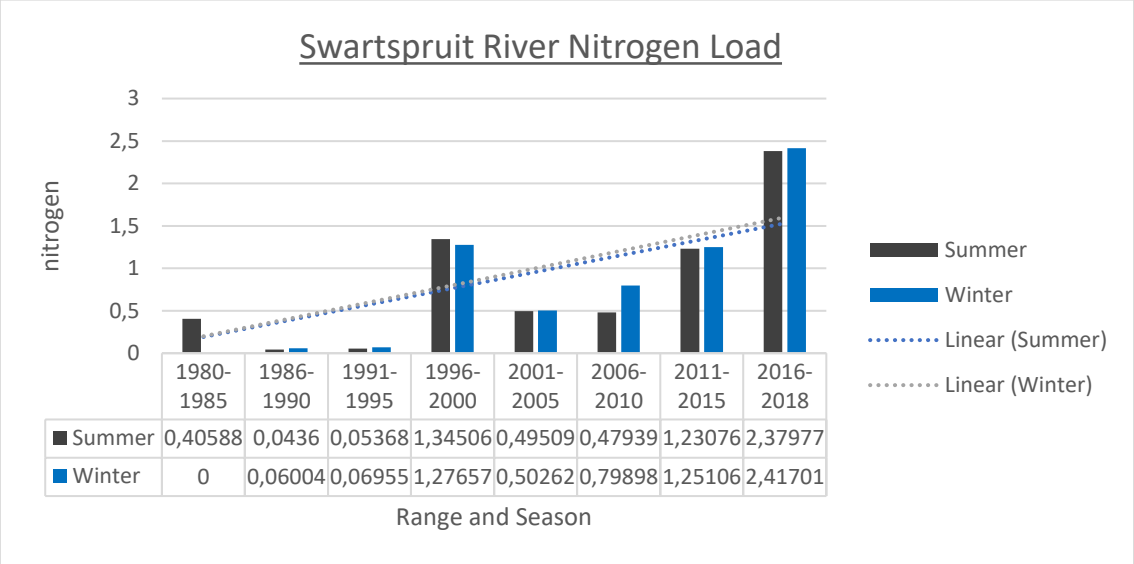



*Figure 34: Swartspruit River temporal nitrogen load spanning 38 years*

Nitrogen loading (Figure 34) has a similar trend to that of sulphate loading and other graphs with low summer and winter loading rates in 1986–1995, followed by a strong rise in nitrogen loading in the 1996–2000 period to 1.34506 kg/hr and 1.27657 kg/hr respectively, This is followed by a drop in the 2001–2005 period, although nitrogen loading rates increased from 2006 to 2018, with the 2016–2018 period peaking at 2.37977 kg/hr and winter loading rates of 2.41701 kg/hr. The increases and decreases could be due to El Niño and La Niña events influencing discharge rates. The general trend within the nitrogen loading calculation during the period showed an increase in overall nitrogen loading rates over time. It ties in with the changes observed in land use changes which resulted in overall development as seen around the Hartbeespoort River. Agricultural activities were the most water-intensive and were responsible for the overall increase in nitrogen loading following the 2001–2005 period.

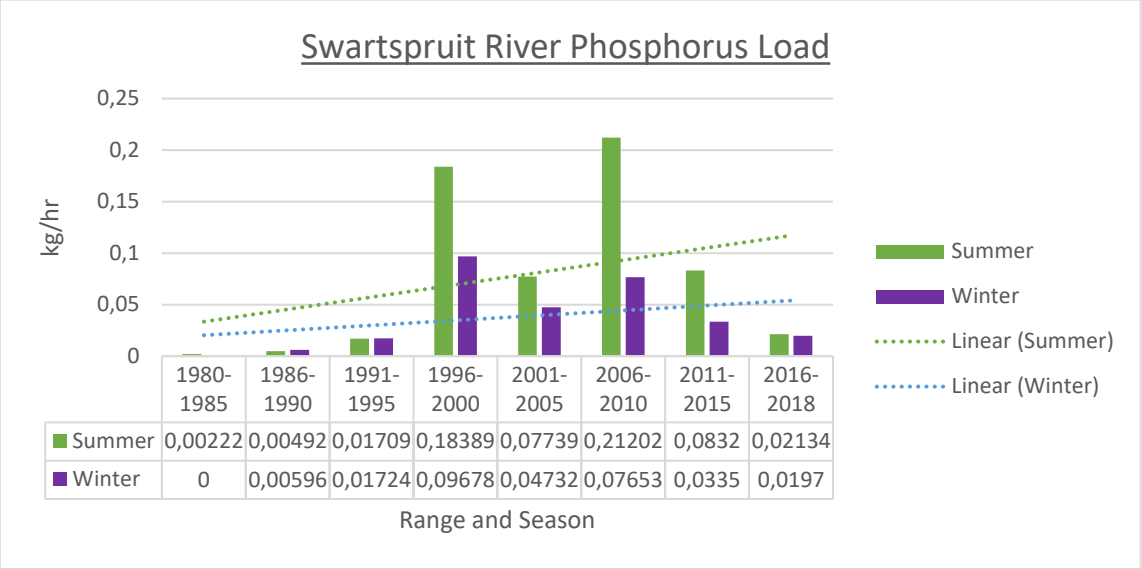



*Figure 35: Swartspruit River temporal phosphorus load over 38 years.*

Phosphorus loading rates (Figure 35) increased in the 1996–2000 period to 0.18389 kg/hr in summer and 0.09678 kg/hr in winter. A drop was noted in the 2001–2005 period, which is consistent with other nutrient evaluations. The all-time peak of summer phosphorus loading rate was seen during the 2006–2010 period to 0.21202 kg/hr, followed by a decrease in the 2011–2018 period. The presence of phosphorus loading was strongly attributed to the use of fertilisers in agricultural activities, and small farm activity within the vicinity surrounding the Swartspruit River could be the result of increased phosphorus loading when yield demands increase.

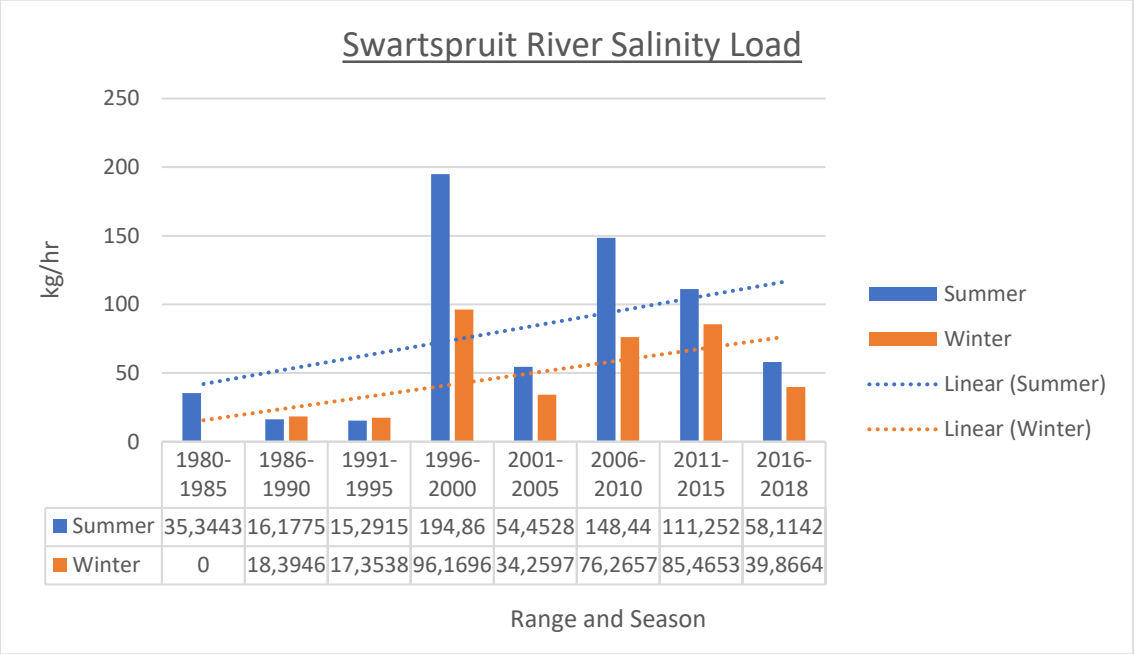



*Figure 36: Swartspruit River temporal salinity load spanning 38 years*

Salinity loading (Figure 36) shows an increasing trend in salinity loading during summer and winter throughout the period of study. Winter salinity loads were significantly lower than those in summer. The peak summer salinity loading rates occurred during the 1996–2000 period, with an average loading rate of 194.8598 kg/hr and winter loading rate of 34.25974 kg/hr. This was followed by the drop in the 2001–2005 period, attributed to drought-induced climatic changes under El Niño conditions. An increase in overall salinity was observed, with summer salinity loading rates increased during the 2006–2010 period to 148.4396 kg/hr and to 111.2524 kg/hr during the 2011–2015 period. This was followed by a decrease in TDS during the 2016–2018 period. Summer salinity loading rates were significantly higher than those in winter from 1996 to 2018. During the period 1986–1995, salinity loadings for summer and winter were below 20 kg/hr. The increase in overall salinity during the respective periods as previously mentioned, was in response to land use around the Hartbeespoort River, driving the TDS values to increase. Sodium and chloride contributed significantly to the overall TDS values.

## 5.6. Brandvlei River Nutrient and Salinity Loading

The Brandvlei River is an isolated tributary that forms part of the UCRB. The nutrient and salinity loading has been determined using site A2H024. The river forms part of the A21F quaternary catchment, as seen in Figure 37.

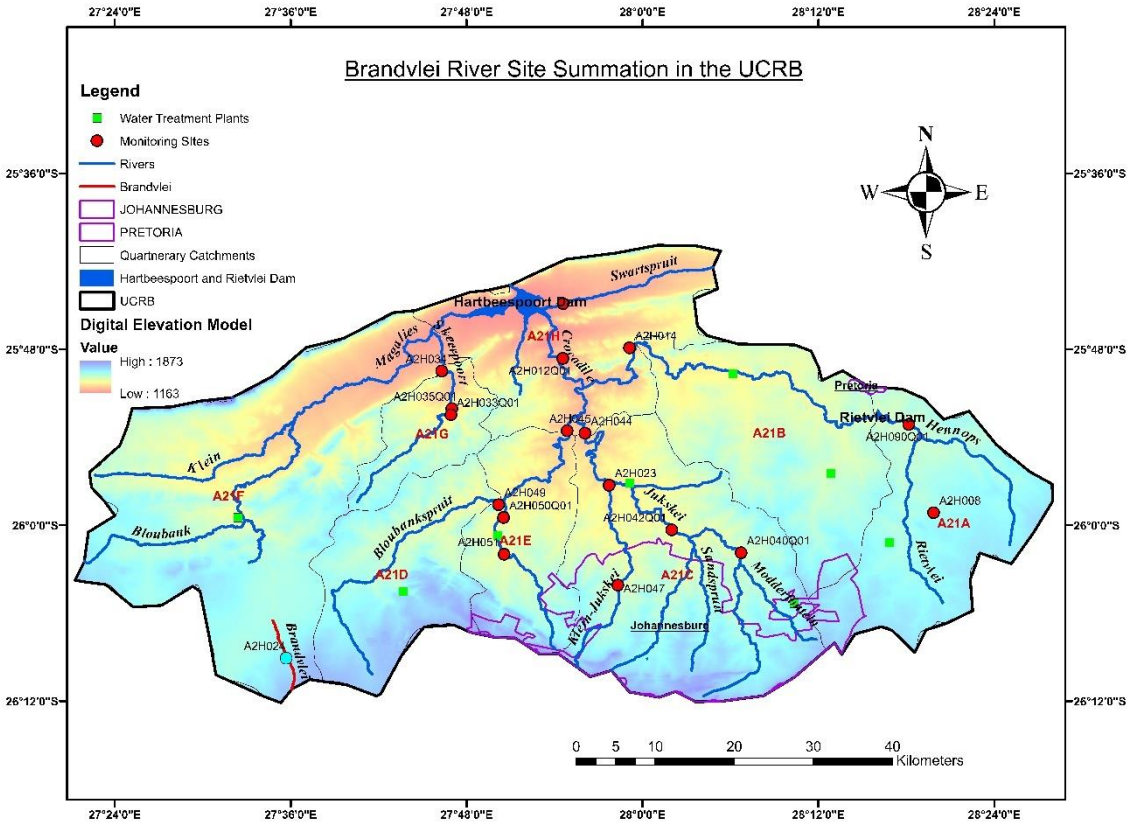



*Figure 37: Brandvlei River gauging station summation*
*(including quaternary catchments, sites and water treatment plants)*

As depicted in Figure 38, sulphate loading rates peaked between 1996 and 2000 with a summer loading rate of 0.66938 kg/hr and winter loading rate of 1.39542 kg/hr.

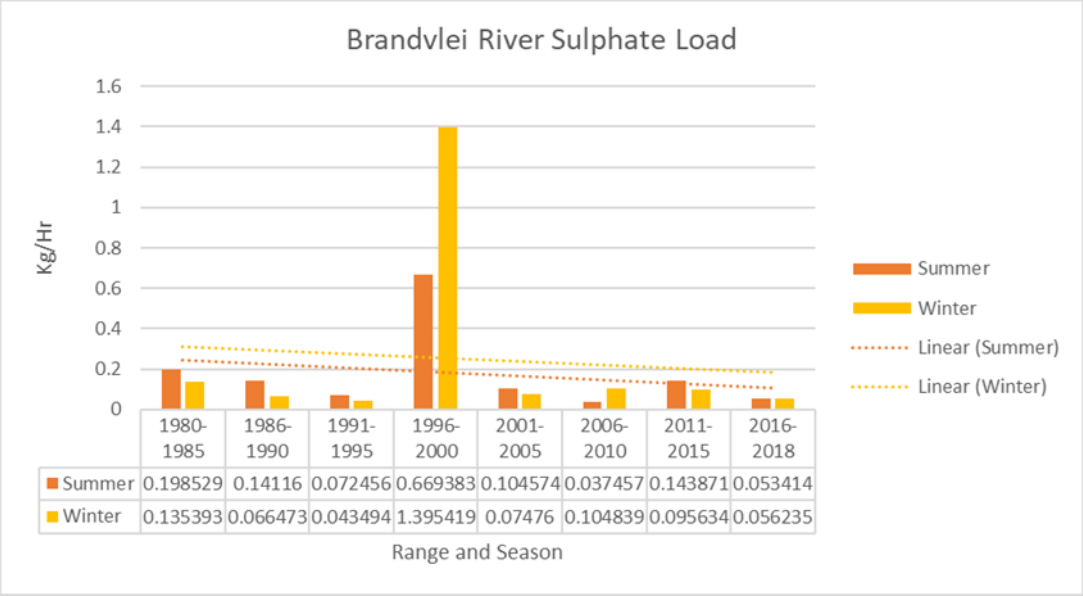



*Figure 38: Brandvlei River temporal sulphate load spanning 38 years*

Annual intervals in the period of 1996–2000, show the lowest sulphate loading rate throughout the UCRB river networks. The significantly low sulphate loading rate was strongly related to the spatial relationship between land use and river. The Brandvlei River has little to no mining activity, hence the very low sulphate loading rates. Summer and winter sulphate loading rates decrease over time, with winter loading rates higher during the 1996–2000 and 2006–2010 periods, and those of summer being higher throughout the annual intervals.

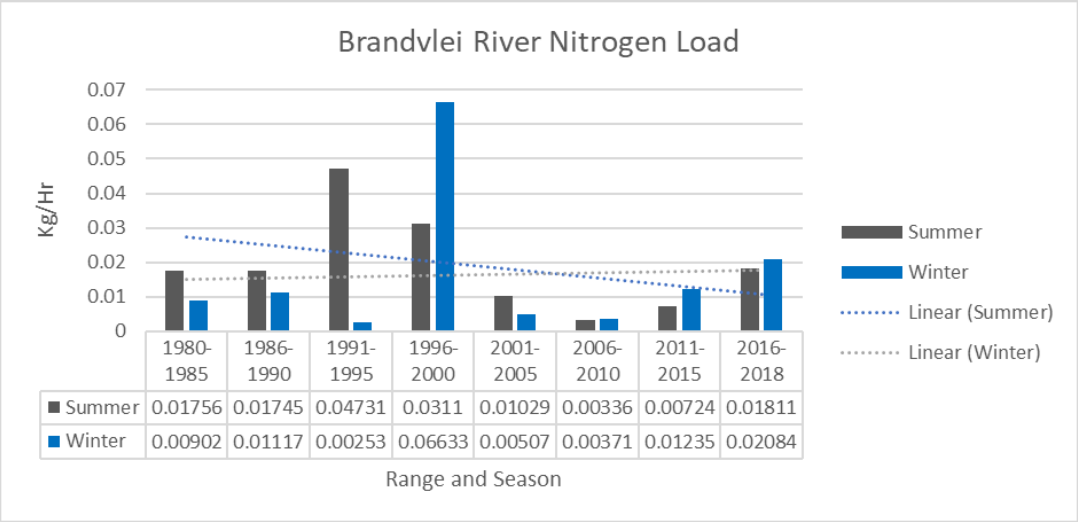



*Figure 39: Brandvlei River temporal nitrogen load spanning 38 years*

The overall loading rate of nitrogen in the Brandvlei River was low in relation to the rest of the river networks in the basin, yet despite this, a general trend of the nitrogen loading rates was noted (Figure 39). Summer loading rates were consistently higher than winter loading rates from 1980 to 1995, with winter loading surpassing summer loading rates in the 1996–2000 period, increased to 0.06633 kg/hr. A steady decline was recorded during the 2001–2005 and 2006–2010 periods. Nitrogen loading rates in the Brandvlei River began to increase from 2011 to 2018, with summer and winter levels reaching a high in the 2016 - 2018 period of 0.01811 kg/hr and 0.02084 kg/hr respectively. Over time, the winter loading rate in the Brandvlei River (Figure 39), reflects an increase in load, with the summer loading rate decreasing. This could be a result of the shape of the drainage basin and relative drainage which increased the overall lag time and resulted in higher loading rates during the winter season.

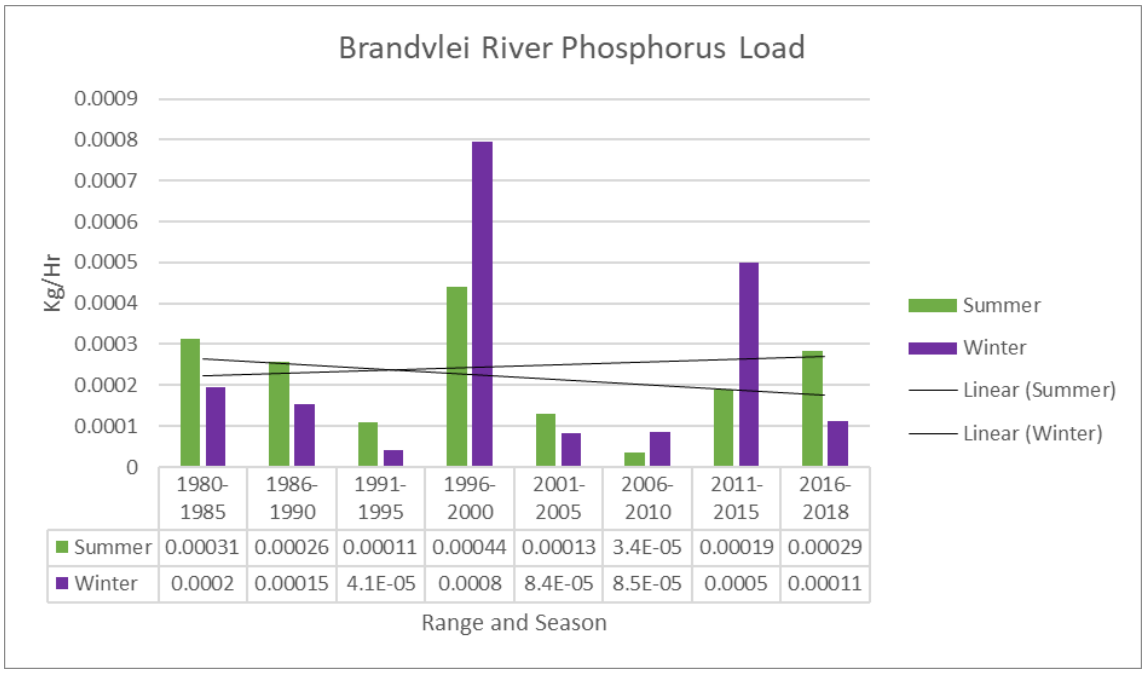



*Figure 40: Brandvlei River temporal phosphorus load spanning 38 years*

Phosphorus loading rates throughout the period of study (38 years) are relatively low (Figure 40). As a result, the phosphorus load did not pose a significant threat to the water or adversely affect the water quality. Similar trends were observed in phosphorus loading in the Brandvlei River to nitrogen loading rates, with

increased summer phosphorus loading during the 1980–1995 period. Summer and winter loading rates peaked in the 1996–2000 period, while a strong decrease was noted in the 2001–2005 and 2006–2010 periods, followed by a rise during the 2011–2015 periods with winter loading rates measuring higher than summer loading. For the 2016 to 2018 period, summer loading rates increased above winter loading rates. The relatively low phosphorus loading was due to less agricultural activity in and around the Brandvlei River.

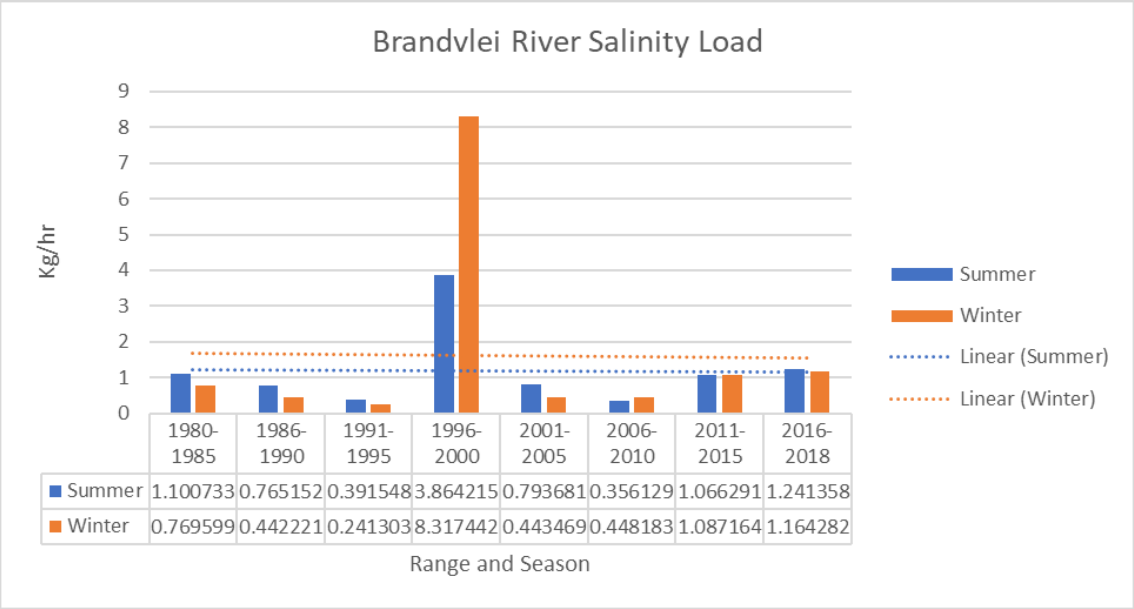



*Figure 41: Brandvlei River temporal salinity load spanning 38 years*

Salinity loading from 1980 to 1995 (Figure 41), shows a summer high of 1.10 kg/hr, and a decrease in overall summer and winter loading rates. The decrease in overall salinity experienced was due to a rise in temperatures. During the 1996–2000 period, a peak high in salinity loading rate was seen during winter (8.31 kg/hr), and summer (3.86 kg/hr). A decrease followed during the 2001–2005 period with a gradual increase in overall salinity loads from 2006 to 2018, as previously seen. The increase in salinity can directly be attributed to a rise in TDS values over time because of changes in land use activity, primarily construction and development. Higher summer salinity loading rates during the 2016–2018 period can be attributed to increased discharge, due to precipitation rates being higher.

## 5.7. Gauging station A2H012Q01

Gauging station A2H012Q01 is the last station of measurement along the Crocodile River. The results are a collective representation of the Jukskei River, the Hennops River and the Crocodile River. They represent the minimum nutrient and salinity load entering the Hartbeespoort Dam from the South of the UCRB. The A2H012Q01 is in the A21H quaternary catchment area and it is a stream order of four order (Figure 42). The A2H012Q01 is the closest estimation of nutrient and salinity loads entering the Hartbeespoort Dam through surface water.

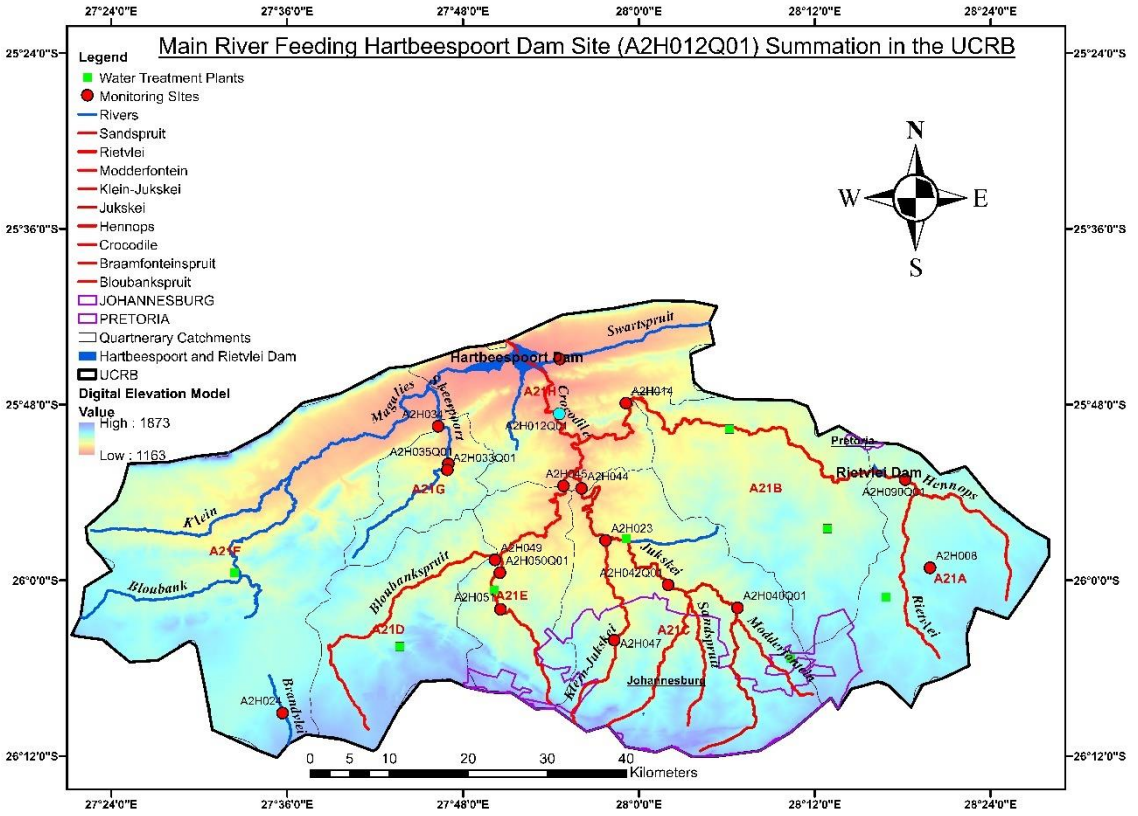


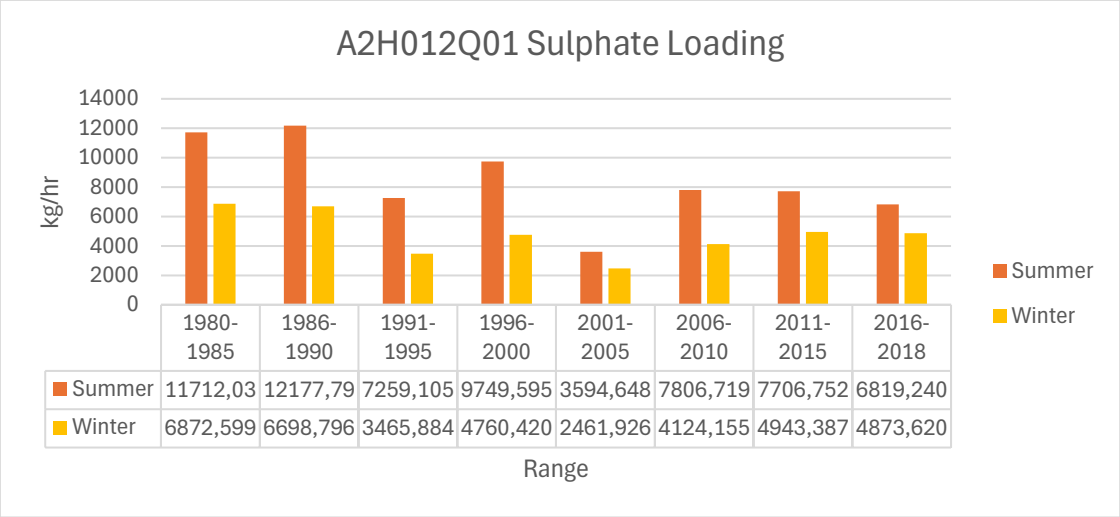

*Figure 42: A2H012Q01 Main Crocodile River gauging station summation (including quaternary catchments, sites and water treatment plants)*

The gauging station at A2H012Q01 is pertinent in that it gives an indication of how humans have impacted the surface water quality. This is the last monitoring station before water from the South end drains into the Hartbeespoort Dam. The graphs are key representations of the Hennops River, Crocodile River and

Jukskei River which merge into the larger Crocodile River before it feeds into the Hartbeespoort Dam. The rivers from the South end of the study area carry nutrient-rich waters, directly from Johannesburg and Pretoria, where mining and industrial effluents discharge into the UCRB, and are restricted by the Hartbeespoort Dam.

The nutrients and salinity drivers are directly attributed to the anthropogenic sources including the development of roads, urbanisation, sewage spills and AMD, and industrial effluent which directly discharges from the cities and into the UCRB. Increased water demands and the development of roads increase the overall runoff by reducing infiltration, thus causing a rise in discharge rates that results in salinity and nutrients entering the UCRB.

In Figure 43, the minimum sulphate load was determined for the gauging site A2H012Q01 along the Crocodile River. The observed linear trend shows an overall decrease in sulphate loading in both summer and winter; however, the winter trend is a lot gentler.




| | 1980-1985 | 1986-1990 | 1991-1995 | 1996-2000 | 2001-2005 | 2006-2010 | 2011-2015 | 2016-2018 |
|---|---|---|---|---|---|---|---|---|
| Summer | 11712,03 | 12177,79 | 7259,105 | 9749,595 | 3594,648 | 7806,719 | 7706,752 | 6819,240 |
| Winter | 6872,599 | 6698,796 | 3465,884 | 4760,420 | 2461,926 | 4124,155 | 4943,387 | 4873,620 |

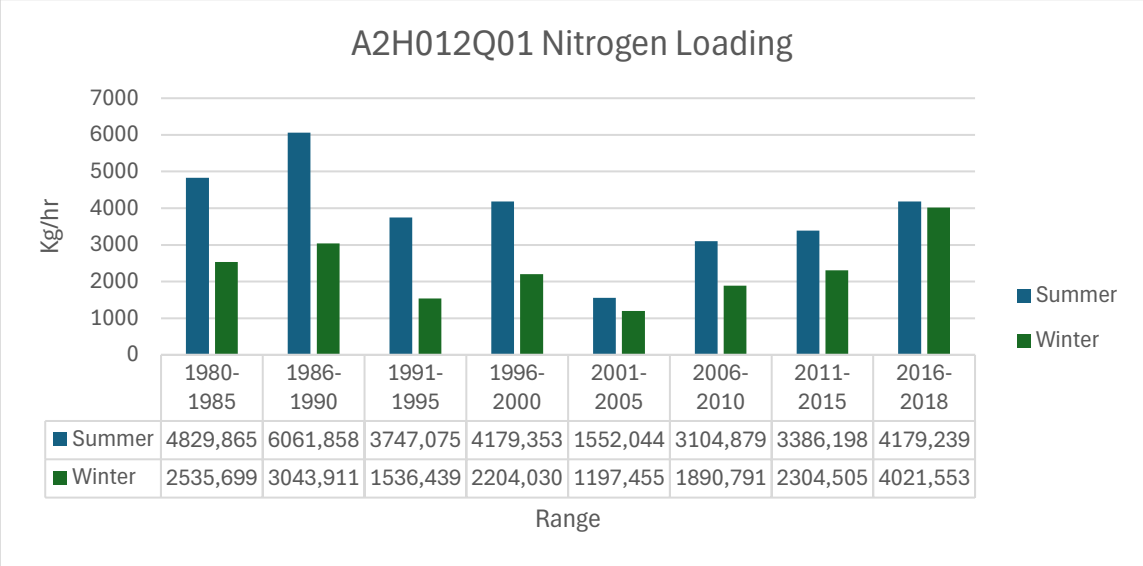
*Figure 43: A2H012Q01 temporal sulphate load spanning 38 years*

Sulphate loading rates are indicated in Figure 43 which illustrates a summer loading rate that is consistently higher than the winter loading rate. This is due to the UCRB receiving summer rainfall during the months of October to March (DWAF, 2004). Mining activities that occur South of the study areas have

abandoned mines and landfills from the gold rush era that occurred in the Witwatersrand basin. These landfill sites are a threat to water quality, due to precipitation rates increasing in the summer months which result in the leaching of sulphate-rich metals entering rivers and streams, and which follow into Hartbeespoort Dam.

The summer sulphate load between 1980 and 1985 is measured at 11712.038 kg/hr and has a winter load of 6872.599 kg/hr. The sulphate load increased in the summer seasons of 1986–1990 to a rate of 12177.794 kg/hr and then decreased in winter to 6698.796 kg/hr. This was due to the occurrence of El Niño during the 1982–1983 period, which caused a decrease in discharge rates (Ali et al., 2022). During the 1986–1990 period, the overall sulphate loading rate was at its highest across the thirty-eight years of study. The peak sulphate loading rate is directly attributed to the combination of poor water management strategies and limited awareness by the Department of Water Affairs of the adverse effects of sulphate entering the UCRB. During the 1991–1995 period, El Niño brought about drought in 1992 and caused an overall decrease in summer and winter loading rates, due to reduced precipitation increasing discharge rates (Ali et al., 2022). In the years 1998–1999, La Niña dominated the interior of South Africa as rainfall increased; this pushed the overall discharge rates in the basin to increase and caused a rise in summer loading rates. Figure 43 shows an increase in sulphate loading following the 1991–1995 and 1996–2000 periods, with a summer loading rate of 9749.595 kg/hr. This could be attributed to increased rainfall accelerating rates of leaching, and seepage of AMD into the river basin. A drastic decrease in 2001–2005 was observed in sulphate loading rates due to the droughts experienced in South Africa between 2002 and 2003. An increase in overall summer sulphate loading rates was noted in the 2006–2018 periods, with loading rates consistently higher than 5000 kg/hr. A steady decrease in sulphate loading rates is observed throughout the thirty-eight years in summer and winter due to improved landfill management strategies. Winter sulphate loading rates were consistently lower than summer sulphate loading rates because of reduced precipitation – as the UCRB does not receive winter rainfall (Leketa and Abiye, 2019).

Figure 44 shows the minimum nitrogen load determined for the A2H012Q01 station, where it can be seen that the general summer and winter trends indicate a decrease in summer loading rates and an increase in winter nitrogen loading.



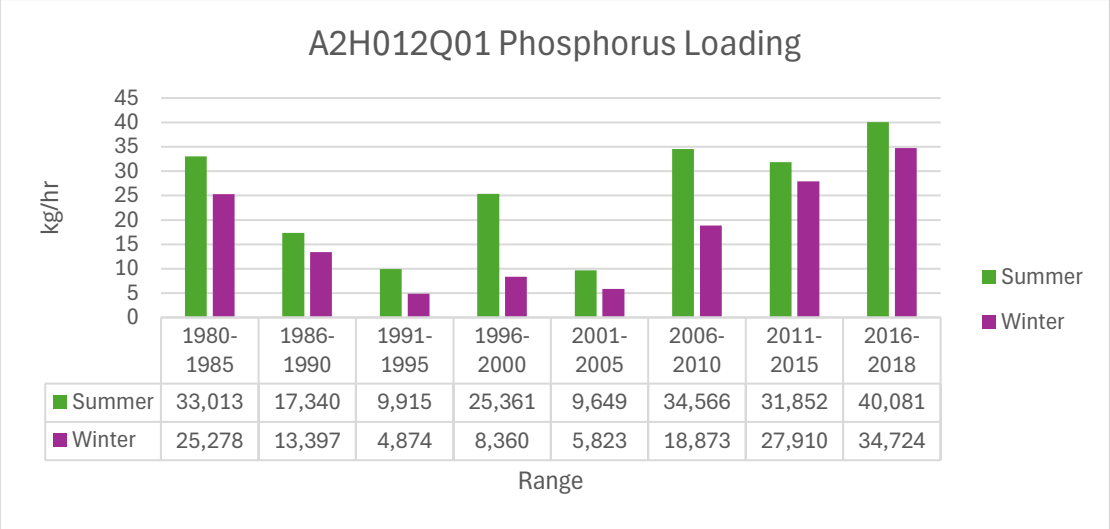

| | 1980-1985 | 1986-1990 | 1991-1995 | 1996-2000 | 2001-2005 | 2006-2010 | 2011-2015 | 2016-2018 |
|---|---|---|---|---|---|---|---|---|
| Summer | 4829,865 | 6061,858 | 3747,075 | 4179,353 | 1552,044 | 3104,879 | 3386,198 | 4179,239 |
| Winter | 2535,699 | 3043,911 | 1536,439 | 2204,030 | 1197,455 | 1890,791 | 2304,505 | 4021,553 |

*Figure 44: A2H012Q01 temporal nitrogen load spanning 38 years*

Nitrogen loading rates before entering the Hartbeespoort Dam (Figure 44) show an overall similar summer loading rate trend to sulphate loading represented in Figure 43. Winter nitrogen loading rates are observed to have increased through time and are a consequence of increases in point and nonpoint sources in Johannesburg. Sewage spills – due to poor management of piping infrastructure – which can be observed across areas of Johannesburg that resulted in an unaccounted-for increase of nitrogen entering the river basin. This is further exacerbated by the runoff rates that increased due to road development and urbanisation, reducing overall infiltration rates. Nitrogen loading rates are rising as a result of untraceable sources, but known atmospheric deposition. This is pertinent due to industrial gases and fossil fuel burning increasing air pollution, which is causing a rise in inception and precipitation of toxic gases being deposited into the river basin(Abiye, 2021). An increase in summer nitrogen loading rates was observed during the period 1980–1990, with winter rates also increased (Figure 44). A decrease in loading rates in 1991–1995 was detected; this is due to the 1992–1995 El Niño bringing drought and decreasing the overall

nitrogen loading rates (Ali et al., 2022). Dilution and denitrification processes break down and reduce overall nitrogen when feeding into the rivers, because of the nature of the drainage basin. For the 1996–2000 period, summer nitrogen loading rates were observed to have increased as a result of elevated precipitation brought by La Niña during the 1998-1999 period. A drastic drop in summer and winter loading rates was observed during the 2001–2005 period due to droughts across the interior by El Niño in 2002. A drastic increase in overall summer and winter loading rates was observed from 2006 to 2018; this is connected to more sewage spills in tandem with accelerating urbanisation. Industrial production during this period increased, inducing a greater inception of toxic gases, which caused a rise in atmospheric deposition. This was compounded by increased farming demands and resulted in increased fertiliser runoff into the basin and rising loading rates.

Phosphorus loading represented by site A2H012Q01 (Figure 45), shows increasing phosphorus loading rates in both summer and winter converse to nitrogen and sulphate loading rates.



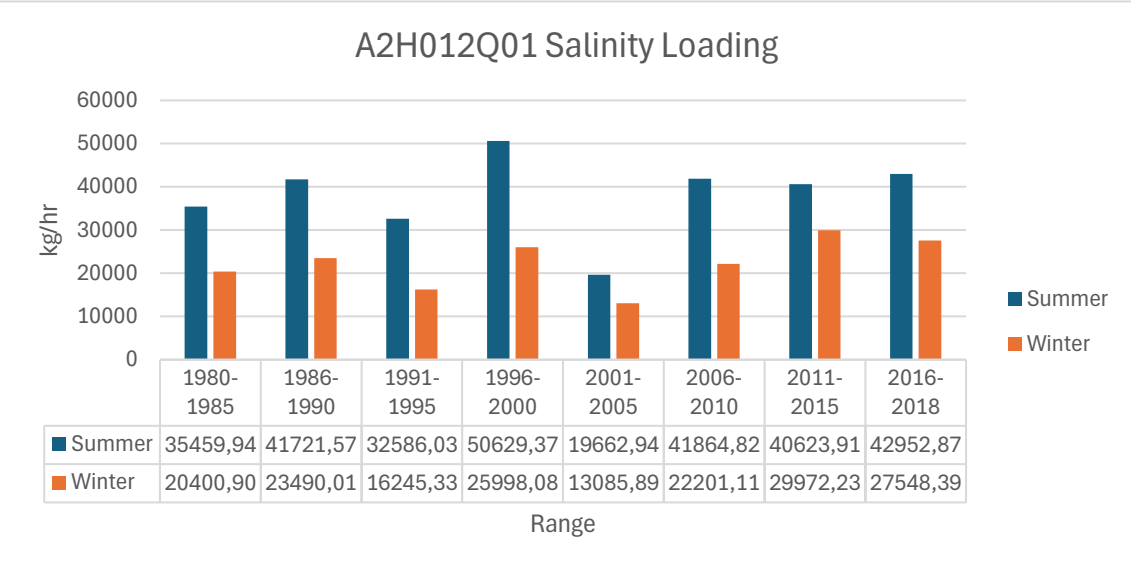

| | 1980-1985 | 1986-1990 | 1991-1995 | 1996-2000 | 2001-2005 | 2006-2010 | 2011-2015 | 2016-2018 |
|---|---|---|---|---|---|---|---|---|
| Summer | 33,013 | 17,340 | 9,915 | 25,361 | 9,649 | 34,566 | 31,852 | 40,081 |
| Winter | 25,278 | 13,397 | 4,874 | 8,360 | 5,823 | 18,873 | 27,910 | 34,724 |

*Figure 45: A2H012Q01 temporal phosphorus load spanning 38 years*

High phosphorus loading rates during the 1980–1985 period were recorded during the first two decades of the study with a summer and winter loading rate of 99.6885 kg/hr and 76.3408 kg/hr, respectively. A drastic decrease in summer

and winter loading rates followed from 1986–1995, due to bioremediation plans occurring during the early 1990s (Ali et al., 2022). For the 1991–1995 and 2001–2005 periods, the phosphorus loading rates during summer and winter were low due to bioremediation, and El Niño decreased the summer loading rate to below 30 kg/hr and that of winter to below 20 kg/hr. From 2006 to 2018, summer and winter phosphorus loading rates increased. This increase adversely affected the Hartbeespoort Dam, which drives up eutrophication rates and leads to an increase in HABs and cyanobacteria. The increases reduced overall dissolved oxygen levels and threaten aquatic ecosystems and human health (Ali et al., 2022).

In Figure 46, the salinity loading was calculated for A2H012Q01 station – the general salinity trend showed a gradual increase for summer and winter salinity loading.




| | 1980-1985 | 1986-1990 | 1991-1995 | 1996-2000 | 2001-2005 | 2006-2010 | 2011-2015 | 2016-2018 |
|---|---|---|---|---|---|---|---|---|
| Summer | 35459,94 | 41721,57 | 32586,03 | 50629,37 | 19662,94 | 41864,82 | 40623,91 | 42952,87 |
| Winter | 20400,90 | 23490,01 | 16245,33 | 25998,08 | 13085,89 | 22201,11 | 29972,23 | 27548,39 |

*Figure 46: A2H012Q01 temporal salinity load spanning 38 years*

Salinity loading in the UCRB showed an increase in both seasons' salinity loading rates with time; summer salinity loading rates increased over time as a result of temperature increases in the UCRB as mentioned in Ali et al. (2022). This resulted in increased evaporation driving up overall TDS values, hence increased overall salinity loading. Summer salinity loading rates were consistently higher than winter salinity loading rates by a minimum of 5000 kg/hr, due to the summer

rainfall increasing discharge. Salinity loading rates decreased in the 1991–1995 and 2001–2005 period due to El Niño drying up the interior region. Within the first two decades (1996–2000), summer and winter salinity loading rates increased at a rate of 152901 kg/hr and 78514.2 kg/hr respectively – this is driven by discharge rates increasing due to La Niña. In the eighteen years following the 2001–2005 period, overall summer and winter loading rates increased which can be attributed to the increase in overall summer temperatures, noted by Ali et al. (2022), increasing the overall TDS load. Due to lower temperatures in winter, less dilution, evaporation, precipitation and overall discharge occurred, reducing the overall salinity loads as a result of lower temperatures in winter. When monitoring water, the major cations and anions driving TDS levels up in the UCRB are the increase in chlorine, sodium, calcium and magnesium. Chlorine concentrations increase with time due to swimming pool backwashes, discharging large quantities of salt into the water system. It has been noted, and further supported by Ali et al. (2022), that due to human activities and urbanisation, increased discharge rates and untreated wastewater discharges are forcing up overall salinity levels. The increasing rate of urban growth caused the salinity loading rates to increase from 2006 to 2018.

# 6. DISCUSSION

From 1980 to 2018 in the UCRB, anthropogenic influence drastically altered and affected the water quality. The calculated nutrient and salinity loads were determined for various rivers within the UCRB. The Hennops, Jukskei and Crocodile rivers discharge the highest nutrients to the Hartbeespoort Dam of 500 to 1500 kg/hr of phosphorus, nitrogen and sulphate. From the spatial variability of the UCRB, it can be concluded that with the rapid increase in urbanisation and industrial development (supplemented with increasing water demand), the nutrient and salinity loading has increased. It was observed that there was seasonal variability with the summer loading rates that were consistently higher than the winter loading rates which occurs throughout all the major rivers. The reason for this could be that the UCRB receives its rainfall during October–March (Department of Water Affairs and Forestry, 2008a), which results in direct recharge into the major rivers in the UCRB, driving up overall surface runoff and inherently increasing the discharge into the rivers. From the observed elevation maps, the drainage network and density supplement an increased discharge into the rivers on the way to convergence at the Hartbeespoort Dam. Increased precipitation during summer months and supplemented discharge from the WMA increase the overall discharge (Department of Water Affairs and Forestry, 2008a), which drives up loading and dilution rates. The inter-basin water transfer from the WMA has inflated the discharge in the Jukskei and Hennops streams, thus resulting in the disposal of urban wastewater from the water treatment works into the major rivers. The disposal of wastewater has adversely affected the quality of surface water resources in the UCRB (Department of Water Affairs and Forestry, 2008a).

The general temporal trend observed in the Jukskei, Hennops and Crocodile rivers in the early 1980s, shows low loading rates followed by a further decrease into the early 1990s due to El Niño in 1982–1983 (Abiye and Ali, 2022). Following La Niña, an increase in loading rates was observed in 1996–1998, bringing increased precipitation, increased recharge and runoff between 1996 and 2000. A strong decrease followed during the 2001–2005 period due to El Niño where

drought was experienced across the extent of the UCRB, bringing down overall loading. Following on to the 2006–2018 period, supply by the CWMWMA through the inter-basin water transfer, there was an increase in the Hennops River, Jukskei River and Crocodile River where through urban wastewater and water treatment works, discharging water adversely affected the UCRB (Department of Water Affairs and Forestry, 2008a). This increased the overall sulphate, phosphorus and nitrogen loading rates in all major rivers draining from the Johannesburg region.

The Jukskei River discharges and drains the Johannesburg region, and is the largest contributor to nutrients entering the basin. The river drains the Johannesburg region through four subsidiary rivers, including Klein-Jukskei, Braamfontein Spruit, Sandspruit, and Modderfontein. The potential industrial influencers contributing to increased nitrogen loads around the Jukskei River are the African Explosives and Chemical Industries (AECI) factory and the Kelvin Power Station situated along the Modderfontein Spruit (Huizenga and Harmse, 2005). The increase in nitrogen loading along the Jukskei River is directly attributed to increased discharge through the inter-basin water transfer and to the rise in overall nitrogen levels that result from increases in industrial and communal effluent and population growth. The rise in informal settlements and poor sewage disposal practices along the Jukskei River in the vicinity of Alexandra could be responsible for the rising nitrogen loading rate (Huizenga and Harmse, 2005). The nonpoint sources of nitrogen considerably increase and make it difficult to trace the exact sources of nitrogen. Nitrogen loads increased considerably from 2005 to 2018 because of poor maintenance, urbanisation and industrial discharge compounded by untreated wastewater entering the Jukskei River.

Sulphate loading rates throughout the Jukskei River were found to decline gradually between 1980 and 2018, although the sulphate loading rates are higher than peak sulphate discharges in the Crocodile River and the Hennops River. The sulphate loading rates are high due to abandoned landfills and mining activity occurring south of the Modderfontein River, the Sandspruit and Braamfontein-

Spruit. According to Mengistu et al. (2019), the Witwatersrand Goldfields ground and surface water interaction are responsible for Crocodile River and Jukskei River sulphate concentrations. Throughout the 1980–2018 period, the sulphate loading rates are considerably higher than the Crocodile River and the Hennops River. This is also supported by Naicker et al. (2003); the central Rand area where acid mine drainage is a potential problem contributes to the increased sulphate loads along the Jukskei River. The source of sulphate pollution along the Jukskei River is due to gold mining activities (due to the oxidation of pyrite in tailings dams and erosion or reworking when exposed to air), thus contributing to sulphate leaching into the Jukskei River (Venter, 1995; Nordstrom and Alpers, 1999; Naicker et al., 2003).

The Jukskei River is the major contributor to the concentration of high nutrients. As per prior research conducted on the Hartbeespoort River by Ali et al. (2022), it is noted that total phosphorus is the limiting nutrient in the overall increase in Harmful Algal Blooms. The phosphorus loading rates from 1980 to 1985 are high which ties in with research done by Huizenga and Harmse (2005), which highlights the eutrophication problem in the Hartbeespoort Dam, strongly attributed to the high phosphate concentration coming from the Jukskei River. The presence of high phosphorus loads results in the invasive aquatic macrophyte (hyacinth), growth dropping overall dissolved oxygen levels and further affecting Hartbeespoort Dam ecosystems (Ali et al., 2022). Following 1986–1995, phosphorus loading rates decreased drastically due to the implementation of a phosphate standard in 1985 to 1 mg/L and calcite precipitation occurring at a high pH (Huizenga and Harmse, 2005), – and a further bioremediation project to reduce the hypereutrophic status of the Hartbeespoort Dam. Due to poor water resource management in the late 1990s, total phosphorus levels increased (Ali et al., 2022). Following the La Niña event in 1996–1998 and El Niño in the early 2000s, total phosphorus loading increased and posed an immense threat to overall water quality in the UCRB (Abiye and Leketa., 2021). The general summer and winter phosphorus loading rate increased in the Jukskei River, reaching a loading rate of 20.39 kg/hr during summer and 17.4427 kg/hr during winter in 2016–2018. The rise in phosphorus

loading rates is conjugated with the supplemented discharge from the WMA and was exacerbated by increased population and urbanisation. The point sources responsible are golf courses and agricultural runoffs along the Jukskei River, driving up phosphorus concentrations, supplemented with untreated wastewater discharge (Ali et al., 2022).

The Hennops River is threatened by AMD with the sulphate loading rates rising drastically over time – this is attributed to abandoned mines and landfill sites that are poorly managed resulting in seeping and leakage of harmful metals into the Hennops River. The landfill sites are located southeast of the UCRB, draining into the Hennops River. Sulphate loading rates doubled for both summer and winter during the late 1990s, although it dropped moving into the early 2000s and then increased from 2006 to 2018. This is strongly attributed to mining activities within the vicinity of the larger Hennops River, which feeds into the region of the Hennops River in the UCRB and the inter-basin transfer increasing the discharge and driving up the loading rates. The values are a minimum and strongly subjected to dilution that occurs in the Rietvlei Dam, acting as a restrictive and dilutive body.

The calculated nitrogen loading rates indicated an exponentially increasing trend for summer and winter, forecasting further increases in nitrogen concentration and a rise in nitrogen loads. The loading is strongly subjected to spatial variability with a growing population and urbanisation, posing a threat to water quality. Untreated wastewater is compounding the threat of nitrogen in the Hennops River (Department of Water Affairs and Forestry, 2008a). After 2005, phosphorus loading rates rose drastically in the Hennops River, due to the rise in phosphate concentrations which resulted from agricultural practices that use fertiliser, responsible for increasing phosphorus runoff into the Hennops River, with additional inter-basin CWMWMA discharge.

The Crocodile River has minimal phosphorus loading rates due to reduced agricultural practices along the Crocodile River, resulting in a lower concentration of phosphate runoff. The Crocodile River is largely threatened by the rise in sulphate concentration and subsequently the increasing sulphate loading rate.

The discharge of untreated wastewater is increasing the loading rates and exacerbating the sulphate loads as seen from 2006 to 2018. This is strongly related to landfill seepage and mining activity around the periphery of Johannesburg. The possible effect of groundwater and surface water interaction could be a result of increasing sulphate concentration that caused an increase in the loading rates. The Crocodile River had a loading trend moderately consistent in the 1980–1995 period, with a strong increase in the 1996–2000 period attributed to the La Niña occurrence, and supplemented discharge from the WWTW (Department of Water Affairs and Forestry 2008a; Abiye and Leketa, 2021). Nitrogen levels along the Crocodile River increased drastically post the 2001–2005 period because of population increase, urbanisation, sewage effluent and informal settlements along the Crocodile River.

Anthropogenic pollution (such as sewage treatment plant discharges and industrial development along the channel) is adversely affecting and increasing the nitrogen loading rate (Wernick et al., 1998; Hall et al., 1999). The result of increased runoff during the summer periods is evident, hence summer loading rates are higher than those in winter, attributed to atmospheric deposition, industrial development and increasing urban development (Fisher and Oppenheimer, 1991).

Gauging station A2H012Q01 monitors the inflow of water from all major rivers in the South; the site itself is represented as a fourth-order stream. As a result, the expected nutrient and salinity loads are increased with a high volume of water. The gauging station with its represented nutrient loads is an indicator of the quantity of nutrients entering the Hartbeespoort Dam. As shown on the maps, there are no wastewater treatment works along this channel. The sulphate load is seen to be high in the summers and decreases in the winters and from 1980 to 1990, very high sulphate loads were observed which correlates with research done by Huizenga and Harmse (2005). A decrease was followed by a rapid increase which is consistent with other results due to the climatic variations (including El Niño and La Niña, respectively). Sulphate loading rates entering the Hartbeespoort Dam after 2006 show a seasonal and temporal increasing trend;

this is attributed to increased sulphate concentrations and discharge from the wastewater treatment plants increasing sulphate loading rates. Secondly, it is noted that groundwater and surface water interactions within the Central Rand Group, West Rand Group and Malmani Dolomites ensue (Abiye et al., 2015), hence, sulphate concentration occurrence increased into the latter years. Nitrogen loads across the UCRB are a threat to water sources. From the early 1980s to 1990, nitrogen loading rates were very high, with climatic phenomena in the late 1990s and early 2000s supplemented by bioremediation plans, which account for the decrease and increase in the loading rates. Following 2006, nitrogen loading rates increased due to sewage, and commercial and industrial effluents. Disposal of untreated waste, decentralised and onsite septic tanks and centralised wastewater treatment plants discharging poor quality wastewater into streams also threaten surface water and groundwater quality (Satterthwaite, 2008; Humphrey et al., 2013; De and Toor, 2017; Toor et al., 2017).

Phosphorus loads (being the limiting nutrient for HAB), are indicated to have posed an immense threat to the Hartbeespoort Dam post 2006. As mentioned, the early 1980s to 1995 show a decrease in phosphorus loading, and a rise in summer loads is evident in 1996 due to La Niña (Ali et al., 2022), followed by a decrease in the early 2000s due to El Niño. Phosphorus loading post the bioremediation project (Ali et al., 2022), indicated a rise in phosphorus concentration, although the Hartbeespoort Dam has not been hypereutrophic. The quality of water entering the dam is under severe threat with the rise in urbanisation and increased fertiliser used to keep farm yields to meet population demands. Runoff and disposal of phosphate into water systems is increasing and there is reduced quality in the discharge of partially treated wastewater into streams (Ali et al., 2022). The mismanagement and presence of informal settlements within the proximity of runoff impacts the larger rivers, with poor sanitary practices increasing the risk of water-borne diseases in the UCRB in future. Lastly, poor management of old infrastructure (including septic tanks and piping that contains and distributes effluent discharge to the wastewater treatment plants and could potentially burst), adversely affects water resources in the UCRB.

The Skeerpoort River is mainly adversely affected by sulphate loading while regarding the sites evaluated and discharge values returned, nitrogen and phosphorus loading is low. The possible reason for the high sulphate loading rates around the Skeerpoort River is the mining activities in the catchment. The Skeerpoort River is located on the Malmani Dolomite. It is known that the mixing of groundwater and surface water can have major effects on aquatic environments if factors like acidity, temperature and dissolved oxygen are altered (Winter et al., 1998). Research on the interaction of groundwater and surface water through environmental isotopes concluded the interaction of mixing between them in the Malmani Dolomites (in the Karstic Aquifers) (Abiye et al., 2015). The presence and variability observed in the Skeerpoort River concerning a general increase in sulphate is due to the groundwater interaction caused by the advection of mine water within the rock fractures of the karstic rock (Abiye, 2014). Emptying of mine water into the streams and seepage into the fractured crystalline rocks and karstified dolomitic aquifer due to the influence of increased sulphate concentrations (Abiye, 2011), over time has resulted in increased sulphate loading across the extent of the Skeerpoort River.

Salinity loading across the UCRB shows strong trends of seasonal variation as summer loading rates are considerably higher than winter loading rates. This is due to most of the UCRB receiving recharge through precipitation which occurs in the summer months (DWA, 2013b). The direct recharge from precipitation increases the overall runoff, and the runoff from built-up areas and peripheries around the Hennops, Jukskei and Crocodile rivers which have informal settlements is escalating overall contamination. During the early 1980s, TDS values in the summer months were high because all major cation and anion concentrations increased due to higher temperatures and evaporation that increased overall TDS, and therefore salinity. This is supported by Huizenga and Harmse (2005). After 2005, the $Cl^-$, $Na^+$, Mg, $F^-$, TN, TP, $SO_4$, $NH_4$ and $Ca^{2+}$ concentrations increased during the summer period and controlled most of the TDS values, possibly due to increased temperature and evaporation. The leakage and seepage of mine water into the river systems are responsible for high SO  concentrations. Chloride from commercial and domestic water softeners

(from the use of NaCl resins water purification processes) and backwash from swimming pools could be responsible for the increasing chloride concentration, which was high during the summer months. Increased nitrogen and phosphorus concentrations due to effluent discharge, partially treated wastewater disposal and agricultural runoff over time (as a result of population growth and urbanisation), are responsible for the increase in the concentrations over the years – driving up the water salinity.

The Hennops River at the A2H008 gauging station receives flow from a natural spring; an erosion of sediments and concentrating effects from rising temperatures over time that are responsible for increasing evaporation levels and the overall salinity of the spring (Venkatesan et al., 2011). The natural spring's salinity, increasing evaporation rates and discharge of partially untreated wastewater are responsible for the increase in higher summer loading rates. During winter, due to reduced overall temperatures, lower evaporation and more dilution, lowered TDS values account for the decrease in salinity loading rates. The Jukskei River shows a similar trend in TDS values with summer values being considerably higher than winter loading rates due to the climatic variation in temperature and rainfall. The TDS concentrations were higher and decreased with time, from the early 1980s to 1990; they peaked during the 1996–2000 period resulting from increased precipitation and further runoff as a consequence of La Niña. Following a strong salinity decrease in the 2001–2005 period due to El Niño, the loading rates have decreased due to reduced discharge and its directly proportional relationship in the salinity loading calculation. TDS values were higher in summer and a rise in salinity loading rates into the next eighteen years followed.

An increase in urban water demands resulted in the supplemented inter-basin water programme subsidising the growing Johannesburg population. This increased the discharge rates across the Jukskei River and the Hennops River, intensifying salinity loading. The TDS values increased during the eighteen years, due to wastewater effluents and runoff from the Johannesburg area being diverted into the major rivers in the UCRB. The demands from agricultural use of

fertiliser runoffs and irrigation groundwater discharge into the UCRB have increased salinity rates over the period. The consistent climatic changes and rise in temperatures during the summer, with the increasing evaporation rates (Markstrom et al., 2015), resulted in increased salinity. The additional discharge entering from the inter-basin water transfer has inflated the loading rates through the disposal of partially treated urban wastewater from wastewater treatment works (Department of Water Affairs and Forestry, 2008a). According to DWAF (2004), the Johannesburg urban water demand was increasing; during the year 2000, 291.4mm$^3$ of water was added from the inter-basin water transfer. The demands have been increasing ever since (hence the rise in overall nutrient and salinity loading rates), with the forecasted demand for the year 2025 for more wastewater (409 million m$^3$) to be pumped into the UCRB. This poses an even greater threat to the UCRB streams and water quality. The Crocodile River, located on the West, follows a similar salinity loading trend to the Jukskei and Hennops rivers (before joining into the Jukskei River, which joins the Hennops River). The Crocodile River is subject to TDS driving mechanisms from resorts and golf courses (partially purified wastewater discharge), informal settlements (groundwater contamination) and mining being responsible for increased TDS levels (Nde and Mathuthu, 2018). Resorts and accommodation sites normally have their own storage and pumping facilities, including JoJo tanks and boreholes; the water is then cleaned using resins and water softeners and discharged into the larger municipal lines, which are partially purified out of the wastewater treatment plants (Venkatesan et al., 2011). The rise in overall TDS and salinity loading in the UCRB (as seen at A2H012Q01 station), indicates that increased salinity can pose a threat to municipal pipes transporting water to water treatment works, as it can corrode pipes (Venkatesan et al., 2011). With the excessive use of water and recycling of water, TDS levels are bound to rise and further increase the TDS values entering the larger river (Venkatesan et al., 2011), as seen in the A2H012Q01 station (Figure 46). According to Venkatesan et al. (2011), drought and increased water usage by a rising population are attributed to increased TDS concentration. This is observed in the UCRB and is responsible to some degree for the rise in salinity loading in the UCRB.

# 7. CONCLUSION

Based on the analysed water quality monitoring data, the water quality in the UCRB has been largely influenced by anthropogenic activities. The rapid urban growth and development of industries, agriculture and mining across the basin's spatial extent have adversely affected the water quality. The nutrient and salinity loading across the UCRB are driven primarily by changes in chemical and nutrient concentration in the water, besides an increased wastewater discharge from the inter-basin water transfer (the adjacent Vaal basin), resulting in higher loading rates. The wastewater treatment works are struggling to maintain the quality of treated wastewater which affects the nutrient and salinity loads.

From the findings in this study, it can be concluded that during the early 1980s to early 1990s, summer and winter loading rates were high. The loading rates dropped drastically in the mid-1990s due to the application of bioremediation strategies and were followed by a significant spike in the late 1990s and early 2000s due to La Niña. The nutrient and salinity loading rates throughout the UCRB dropped again in the early 2000s due to the El Niño occurrence. From the onset of the inter-basin transfer in the late 2000s into the following two decades, an overall rise in nutrient and salinity loading rates was observed. Mining activities (compounded by poor landfill and tailing storage facilities) have resulted in seepage and leaching of harmful metals and oxidation of pyrite, a consequence of which is increasing sulphate loading, gradually declining through the four-decadal period. Nitrogen levels rise due to an increase in urbanisation and population, with urban development, poor maintenance of sewage lines, industrial discharge from power plants, informal settlements and poor access to basic lavatories and sanitary facilities causing a rise in nitrogen and phosphorus levels. When the surface runoff from fertilisers began to flow into river systems, phosphorus loading rates increased together with the expansion of agricultural practices across the UCRB. This is due to a rising population and an increasing demand for food security. The anthropogenic influence compounded by a crippling water management system across the extent of the UCRB, poses a large threat to water quality and security, which in turn poses serious health

implications. The seasonal variation in nutrient and salinity loading rates (with increased summer loading rates relative to winter loading rates), reflects the urgency for an enhanced water management strategy to improve overall water quality and the country's economy. From the following results found in this study, sulphate, nitrogen and phosphorus loads are entering the Hartbeespoort dam during summer at a rate of 6819.24 kg/hr, 4179.24 kg/hr and 40.081 kg/hr and during winter the loading rates for sulphate, nitrogen and phosphorus decrease, but are still elevated to 4873.62 kg/hr, 4021.55 kg/hr and 34.724 kg/hr respectively. The Salinity loading rates during summer are 42952.87 kg/hr and 27548.39 kg/hr. It is evident that nutrient and salinity loading rates are certain to increase, further exacerbating the decrease in overall water quality which could pose severe health and economic risks for urban centres.

## 8. RECOMMENDATIONS AND LIMITATIONS

- Wastewater treatment discharge has not been monitored consistently throughout the 38 years, this has resulted in overestimated nutrient and salinity loading rates, as the overall inflow and outflow water chemistry and discharge results have not been provided/recorded upon request from the DWA.
- The results from the study indicate a need for immediate attenuation planning for the upcoming decade to protect the water quality in the UCRB by utilizing the results from this study.
- Water resource management of South Africa needs to investigate and concentrate their efforts on improving and adapting wastewater treatment facilities to accommodate for the inter-basin water transfer discharge and effluent entering the rivers and wastewater treatment plants.
- Further research needs to be done on adaptive wastewater treatment works, to changes in water use through time as seen by the rapid changes in loading rates

## 9. REFERENCES

Abiye, T. A., Mengistu, H. and Demlie, M.B. 2011. Groundwater Resource in the Crystalline Rocks of the Johannesburg Area, South Africa. *Journal of Water Resource and Protection*, 3:199–212.

Abiye, T. 2016. Synthesis on Groundwater Recharge in Southern Africa: A Supporting Tool for Groundwater Users. Groundwater for Sustainable Development, 2: 182–189.

Abiye, T.A. 2021. Physicochemical and metal composition of rainfall in the Johannesburg region, South Africa. *Environmental Monitoring and Assessment*, *193*(6), p.348.

Abiye, T.A. and Ali, K.A. 2022. Potential role of acid mine drainage management towards achieving sustainable development in the Johannesburg region, South Africa. *Groundwater for Sustainable Development*, p.100839.

Abiye, T.A. 2011. Provenance of groundwater in the crystalline aquifer of Johannesburg area, South Africa. *International Journal of Physical Sciences*, 6(1):.98-111.

Abiye, T.A., Mengistu, H., Masindi, K. and Demlie, M. 2015. Surface water and groundwater interaction in the upper Crocodile River Basin, Johannesburg, South Africa: environmental isotope approach. *South African Journal of Geology*, *118*(2), pp.109-118.

Abiye, T.A.; Leketa, K.C. 2021. Historic Climatic Variability and Change: The Importance of Managing Holocene and Late Pleistocene Groundwater in the Limpopo River Basin, Southern Africa. In Climate Change and Water Resources in Africa; Springer: Berlin/Heidelberg, Germany, pp. 131–143

Ali, K., Abiye, T. and Adam, E. 2022. Integrating in Situ and Current Generation Satellite Data for Temporal and Spatial Analysis of Harmful Algal Blooms in the Hartbeespoort Dam, Crocodile River Basin, South Africa. *Remote Sensing*, *14*(17), p.4277.

Ashton, P.J., Moor, F.C. De, Chutter, F.M., Cochrane, K.L., Jarvis, A.C., Robarts, R.D., Scott, W.E., Thornton, J.A., et al. 1985. *The Limnology of Hartbeespoort Dam*.

Barnard H.C. 2000. An explanation of the 1:500 000 general hydrogeological map. Pretoria, South Africa.

Chang, H., Evans, B.M. and Easterling, D.R. 2001. The effects of climate change on stream flow and nutrient loading 1. *JAWRA Journal of the American Water Resources Association*, *37*(4), pp.973-985.

Chapman P. M., Bailey H, Canaria E. 2000. Toxicity of total dissolved solids associated with two mine effluents to chironomid larvae and early stages of rainbow trout. Environ. Toxicol. Chem.;19(1):210–4.

Colman, J.A., Massey, A.J. and Brandt, S.L. 2016. Determination of dilution factors for discharge of aluminium-containing wastes by public water-supply treatment facilities into lakes and reservoirs in Massachusetts (No. 2011-5136). US Geological Survey.

Conley DJ. 2000. Biogeochemical nutrient cycles and nutrient management strategies. Hydrobiologia, 410: 87–96.

Cukic, E.Z. and Venter, P. 2012. Sediment removal and management: Hartbeespoort Dam remediation. *Civil Engineering= Siviele Ingenieurswese*, *2012*(7), pp.42-47.

De M, Toor GS. 2017. Nitrogen transformations in the mounded drain fields of drip dispersal and gravel trench septic systems. Ecol Eng 102:352–360. https ://doi.org/10.1016/j.ecoleng.2017.02.039

Department of Agriculture and Rural Development (DARD). 2011. Gauteng State of Environment Report 2011, Gauteng Provincial Government, Johannesburg, pp. 140

Department of Agriculture Conservation and Environment (DACE), 2004. Gauteng State of Environment report 2004, Gauteng Provincial Government, Johannesburg, pp. 118.

Department of Water Affairs (DWA). 2013b. Feasibility Study for a Long-Term Solution to Address the Acid Mine Drainage Associated with the East, Central and West Rand Underground Mining Basins. Study Report No. 5.4: Treatment Technology Options –DWA Report No. P RSA 000/00/16512/4, Pretoria, South Africa.

Department of Water Affairs and Forestry (DWAF). 2004. Crocodile River (west) and Marico Water Management Area: Internal strategic perspective Crocodile West Marico Water Management Area: Crocodile River (west) catchment. DWAF Report 03/000/00/0303, Report prepared for the Directorate: National Water Resource Planning, Pretoria, pp. 160.

Department of water affairs and forestry, S. A. 2008. The Development of a Reconciliation Strategy for the Crocodile (West) Water Supply System: Summary of Previous and Current Studies. BKS (PTY) LTD & ARCUS GIBB (PTY) LTD (P WMA 03/000/00/3408).

DH Environmental. 2004. Hartbeespoort Dam Remediation Project (Phase 1).

Dudula, M.Z. 2007. A situation analysis of the water quality in the Hartbeespoort dam catchment: nutrients and other pollutants' assessment on rivers entering the dam (Doctoral dissertation).

Farrington JW. 1992. Marine organic geochemistry: review and challenges for the future. Workshop in Honolulu, HI, USA, 8-12 January 1990. Foreword. Mar Chem 39:1–4.

Fisher TR, Peele ER, Ammerman JW, Harding LW. 1992. Nutrient limitation of phytoplankton in the Chesapeake Bay. Mar Ecol Prog Ser 82:51–63.

Goolsby DA, Battaglin WA, Aulenbach BT Hooper RP. 2000. Nitrogen flux and sources in the Mississippi River Basin. Sci Total Environ 248:75–86.

Guo L, Santschi PH, Bianchi TS. 1999. Dissolved organic matter in estuaries of the Gulf of Mexico. In: Biogeochemistry of Gulf of Mexico Estuaries (Bianchi TS, Pennock JR, Twilley RR, eds). New York: John Wiley and Sons, 269–299.

Howarth RW, Billen G, Swaney D, Townsend A, Jaworski N, Lajtha K, Downing JA, Elmgren R, Caraco N, Jordan T, et al. 1996. Regional nitrogen budgets and riverine N & P fluxes for the drainages to the North Atlantic Ocean: natural and human influences. Biogeochemistry 35:75–139

Huizenga, J.M. and Harmse, J.T. 2005. Geological and anthropogenic influences on the inorganic water chemistry of the Jukskei River, Gauteng, South Africa. *South African Journal of Geology*, *108*(3), pp.439-447

Humphrey CP Jr, O'Driscoll MA, Deal NE, Lindbo DL, Thieme SC, Zarate-Bermudez MA. 2013. Onsite wastewater system nitrogen contributions to groundwater in coastal North Carolina. J Environ Health 76:16–22

Jalpaiguri. 2021., India: A Multiple Indicator-Based Analysis. Environ. Monit. Assess, 193, 667

Kusangaya, S., Warburton, M.L., Van Garderen, E.A. and Jewitt, G.P. 2014. Impacts of climate change on water resources in southern Africa: A review. *Physics and Chemistry of the Earth, Parts A/B/C*, *67*, pp.47-54.

Lawrence, D., Valiela, I. and Tomasky, G. 2004. Estuarine calanoid copepod abundance about season, salinity, and land-derived nitrogen loading, Waquoit Bay, MA. *Estuarine, Coastal and Shelf Science*, *61*(3), pp.547-557.

Leketa, K. and Abiye, T. 2019. Modelling the impacts of climatic variables on the hydrology of the Upper Crocodile River Basin, Johannesburg, South Africa. *Environmental Earth Sciences*, *78*(12), p.358.

Leketa, K., Abiye, T., Zondi, S. and Butler, M. 2019. Assessing groundwater recharge in crystalline and karstic aquifers of the Upper Crocodile River Basin, Johannesburg, South Africa. *Groundwater for Sustainable Development*, *8*, pp.31-40.

Leketa, K.C. 2019. A holistic approach to groundwater recharge assessment in the Upper Crocodile River Basin, Johannesburg, South Africa (Doctoral dissertation).

Lusher, J.A. and Ramsden, H.T. 2000. Water pollution. In: R.F. Fuggle and M.A. Rabie, (Editors), Environmental Management in South Africa. (3rd impression). Juta and Company, Limited., Cape Town, South Africa,456-492.

Markstrom SL, Regan RS, Hay LE, Viger RJ, Webb RMT, Payn RA, LaFontaine JH. 2015. PRMS-IV, the precipitation-runoff modelling system, version 4: US geological survey techniques and methods, book 6, chap. B7. United States Geological Survey, Colorado, USA. http://dx.doi.org/10.3133/tm6B7. https ://pubs.usgs.gov/tm/6b7/

McCarthy, T. & Rubidge, B. 2005. The Story of Earth and Life A Southern African perspective on a 4.6-billion year journey. published by Struik, Cape Town, pp. 333.

McCleskey, R.B., Cravotta III, C.A., Miller, M.P., Tillman, F., Stackelberg, P., Knierim, K.J. and Wise, D.R. 2023. Salinity and total dissolved solids measurements for natural waters: An overview and a new salinity method based on specific conductance and water type. *Applied Geochemistry*, p.105684.

Mengistu, H.A., Demlie, M.B., Abiye, T.A., Xu, Y. and Kanyerere, T. 2019. Conceptual hydrogeological and numerical groundwater flow modelling around the Moab Khutsong deep gold mine, South Africa. *Groundwater for Sustainable Development*, *9*, p.100266.

Mikalsen, T. 2005. Causes of increased total dissolved solids and conductivity levels in urban streams in Georgia.

Mondal, S.; Mitra, S.; Dey, J.; Tamang, L. 2021. Assessment of the Anthropogenic Interventions and Related Responses of Karala River.

Naicker, K., Cukrowska, E. and McCarthy, T.S. 2003. Acid mine drainage arising from gold mining activity in Johannesburg, South Africa and its environs. Environmental Pollution, 122, 29-40.

Nde, S.C. and Mathuthu, M. 2018. Assessment of potentially toxic elements as non-point sources of contamination in the upper crocodile catchment area, northwest province, South Africa. *International Journal of Environmental Research and Public Health*, *15*(4), p.576.

Nde, S.C., Bett, S.K., Mathuthu, M. and Palamuleni, L. 2022. Anthropogenic Land Use and Land Cover Change as Potential Drivers of Sediment Sources in the Upper Crocodile River, North West Province, South Africa. *International Journal of Environmental Research and Public Health*, *19*(20), p.13313.

Neswiswi, A.B. 2014. Development of a Water Quality Index (WQI) for the Jukskei River Catchment. *Johannesburg [Masters Thesis] Wits Institutional Repository on DSpace*.

Nordstrom, D.K. and Alpers, C.N. 1999. Geochemistry of acid mine waters. In: S. Geoffrey and M.J. Logsdon (Editors), The Environmental Geochemistry of Mineral Deposits. Part A: Processes, Techniques and Health Issues. Reviews in Economic Geology, 6A, 229-248.

Odum WE, Odum EP, Odum HT. 1995. Nature's pulsing paradigm. Estuaries 18:547–555.

Oliva P., Viers, J. and Dupré, B. 2003. Chemical weathering in granitic environments. Chemical Geology, 202, 225-256.

Paerl HW. 1997. Coastal eutrophication and harmful algal blooms: the importance of atmospheric deposition and groundwater as "new" nitrogen and other nutrient sources. Limnol Oceanogr 42:1154–1165.

Paul V.R. 2013. Snelgrove, in Encyclopedia of Biodiversity (Second Edition).

Pinckney, J.L., Paerl, H.W., Tester, P. and Richardson, T.L. 2001. The role of nutrient loading and eutrophication in estuarine ecology. *Environmental health perspectives*, *109*(suppl 5), pp.699-706.

Rast, W. and Lee, G.F. 1983. Nutrient loading estimates for lakes. *Journal of Environmental Engineering*, *109*(2), pp.502-517.

Satterthwaite D. 2008. Cities' contribution to global warming: notes on the allocation of greenhouse gas emissions. Environ Urbanization 20:539–549. https ://doi.org/10.1177/09562 4780809612 7

Scanlon, B.R., Healy, R.W., Cook, P.G. 2002. Choosing appropriate techniques for quantifying groundwater recharge. Hydrogeol. J. 10, 18–39. https://doi.org/10.1007/s10040-001-0176-2. (ISSN 1435-0157).

Thornton, J.A., Mcmillan, P.H. & Romanovsky, P. 1989. Perceptions of water pollution in South Africa: Case studies from two water bodies (Hartbeespoort Dam and Zandvlei) *South African Journal of Psychology*. 19(4):199–204.

Toerien, D. & Walmsley, R. 1978. The Dissolved Mineral Composition of the Water Flowing into and out of the Hartbeespoort Dam. *Water SA*. 4(1):25–38.

Toor GS, Yang Y-Y, Mechtensimer S, De M, Obreza TA. 2017. A review of the fate and transport of nitrogen, phosphorus, pathogens, and trace organic chemicals in septic systems AU—Lusk. Mary G Critical Reviews in Environ Sci Technol 47:455–541. Available: https ://doi.org/10.1080/10643 389.2017.13277 8

United States Bureau of Reclamation (USBR). 2005. Quality of water Colorado River Basin. Progress report no. 22; Available: http://www.usbr.gov/uc/progact/salinity/pdfs/PR22. pdf.

Venkatesan, A.K., Ahmad, S., Johnson, W. and Batista, J.R. 2011. Systems dynamic model to forecast salinity load to the Colorado River due to urbanization within the Las Vegas Valley. *Science of the Total Environment*, *409*(13), pp.2616-2625.

Venter, A.J.A. 1995. Assessment of the Effect of Gold-Mine Effluent on the Natural Aquatic Environment. Unpublished PhD thesis, Rand Afrikaans University, Johannesburg, South Africa

Venter, P. 2004. 16 eutrophication management. *Water Wheel*. (January/February).

Weber-Scannell P, Duffy LK. 2007.Effects of total dissolved solids on aquatic organisms: a review of literature and recommendation for Salmonid species. Am. J. Environ. Sci. 2007;3(1):1–6.

Williams WD. 1987. Salinization of rivers and streams: an important environmental hazard. AMBIO 1987;16(4):180–5

Winter, T.C., J.W. Harvey, Franke, O.L. and Alley, W.M. 1998. Groundwater and Surface water: a single resource. U.S. Geological Survey circular 1139, 30pp.

Wittmann, G. & Forstner, U. 1975. Metal Enrichment of Sediments in Inland Waters- The Hartbeespoort Dam. *Water SA*. 1(2):76–82.

Zohary T, Jarvis AC, Chutter FM, Ashton PJ, Robarts R. 1988. The Hartbeespoort dam ecosystem programme—1980–1988. Council for Scientific and Industrial Research, Pretoria, RSA. http://www.dwa.gov.za/iwqs/eutrophication/Zohary_1988_The_Hartbeespoort_Dam_ecosystemprogramme.pdf